

AN ABSTRACT OF THE DISSERTATION OF

Joel E. Johnson for the degree of Doctor of Philosophy in Oceanography presented on July 19, 2004.

Title: Deformation, Fluid Venting, and Slope Failure at an Active Margin Gas Hydrate Province, Hydrate Ridge Cascadia Accretionary Wedge

Abstract Approved:

Signature redacted for privacy.

Chris Goldfinger

During the last 15 years, numerous geophysical surveys and geological sampling and coring expeditions have helped to characterize the tectonic setting, subsurface stratigraphy, and gas hydrate occurrence and abundance within the region of the accretionary wedge surrounding Hydrate Ridge. Because of these investigations, Hydrate Ridge has developed as an international site of active margin gas hydrate research. The manuscripts presented in this dissertation are focused on the geologic setting hosting the gas hydrate system on Hydrate Ridge. These papers examine how active margin tectonic processes influence both the spatial and temporal behavior of the gas hydrate system at Hydrate Ridge and likely across the margin. From a high resolution sidescan sonar survey (Chapter II) collected across the region, the distribution of high backscatter, as well as the locations of mud volcanoes and pockmarks indicates variations in the intensity and activity of fluid flow across the Hydrate Ridge region. Coupled with subsurface structural mapping, the origins for many of these features as well the locations of abundant gas hydrates can be linked to folds within the subsurface. Continued structural mapping, coupled with age constraints of the subsurface stratigraphy from ODP drilling, resulted in a model for the construction of the accretionary wedge within the Hydrate Ridge region (Chapter III). This model suggests the wedge advanced in three phases of growth since the late Pliocene and was significantly influenced by the deposition of the Astoria fan on the abyssal plain and left lateral strike slip faulting.

Changes in structural vergence, documented here, also help explain the variability in bathymetric relief across the region. Determination of the occurrence and timing of Holocene slope failures derived from Hydrate Ridge (Chapter IV) and comparison with a Holocene marine record of Cascadia subduction zone earthquakes suggests earthquake induced slope failure within the gas hydrate stability zone does occur at Hydrate Ridge and thus, may represent a high frequency mechanism for the mobilization of seafloor and subseafloor gas hydrates across the margin.

©Copyright by Joel E. Johnson

July 19, 2004

All Rights Reserved

Deformation, Fluid Venting, and Slope Failure at an Active Margin Gas Hydrate
Province, Hydrate Ridge Cascadia Accretionary Wedge

by

Joel E. Johnson

A DISSERTATION

submitted to

Oregon State University

in partial fulfillment of
the requirements for the
degree of

Doctor of Philosophy

Presented July 19, 2004

Commencement June 2005

ACKNOWLEDGEMENTS

I would like to thank my five committee members Chris Goldfinger, Anne Tréhu, Bob Yeats, Alan Niem, and Tom Dietterich for taking the time to serve on my committee and for reading and providing helpful comments during the review of this dissertation. In particular I wish to thank my dissertation advisor, Chris Goldfinger, for introducing me to marine geology, providing excellent opportunities for cruise participation on a variety of expeditions, encouraging me to pursue my own research interests, teaching me the ever-valuable skill of proposal writing, and for excellent guidance and discussion of the research presented here. I also wish to thank Anne Tréhu for helpful and insightful discussions during the course of this research and for inviting me to sail as a shipboard sedimentologist on ODP Leg 204, a forever valuable experience and the starting point for much of my post-dissertation research. I thank Bob Yeats for great discussions of the geology of the Cascadia margin and his supportive guidance over the years. I thank Alan Niem for offering great courses and field trips in sedimentology and stratigraphy and for engaging discussions throughout my time at OSU. I also thank Marta Torres for helpful discussion of the research presented here and supportive guidance and enthusiastic encouragement throughout my time at OSU.

I also wish to acknowledge the following individuals who contributed helpful professional advice and scientific insight during the course of this research: Nathan Bangs, C. Hans Nelson, Andrew Meigs, Bob Collier, Bobbie Conard, and Gerhard Bohrmann. I also thank numerous friends for making my experience at OSU enjoyable and unforgettable, both at sea and onshore. In particular, Dan Myers, Vincent Rinterknecht, Sam VanLaningham, Chris Krugh, Mike Winkler, Heather Petcovic, Drew Eriksson, Jason Chaytor, Chris Romsos, Matt Arsenault, and Ann Morey-Ross. Finally, I offer sincere acknowledgement and thanks to my wonderful wife, Megan. Her endless encouragement, support, and understanding throughout the completion of this research will always be cherished and appreciated.

I acknowledge the following funding sources which made this research possible: National Science Foundation, American Chemical Society-Petroleum Research Fund,

Joint Oceanographic Institutions U.S. Science Support Program, and the Oregon State
University College of Oceanic and Atmospheric Sciences Chipman-Downs Fellowship.

CONTRIBUTION OF AUTHORS

Chris Goldfinger, C. Hans Nelson, and Anne Tréhu were the principal and/or co-principal investigators of the research projects that resulted in the manuscripts presented here. Their collective contributions included assistance with initial development of the research problems, guidance with methodology, and interpretation of the results. Erwin Suess contributed seafloor sample observations and geochemical data from cores collected across the Hydrate Ridge region, which were used to groundtruth portions of the sidescan sonar survey discussed in Chapter II. Nathan Bangs helped process and interpret additional 2-D seismic reflection profiles across northern Hydrate Ridge, which although not presented in Chapter III, provided important insight into the structures of that region. Johanna Chevallier mapped the structures within the 3-d seismic survey at southern Hydrate Ridge, tying them to the ODP Leg 204 down hole data, and determined the timing of landward vergence at southern Hydrate Ridge discussed in Chapter III.

TABLE OF CONTENTS

	<u>Page</u>
I. Introduction.....	1
II. Geophysical Constraints on the Surface Distribution of Authigenic Carbonates Across the Hydrate Ridge Region, Cascadia Margin	4
Abstract.....	5
Introduction.....	6
Tectonic Setting	9
Cascadia Accretionary Prism.....	9
Structure of the Hydrate Ridge Region.....	10
Methods.....	14
Imaging the Carbonates	14
SeaMARC 30 Survey.....	14
High Backscatter and Carbonates	15
Results.....	16
Sidescan Sonar Survey.....	16
Backscatter Patterns and Bathymetric Slope	16
Groundtruthing the Sonar	19
Other Fluid Venting Manifestations	25
Discussion.....	31
Backscatter Distribution.....	31
Relationship to Geologic Structures	32
Landward Limit of Gas Hydrate Stability	35
Backscatter Patterns and Fluid Flow.....	36
Conclusions.....	39
Acknowledgements.....	40
References.....	41
III. Structural Vergence Variation and Clockwise Block Rotation in the Hydrate Ridge Region, Cascadia Accretionary Wedge.....	46
Abstract.....	47

TABLE OF CONTENTS (continued)

	<u>Page</u>
Introduction.....	48
Geologic Setting: Washington and Oregon Margin.....	52
Data and Methods	53
Results.....	55
Structural Vergence Variation	55
Structural Vergence and Hydrate Ridge Morphology	75
Daisy Bank and Alvin Canyon Strike Slip Faults.....	78
Evidence for Clockwise Block Rotation.....	80
Relative Timing of Major Tectonic Events	81
Discussion.....	85
Accretionary Wedge Construction.....	85
Landward Vergence and Deposition of the Astoria Fan.....	86
Cessation of Landward Vergence at the Deformation Front	89
Clockwise Block Rotation	91
Northward Migration of the Cascadia Forearc	93
Structural Control on Dewatering of the Wedge at Hydrate Ridge	96
Conclusions.....	96
Acknowledgements.....	97
References.....	98
IV. Holocene Slope Failure in an Active Margin Gas Hydrate Bearing Region, Hydrate Ridge, Cascadia Margin.....	103
Abstract.....	104
Introduction.....	104
Geologic Setting.....	106
Research Methods.....	111
Results.....	113
Slope Basin Turbidite Stratigraphy.....	113

TABLE OF CONTENTS (continued)

	<u>Page</u>
Correlation of Turbidites Across the Basin	116
Dating the Turbidites	117
Discussion	119
Triggers for Slope Failure	119
Slope Failure Triggers at Hydrate Ridge	120
Correlation to the Earthquake Triggered Turbidite Record	122
A Mix of Earthquakes and Other Triggers	127
Implications for the Mobilization of Seafloor Gas Hydrates	128
Conclusions	130
Acknowledgements	130
References	131
V. Conclusions	134
Bibliography	136

LIST OF FIGURES

<u>Figure</u>	<u>Page</u>
CHAPTER II	
2-1	8
2-2	12
2-3	13
2-4	*AF
2-5	18
2-6	20
2-7	23
2-8	26
2-9	28
2-10	30
2-11	37

*AF (Attached Foldout)

LIST OF FIGURES (continued)

<u>Figure</u>	<u>Page</u>
CHAPTER III	
3-1 Bathymetric map of the offshore portion of the Cascadia subduction zone	49
3-2 Shaded relief bathymetry (100 m pixel) of the Hydrate Ridge region.....	54
3-3 Geologic structures of the Hydrate Ridge region	57
3-4 (A) OR89 Line 15 (interpreted and uninterpreted). (B) OR89 Line 14 (interpreted and uninterpreted)	60
3-5 (A) OR89 Line 13 (interpreted and uninterpreted). (B) OR89 Line 12 (interpreted and uninterpreted)	62
3-6 (A) OR89 Line 11 (interpreted and uninterpreted). (B) OR89 Line 10 (interpreted and uninterpreted)	65
3-7 (A) OR89 Line 9 (interpreted and uninterpreted). (B) OR89 Line 8 (interpreted and uninterpreted)	68
3-8 OR89 Line 5 (interpreted and uninterpreted).....	70
3-9 (A) OR89 Line 2 (interpreted and uninterpreted). (B) OR89 Line 1 (interpreted and uninterpreted)	73
3-10 Summary of structural vergence variation within the three regions (Region north of Hydrate Ridge, Northern Hydrate Ridge, and Southern Hydrate Ridge) and the three structural zones (I-II-III) discussed in the text.....	76
3-11 Schematic diagram showing the interaction of left lateral strike-slip faults with the accretionary wedge	79
CHAPTER IV	
4-1 (A) Bathymetric map of the offshore portion of the Cascadia subduction zone. (B) Shaded relief bathymetry of the Hydrate Ridge region (location shown in A).....	107
4-2 Stratigraphic records from the three core sites located across the western slope basin	114

LIST OF FIGURES (continued)

<u>Figure</u>		<u>Page</u>
4-3	(A) Comparison of the Holocene Hydrate Ridge record (RR0207-56PC; in red) to the Holocene subduction zone earthquake triggered turbidite record at the Juan de Fuca Canyon site (M9907-12PC; in blue) of Goldfinger et al. (2003). (B) Calibrated radiocarbon ages for the Juan de Fuca Canyon and Hydrate Ridge turbidite events (closed symbols, with 2 sigma error ranges also shown)	123

LIST OF TABLES

<u>Table</u>		<u>Page</u>
	CHAPTER IV	
4-1	Individual foraminifera counts by species taken from hemipelagic sediments beneath turbidites (e.g. T2).....	112
4-2	Down core faunal change documented from smear slide analyses taken in the RR0207-01 kasten core.....	115
4-3	Radiocarbon results and correlative foraminifera data obtained from hemipelagic samples taken beneath each turbidite.....	118

Deformation, Fluid Venting, and Slope Failure at an Active Margin Gas Hydrate Province, Hydrate Ridge Cascadia Accretionary Wedge

Chapter I

Introduction

On the Cascadia continental margin offshore central Oregon, Hydrate Ridge has been the focus of numerous geologic and geophysical investigations for nearly two decades. During the mid-1980's, its location within the lower slope of the accretionary wedge initially prompted investigations of seafloor fluid flow and the dewatering processes associated with accretion of abyssal plain sediments and resulted in one of the first discoveries of chemosynthetic cold seep faunas. By the early 1990's this early work was supplemented by detailed structural investigations and ODP (Ocean Drilling Program) drilling, during which gas hydrates were first recovered. Subsequent work, including numerous seafloor observation and sampling expeditions since the late 1990's and more recently a gas hydrate dedicated ODP leg in 2002, has focused on the surface and shallow subsurface gas hydrate system, seeking to characterize the distribution, concentration, and behavior of gas hydrates in an active margin setting.

Toward these recent efforts, the three manuscripts that comprise this dissertation are focused on the geologic setting hosting the gas hydrate system on Hydrate Ridge. Specifically, examining how active margin tectonic processes influence both the spatial and temporal behavior of the gas hydrate system at Hydrate Ridge and likely across the margin. Chapter II addresses the spatial distribution of pore fluid venting manifestations across a transect of the continental margin spanning the gas hydrate stability zone. The goals of this work were to determine the relationship of pore fluid venting sites across the hydrate stability zone to the underlying large scale geologic structures and the gas hydrate system centered at Hydrate Ridge. The major results indicate that authigenic carbonates and mud volcanoes are concentrated in areas of intense deformation in anticlinal structures like Hydrate Ridge. These structures serve to focus methane-rich fluids, resulting in abundant gas hydrates at the surface and in the shallow subsurface. In older, more dewatered portions of the wedge, the distribution of patches of authigenic carbonate, some with gas hydrates, and a field of pockmarks overlying a shallowing base

of gas hydrate stability in the subsurface, suggests diffuse fluid flow is likely occurring in this region and the pockmarks likely result from rapid gas escape during the destabilization of shallow gas hydrate deposits. These results are important because they characterize the nature of the gas hydrate/fluid venting system across a transect that spans the entire gas hydrate stability zone, encompassing several different structural environments. They also serve to focus several seafloor gas hydrate studies, including some of the ODP Leg 204 drill sites.

Chapter III examines the structural and tectonic evolution of the Hydrate Ridge region since the late Pliocene-early Pleistocene. This work serves to emphasize the complex history of accretion and deformation that occurs in an active margin setting hosting gas hydrate and also documents the structural evolution, including the interactions between thrust and strike slip faults, as the wedge was constructed through time. The results indicate Hydrate Ridge is a composite thrust ridge, formed from both seaward and landward vergent structures. The across-strike changes in structural vergence are linked to high pore fluid pressure caused by the rapid deposition of the Astoria fan sediments on the abyssal plain and the upward propagation of left lateral strike slip faults into the wedge. These strike slip faults have also been active through the accretionary process, resulting in the clockwise block rotation of Hydrate Ridge through time. The changes in structural vergence also help explain the variability in bathymetric relief across the region.

Chapter IV addresses the influence of the subduction zone earthquake cycle on the slope failure, and likely gas hydrate destabilization, frequency over the Holocene timescale at Hydrate Ridge. The results suggest earthquake-induced slope failure within the gas hydrate stability zone does occur at Hydrate Ridge and thus could represent a mechanisms for the mobilization of seafloor and subseafloor gas hydrates on a margin wide scale. This research has implications not only for the short term stability of seafloor and shallow subseafloor gas hydrate along the Cascadia margin, but also for the stability of gas hydrate in other active margin settings.

The first paper (Chapter II) entitled “Geophysical constraints on the surface distribution of authigenic carbonates across the Hydrate Ridge region” was published in November 2003 in the journal *Marine Geology*. The second paper (Chapter III) entitled “Structural vergence variation and clockwise block rotation in the Hydrate Ridge region, Cascadia accretionary wedge” will be submitted to the journal *Tectonics* for publication. The third paper (Chapter IV) entitled “Holocene slope failure in an active margin gas hydrate bearing region, Hydrate Ridge, Cascadia margin” will be submitted to the journal *Earth and Planetary Science Letters*.

Chapter II

Geophysical Constraints on the Surface Distribution of Authigenic Carbonates across the Hydrate Ridge Region, Cascadia Margin

Joel E. Johnson¹, Chris Goldfinger¹, and Erwin Suess²

1. Oregon State University, College of Oceanic and Atmospheric Sciences, 104
Ocean Admin. Bldg. Corvallis, Oregon 97331
2. GEOMAR Research Center for Marine Geosciences, 24148 Kiel, Germany

Johnson, J.E., Goldfinger, C., Suess, E., 2003, Geophysical Constraints on the Surface
Distribution of Authigenic Carbonates across the Hydrate Ridge Region, Cascadia
Margin. *Marine Geology*, 202, 79-120.

Abstract

On active tectonic margins methane rich pore fluids are expelled during the sediment compaction and dewatering that accompany accretionary wedge development. Once these fluids reach the shallow subsurface they become oxidized and precipitate cold seep authigenic carbonates. Faults or high porosity stratigraphic horizons can serve as conduits for fluid flow, which can be derived from deep within the wedge and/or, if at seafloor depths greater than ~300 m, from the shallow source of methane and water contained in subsurface and surface gas hydrates. The distribution of fluid expulsion sites can be mapped regionally using sidescan sonar systems, which record the locations of surface and slightly buried authigenic carbonates due to their impedance contrast with the surrounding hemipelagic sediment. Hydrate Ridge lies within the gas hydrate stability field offshore central Oregon and during the last 15 years several studies have documented gas hydrate and cold seep carbonate occurrence in the region. In 1999, we collected deep-towed SeaMARC 30 (SM30) sidescan sonar imagery across the Hydrate Ridge region to determine the spatial distribution of cold seep carbonates and their relationship to subsurface structure and the underlying gas hydrate system. High backscatter on the imagery is divided into three categories, (I) circular to blotchy with apparent surface roughness, (II) circular to blotchy with no apparent surface roughness, and (III) streaky to continuous with variable surface roughness. We interpret the distribution of high backscatter, as well as the locations of mud volcanoes and pockmarks to indicate variations in the intensity and activity of fluid flow across the Hydrate Ridge region. Seafloor observations and sampling verify the acoustic signals across the survey area and aid in this interpretation. Subsurface structural mapping and swath bathymetry suggest the fluid venting is focused at the crests of anticlinal structures like Hydrate Ridge and the uplifts along the Daisy Bank fault zone. Geochemical parameters link authigenic carbonates on Hydrate Ridge to the underlying gas hydrate system and suggest that some of the carbonates have formed in equilibrium with fluids derived directly from the destabilization of gas hydrate. This suggests carbonates are formed not only from the methane in ascending fluids from depth, but also from the shallow source of methane

released during the dissociation of gas hydrate. The decreased occurrence of high backscatter patches and the dramatic reduction in pockmark fields, imaged on the eastern part of the survey, suggests gas hydrate near its upper stability limit may be easily destabilized and thus, responsible for these seafloor features. High backscatter along the left-lateral Daisy Bank fault suggests a long history of deep-seated fluid venting, probably unrelated to destabilized gas hydrate in the subsurface.

Introduction

Pore fluid expulsion is a common process in accretionary wedges on active continental margins and is coincident with the dehydration and compaction of the sediment column during accretionary wedge development. Fluid expulsion can (1) be episodic along high-porosity stratigraphic horizons and/or faults exposed at the seafloor (e.g. Kulm et al., 1986; Lewis and Cochrane, 1990; Moore and Vrolijk, 1992; Sample, 1996; Sample and Reid, 1998), (2) occur during mud volcanism (e.g. Brown, 1990; Kopf, 2002), and/or (3) occur during diffuse, intergranular fluid flow (e.g. Moore and Vrolijk, 1992 and refs. there in). An abundant component in the fluids escaping from organic rich accretionary wedges is dissolved thermogenic and biogenic methane. When subjected to the lower temperature, lower pressure, and oxidizing bacteria-rich environment near the seafloor surface, these methane rich fluids can precipitate cold seep carbonates of aragonite, calcite, and/or dolomite compositions (Ritger et al., 1987; Greinert et al., 2001). In addition, some of this methane is temporarily incorporated as free gas into the gas hydrate fabric near the seafloor prior to expulsion (Suess et al., 2001), if at high enough gas concentrations and appropriate pressure (water depths at least 300m) and temperature (bottom water temperatures approaching 0° C) conditions (Kvenvolden, 1993).

Both surface and deep towed sidescan sonar surveys offer a unique method for regional mapping of seafloor fluid venting sites because the acoustic impedance contrast (density x sound velocity) between the authigenic carbonates precipitated at these sites and the surrounding hemipelagic sediments is detectable. Sidescan sonar surveys are

valuable because they provide a regional scale survey of seafloor fluid venting occurrences and distributions, and they also help guide later seafloor observation and sampling efforts conducted with manned submersibles, ROV's, tv-camera tows, and coring and dredging devices.

The first documentation of authigenic carbonates and chemosynthetic biological communities associated with pore-fluid expulsion on an active continental margin occurred at the first accretionary ridge west of Hydrate Ridge, offshore central Oregon (Fig. 2-1), in the mid-1980's (Suess et al., 1985; Kulm et al., 1986; Ritger et al., 1987). Since then, other sites along the Pacific rim have also been discovered (e.g. Henry et al., 1989; Le Pichon et al., 1992; Ohta and Laubier, 1987). The occurrence of authigenic carbonates on Hydrate Ridge was documented during ODP (Ocean Drilling Program) Leg 146 drilling in 1992 (see Westbrook et al., 1994), inferred from reprocessed GLORIA sidescan sonar imagery by Carson et al. (1994), and further constrained by submersible observations and seafloor sampling (e.g. Torres et al., 1999; Bohrmann et al., 2000; Greinert et al., 2001). Gas hydrates are also well developed at Hydrate Ridge and were first inferred on seismic reflection profiles collected as the site survey for ODP sites 891 and 892 (MacKay et al., 1992). The widespread distribution of the BSR (bottom simulating reflector), marking the base of gas hydrate stability (Hyndman and Spence, 1992), or the top of a free gas zone trapped beneath the hydrate (MacKay et al., 1994), suggests the ridge is capped by gas hydrate (Tréhu et al., 1999). The first recovery of gas hydrate on Hydrate Ridge occurred during ODP Leg 146 at site 892 (Hovland et al., 1995) when the crest of the northern summit was drilled through a hydrologically active fault (Fig. 2-1). Since then, several researchers have returned to collect samples of the gas hydrate and authigenic carbonates and to conduct other geophysical surveys to characterize the behavior of the hydrate system in this active tectonic setting (e.g. Torres et al., 1999; Bohrmann et al., 2000; Suess et al., 1999; 2001; Tréhu et al., 2002; this study). On Hydrate Ridge and in other accretionary ridges within the hydrate stability zone, a close association between gas hydrates and carbonates may exist because fluids

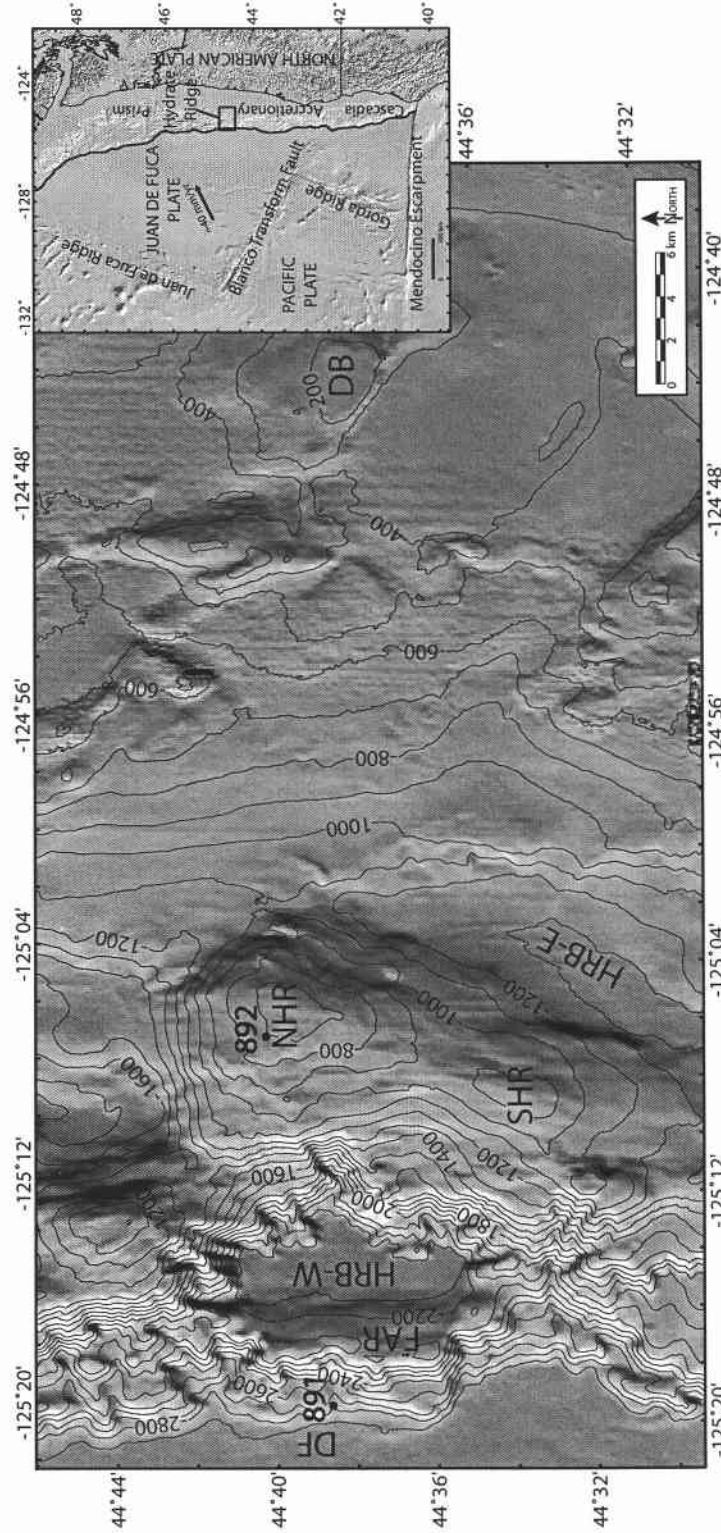


Figure 2-1. Shaded relief bathymetry of the Hydrate Ridge region. Contour interval is 100 m and bathymetric grid is 100 m pixel resolution. Inset shows Pacific Northwest bathymetry and topography (Haugerud, 1999) and the location of Hydrate Ridge region on the lower continental slope of the Cascadia accretionary prism. Hydrate Ridge is a NE-SW trending thrust ridge with northern and southern summits; (NHR) Northern Hydrate Ridge; (SHR) Southern Hydrate Ridge. The ridge is located ~10 km from the deformation front (DF) and bordered on the west and east by slope basins (HRB-W) Hydrate Ridge Basin-West and (HRB-E) Hydrate Ridge Basin-East. ODP (Ocean Drilling Program) site 891 on the crest of the first accretionary ridge (FAR) and site 892 on NHR are shown. Daisy Bank (DB) is also shown.

dewatered from the prism not only supply methane to the gas hydrate stability zone, but also transfer heat to shallower depths, which can induce the destabilization of the gas hydrate (Suess et al., 2001). On both the northern and southern summits of Hydrate Ridge, the authigenic carbonate and pore water carbon and oxygen isotopes support this association by suggesting the carbonates are precipitated in part from methane derived from destabilized gas hydrate (Bohrmann et al., 1998; Greinert et al., 2001). This observation suggests destabilized gas hydrate can contribute to the total accumulation of authigenic carbonate precipitated during accretionary wedge dewatering and compaction. With this in mind, an understanding of the regional distribution of subsurface structures (faults and folds) and the extent of the gas hydrate stability zone is necessary to make interpretations about the possible origins of fluid venting patterns interpreted on sidescan sonar records and observed on the seafloor.

Our recent research efforts have been focused on identifying the structural controls on the distribution of authigenic carbonates in the Hydrate Ridge region and their relationship to the underlying gas hydrate system. In this paper, we present the results of our 1999 SeaMARC 30 deep-towed sidescan sonar survey coupled with seafloor observations and samples and subsurface geologic mapping, based on seismic reflection data, to determine the distribution of authigenic carbonates and their relationship to large scale subsurface structures and the underlying gas hydrate system across the Hydrate Ridge region.

Tectonic Setting

Cascadia Accretionary Prism

The Juan de Fuca Plate is currently being subducted obliquely beneath the North American Plate along the Washington, Oregon, and Northern California continental margins (Fig. 2-1). The Cascadia accretionary prism evolved in response to this oblique subduction and is composed of folded and faulted abyssal plain turbidites and hemipelagic sediments (Kulm and Fowler, 1974). This oblique convergence also creates a right-lateral shear couple within the upper to lower continental slope and off the

Washington and Oregon margins nine WNW trending left-lateral strike-slip faults, antithetic to the shear couple, have been identified on the continental slope and abyssal plain (Goldfinger et al., 1992; Goldfinger et al., 1997). The accretionary wedge widens from 60 km off southern Oregon to 150 km off the northern Olympic Peninsula of Washington, where the thick Pleistocene Astoria and Nitinat Fans are presently being accreted to the margin. The active accretionary thrust faults of the lower slope are characterized by mostly landward vergent thrusts on the Washington and northern Oregon Margins and seaward vergent thrusts on the central and southern Oregon margin (Goldfinger et al., 1992; MacKay et al., 1992; MacKay, 1995). The landward vergent province may be related to the subduction of rapidly deposited and overpressured sediment from the Astoria and Nitinat submarine fans (Seely, 1977; MacKay, 1995). Off Washington and northern Oregon the broad accretionary prism is characterized by low wedge taper and widely spaced accretionary thrusts and folds, which offscrape virtually all of the incoming sedimentary section. Sparse age data suggest the prism is Quaternary in age and is building westward at a rate close to the orthogonal component of plate convergence (Goldfinger et al., 1996). This young accretionary wedge abuts a steep slope break that separates it from the oceanic and volcano-clastic Siletz terrane that underlies the continental shelf (Snively, 1987). Above this basement is a modestly deformed Eocene through Holocene forearc basin sequence (Snively, 1987; McNeill et al., 2000). Hydrate Ridge lies within the northern end of the seaward vergent province, offshore central Oregon, and is the second seaward vergent accretionary thrust ridge from the deformation front (Fig 2-1). It is bordered on east and west by slope basins, Hydrate Ridge Basin-East (HRB-E) and Hydrate Ridge Basin-West (HRB-W).

Structure of the Hydrate Ridge Region

The Hydrate Ridge region is a highly deformed portion of the accretionary wedge that results from oblique subduction-driven compression. The faults and folds in the region were initially mapped by Goldfinger et al. (1992; 1997) and MacKay, et al. (1992; 1995) and document the landward to seaward structural vergence change across the region as well as the presence of two deep-seated left-lateral strike slip faults (the Daisy

Bank and Alvin Canyon faults of Goldfinger et al., 1997). Using the same multichannel seismic data set presented in these papers and in Tréhu et al. (1999) across Hydrate Ridge, we have created a regional structure map that includes the previously mapped structures and the smaller scale folds and faults previously identified, but not correlated across the region (Figs. 2-2 and 2-3). Based on the mapped structures, Hydrate Ridge appears to be bound at its north and south end by the left-lateral strike-slip Daisy Bank and Alvin Canyon faults. The geometry and slip direction of these faults implies clockwise rotation of the block contained between them within an overall right-lateral shear couple (Goldfinger et al., 1997). Oblique subduction-driven right-lateral shear of the Hydrate Ridge block could be responsible for the apparent clockwise rotation of Hydrate Ridge (Johnson et al., 2000; Johnson et al., in prep). The eastern edge of the block occurs at the contact with the Siletz terrane, which forms a strong backstop for the accretionary prism (Fleming and Tréhu, 1999) and is likely the eastern edge of the right-lateral shear couple responsible for the strike slip faults. The concentration of tightly spaced structures at the north end of HRB-E, the apparent bulge in the abyssal plain proto-thrusts SW of Hydrate Ridge, the wider spacing of structures at the south end of HRB-E, and the decrease in abyssal plain protothrusts to the NW may serve as evidence for clockwise block rotation, however, in this paper we focus on the distribution of structures rather than their origins. Although the main fault or faults responsible for the formation of Hydrate Ridge are not imaged on the existing seismic reflection profiles, the asymmetric morphology of the ridge, with its more steeply dipping and eroded western flank, suggests it is cored by one or more seaward vergent thrust faults, similar to the thrust anticlines seen throughout the wedge and commonly observed in fold-thrust belts (Suppe, 1983). The greater relief of the northern summit of the ridge, compared to the southern summit, also suggests net slip along the underlying structures may be greater toward the north.

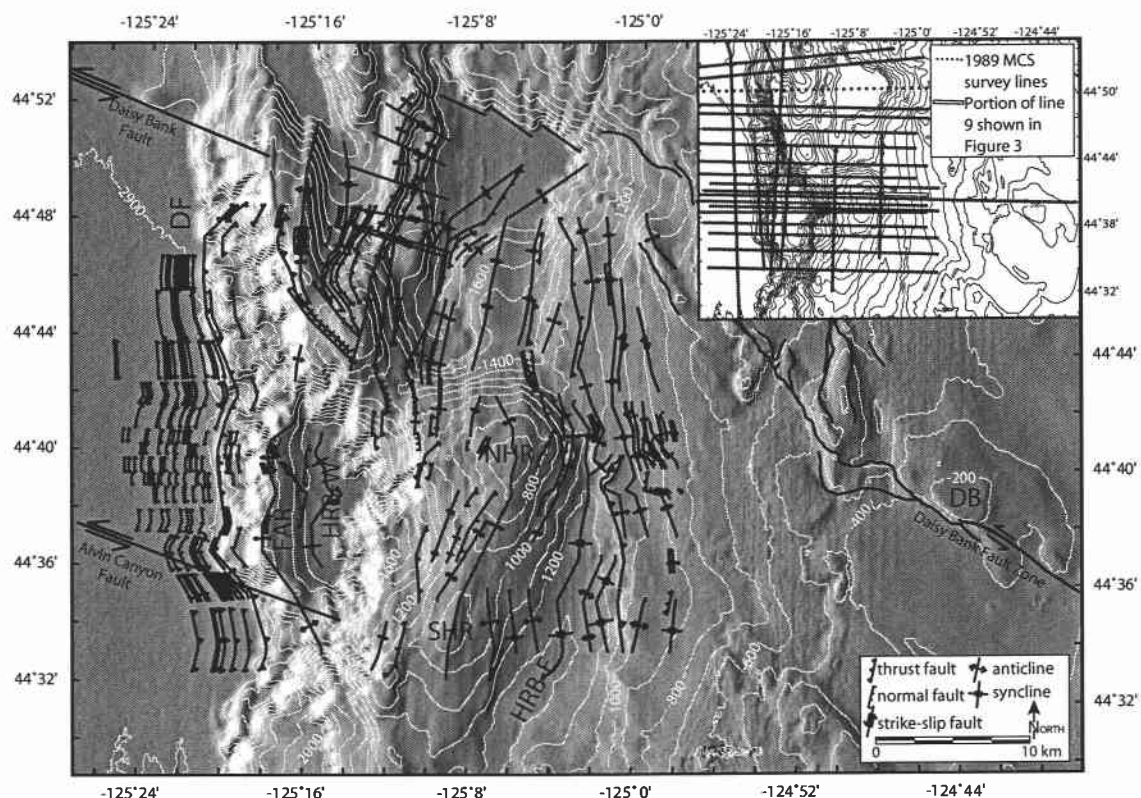


Figure 2-2. Structure map of the Hydrate Ridge region (interpreted from multichannel seismic reflection profiles collected as the site survey for ODP Leg 146, inset), overlain on 100 m shaded relief bathymetry. Deep-seated left-lateral strike-slip faults (Daisy Bank and Alvin Canyon faults) dominate the deformation north and south of Hydrate Ridge and thrusts and folds are common in the region between the strike-slip faults and the apparent clockwise rotation of Hydrate Ridge, suggests deformation may be influenced by oblique subduction-driven right-lateral shear. The eastern end of the Daisy Bank fault is mapped based on the previous work of Goldfinger et al. (1996) and the SM 30 sidescan sonar data presented in this paper. The major geologic and geographical features are labeled as follows; (DF) deformation front; (FAR) first accretionary ridge; (HRB-W) Hydrate Ridge Basin-West; (NHR) Northern Hydrate Ridge; (SHR) Southern Hydrate Ridge; (HRB-E) Hydrate Ridge Basin-East; (DB) Daisy Bank.

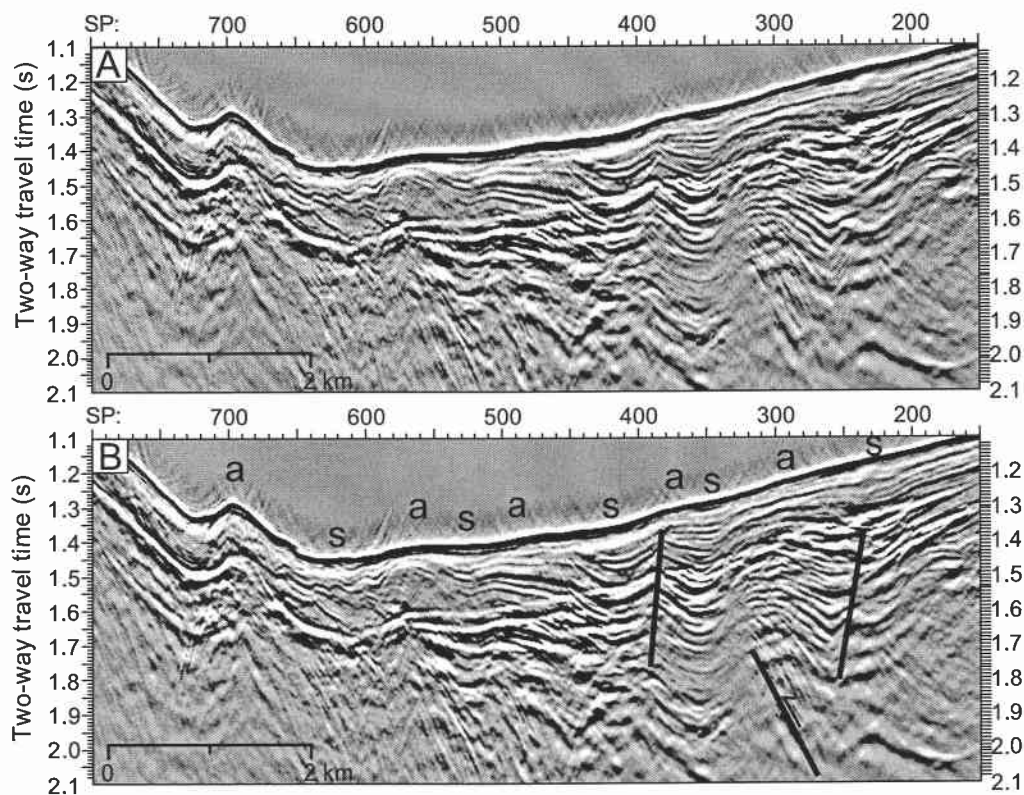


Figure 2-3. (A) Example section of a seismic reflection profile (line 9) from the ODP Leg 146 site survey (location shown in Fig. 2 inset). The data is time migrated and depicts relative true amplitudes. The amplitude scale grades from white to black. (B) Notice the small scale folds (a = anticline; s = syncline) and strike slip faults (sense of slip not detectible). A small thrust fault is also present. Variations in the degree of deformation across the Hydrate Ridge region can be seen by mapping these small scale features along with the previously mapped larger structures (Goldfinger et al. (1992;1997) and MacKay et al. (1992;1995). This line in particular shows the concentration of deformation near the NW corner of Hydrate Ridge.

Methods

Imaging the Carbonates

The observed authigenic carbonates present in the Hydrate Ridge region are exposed at the seafloor or slightly buried by a few centimeters of hemipelagic mud (Bohrmann et al., 1998; Kulm and Suess, 1990; Suess et al., 2001). Because of the acoustic impedance (density x sound velocity) contrast between the carbonates and the surrounding sediments, sidescan sonar can be used to image the distribution of authigenic carbonates across the region at the surface and in the shallow subsurface (Johnson and Helferty, 1990). In regions bearing seafloor gas hydrate, like Hydrate Ridge, there is also an acoustic impedance contrast between the gas hydrate and the surrounding hemipelagic sediments. Although, smaller than that due to carbonate, the impedance contrast between gas hydrate at the seafloor and hemipelagic sediments may be sufficient to produce an intermediate backscatter signal. Because of the limited bandwidth of current analog sonars and variations in the towfish depth during the survey, however, the sonar gain must be adjusted frequently, which makes post-cruise quantitative analysis of variations in backscatter strength problematic. Because of this, we do not attempt to differentiate between authigenic carbonates and seafloor gas hydrate of intermediate backscatter strength across the survey, except where confirmed by seafloor observations.

SeaMARC 30 Survey

To maximize our seafloor resolution and in order to image carbonates buried by a thin veneer of hemipelagic mud we chose the low frequency (30 kHz), deep-towed, SeaMARC 30 (SM 30) sidescan sonar system, operated by Williamson and Associates in Seattle, Washington. The sonar was towed at a depth of ~200 m above the seafloor and collected data in ~3.0 km swaths across the entire region and ~1.5 km swaths across the crest of Hydrate Ridge. The frequency on the port side is 27 kHz and on the starboard side 30 kHz. The gain of the sonar was adjusted manually in 10, 3dB steps to gain approximately equal record intensity across the survey. Navigation was by Sonardyne USBL (Ultra-Short BaseLine acoustic positioning). The R/V New Horizon was used to

tow the SM 30 at 2-3 knots. The sidescan images were acquired and processed using Triton Elics International (TEI) Isis sonar processing software, and ultimately georeferenced and gridded at 1 m pixel resolution for the entire survey using Erdas Imagine software. The survey was designed to image the surface and shallow subsurface authigenic carbonate and gas hydrate in the Hydrate Ridge region, spanning a corridor from the deformation front on the west to beyond the predicted upper hydrate stability limit (450-500 m; Tréhu et al., 2002) on the east. Included on the eastern edge of the survey was the SE extent of the Daisy Bank fault zone, a deep-seated left-lateral strike-slip fault, and likely fluid flow conduit, spanning here, just above the upper depth limit of hydrate stability (Goldfinger et al., 1996). Carson et al. (1994) attempted to remove the bathymetric signal from shallow-towed GLORIA regional sidescan data in an effort to constrain the extent of authigenic carbonate on Hydrate Ridge. These low frequency (6.5 kHz) GLORIA data can record deeply buried features, however, making surficial interpretations problematic. Nevertheless, our deep-towed SeaMarc 30 data support the general interpretations of Carson et al. (1994), but a much higher resolution and across not only Hydrate Ridge, but the slope and shelf to the east.

High Backscatter and Carbonates

The intensity of backscatter on sidescan sonar records is a function of (1) the angle of incidence of each beam (the bathymetric variations on the seafloor-the slope), (2) the physical characteristics of the surface (microscale roughness), (3) the intrinsic nature of the surface (composition-density) and (4) the frequency and pulse characteristics of the sonar (Blondel and Murton, 1997). One of the important effects on the backscatter signal received by the sidescan sonar is the effect due to bathymetric slope (1, above). Steep seafloor bathymetry sloping toward the passing sonar has enhanced backscatter strength compared to those slopes dipping away from the sonar. Because of this signal enhancement, differentiation between sediment types based on backscatter strength is best determined in regions of low slope. On Hydrate Ridge submersible dives, tv-camera tows, and seafloor samples (see *Groundtruthing the Sonar*

below) have documented that authigenic carbonates are present where bathymetric variation is minimal and high backscatter is dominant on the imagery. Similarly, across much of the survey, the seafloor slopes are less than 5° (see *Backscatter Patterns and Bathymetric Slope* below), suggesting high backscatter in these regions is more likely related to changes in rock and sediment composition on the seafloor rather than a bathymetric effect.

Results

Sidescan Sonar Survey

The complete mosaiced survey gridded at 1 m pixel resolution for both the ~3 km and ~1.5 km swaths is presented in Figure 2-4 (attached foldout). The E-W tracklines were collected in order from south (track 1) to north (track 11), beginning at the SE corner of the survey. All odd number tracklines were collected towing the sonar from east to west and even numbered tracks from west to east. Thus, at the overlap between tracklines the same geologic feature is imaged twice, but with insonification from opposing directions. At the overlap, the more detailed swath is generally shown. The 1.5 km swaths over the crest of Hydrate Ridge were towed NE-SW along the axis of the ridge. Dark gray to black lines along the centers of each trackline are the nadirs (no data recovery beneath the towfish). White thin continuous lines across the slope basin east of Hydrate Ridge are surface returns recorded by the sonar. Continuous high backscatter along the nadirs on E-W lines 6-8 is an artifact of the sonar.

Backscatter Patterns and Bathymetric Slope

Examination of the survey mosaic reveals the high backscatter patterns (light tones) generally can be divided into three categories; (I) circular to blotchy with apparent surface roughness, (II) circular to blotchy with no apparent surface roughness, and (III) streaky to continuous with variable surface roughness (Figure 2-4 attached foldout). Category I high backscatter is concentrated mainly on the northern summit and NE end of Hydrate Ridge and to a lesser extent on the southern summit of Hydrate Ridge. Category II high

backscatter is concentrated on the eastern edge of HRB-E, and eastward up to the 700 m bathymetric contour. It also extends spatially from north to south across the entire survey in this region. Category III high backscatter is present on the western edge of the survey in regions of steep bathymetry associated with the large submarine canyon and steep slopes on the western flank of Hydrate Ridge, and in the SE corner of the survey, associated with subtle breaks in slope. Category III high backscatter is also present along the Daisy Bank Fault Zone to the northeast.

To determine the effect of slope on the backscatter intensity, a slope map was created from 50 m gridded bathymetry, which is the highest resolution grid available across the entire survey area (Fig. 2-5). Newly acquired high resolution EM300 data across Hydrate Ridge and HRB-E (from Clague et al., 2001), EM120 data across HRB-W, and EM300 from HRB-E to Daisy Bank (collected by the authors in 2002) are the three primary data sets used in this bathymetric grid. Additional bathymetric data sets (EM300 and EM120 swaths from Jack Barth at Oregon State University and lower resolution data sets, NOAA EEZ SeaBeam 16 and National Ocean Service hydrographic soundings) were used to fill in gaps in coverage. The inclusion of lower-resolution data in the grid limits the resolution to 50 m, however, yields coverage coincident with the SM 30 survey. Examination of bathymetric slope reveals much of the high backscatter (Category I and II) on Hydrate Ridge, HRB-E, and the seafloor west of Daisy Bank occurs in regions with the lowest slope, $<10^\circ$, mostly $<5^\circ$. The high backscatter observed in regions with the highest slope, on the western edge of the survey where slopes exceed 15° surrounding HRB-W and along some of the Daisy Bank fault uplifts, is likely enhanced by the steep bathymetry. The only major exception to this is observed on some of the low slope, high-to-moderate backscatter seen on the flat-topped ridges of the Daisy Bank Fault zone (Figs. 2-4 attached foldout and 2-5; see *Groundtruthing the Sonar* below). With the slope effect to the backscatter intensity minimized in regions of low slope, the backscatter can be interpreted to result from contrasts in surface roughness and/or harder or denser sediment composition across the survey.

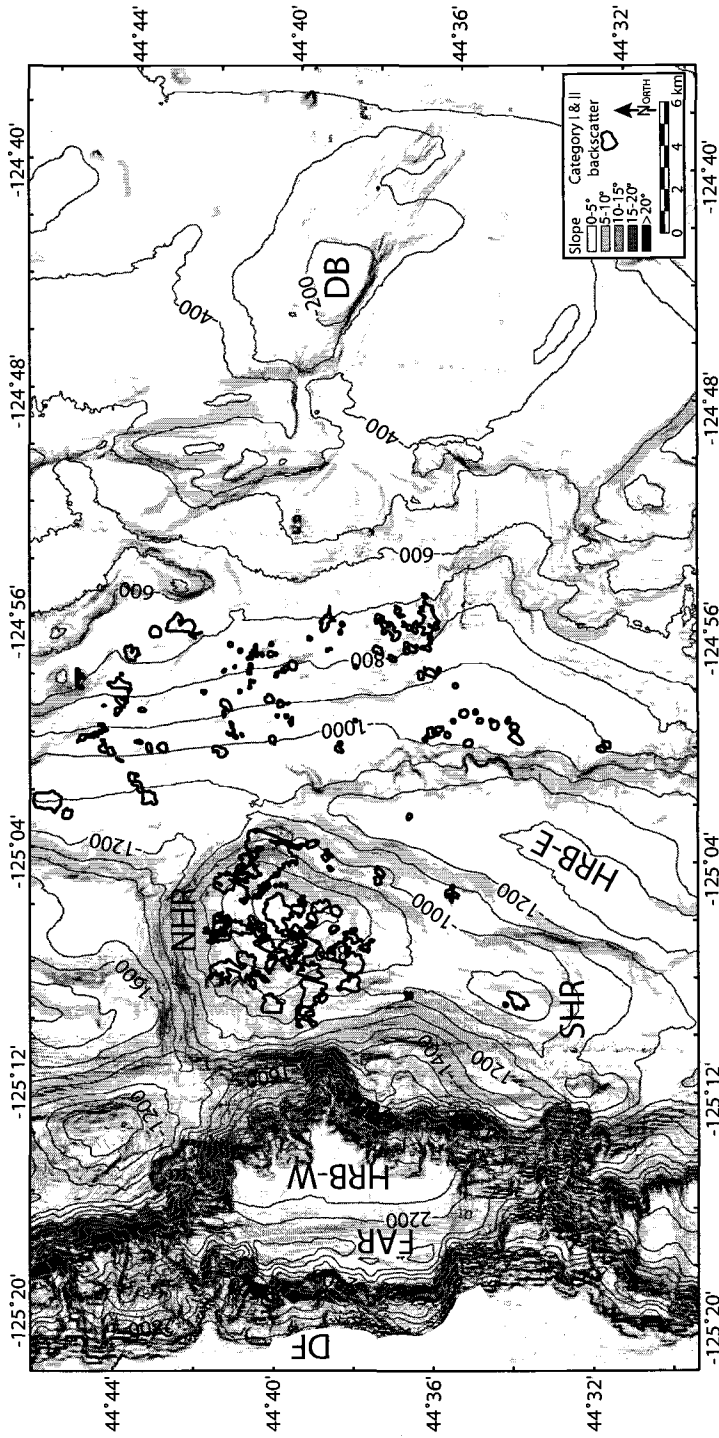


Figure 2-5. Slope map of the Hydrate Ridge region created from swath bathymetric data gridded at 50 m (see *Backscatter Patterns and Bathymetric Slope* for data sources). Slope variations were calculated from the 50 m grid using Erdas Imagine software. Slopes are shaded in 5-degree increments. Category I and II backscatter patches are outlined in black. Notice the coincidence of the backscatter with the regions of lowest slope. Category III backscatter occurs in the low slope regions only on the tops of uplifts associated with the Daisy Bank Fault zone. The coincidence of high backscatter with low slope suggest the backscatter signal is most likely due to changes in surface roughness and sediment composition rather than bathymetry.

Groundtruthing the Sonar

Category I Backscatter-Hydrate Ridge

Samples from the seafloor and deep-towed video camera data (Bohrmann et al., 1998; Greinert et al., 2001; Suess et al., 2001) as well as Alvin observations (Torres et al., 1999) on both the northern and southern summits of Hydrate Ridge have confirmed the presence of extensive authigenic carbonates and gas hydrates. During R/V Sonne Legs 143-1, 2, and 3, deep towed tv-cameras, termed OFOS (Ocean Floor Observation System) and TVG's (tv-guided grab samplers) were deployed across the Hydrate Ridge region (Fig. 2-6a). A graphic log representing the video observations along OFOS track 216 is shown in Figure 2-6b. We observe a close correlation between high backscatter on the sidescan sonar and the slabs, cobbles, and boulders of authigenic carbonates observed in the OFOS videos along all three tracks, 216, 213 and 223 (Fig. 2-6a). OFOS track 223 documents carbonate only near the crest of Hydrate Ridge, where the backscatter is of intermediate intensity but the pattern resembles a pavement of carbonate that extends well into the saddle between the south and north summits (Fig. 2-6a). In all of the TVG samples shown (Fig. 2-6a), authigenic carbonates were also recovered from the seafloor, again coincident with locations of high backscatter.

Observations made during five Alvin dives on the northern summit of Hydrate Ridge resulted in a map of the bottom types, characterizing the seafloor as consisting of massive carbonates, mostly carbonates, mixed sediments and carbonates, sediments, or clams and/or microbial mats (Torres et al., 1999; Fig. 2-6c). On the southern summit of Hydrate Ridge, six Alvin dives resulted in the discovery of a very large carbonate chemoherm pinnacle, which stands nearly 50 m above the seafloor (Torres et al., 1999). The dive sites were concentrated at the largest high backscatter patch on the southern summit of Hydrate Ridge. In the middle of this patch, the acoustic shadow cast by the large pinnacle carbonate can be seen (Figs. 2-4 attached foldout; 2-6a and d). Investigation by Alvin of the intermediate intensity backscatter present northeast of the pinnacle resulted in the identification of gas hydrate at the seafloor, which was previously sampled with

Figure 2-6. (A) SeaMARC 30 coverage and ground truth across Hydrate Ridge. TVG (tv-grab) and OFOS (tv-camera tow) tracks from Sonne Leg 143 are shown. Mud volcanoes MV1, MV2, and MV3 are shown (see *Other Fluid Venting Manifestations*) as well as the Southern Hydrate Ridge (SHR) pinnacle (note the acoustic shadow on the imagery). The intermediate backscatter on SHR represents seafloor gas hydrate as observed in ALVIN dives (Torres et al., 1999). (B) OFOS track 216 across NHR (from Bohrmann et al., 2000). The diagram was constructed from deep towed video observations of the seafloor. Note the coincidence of the chemoherm carbonates and carbonate crusts with the regions of highest backscatter along the track. (C) A bottom type map constructed from ALVIN observation on NHR (from Torres et al., 1999). Again note the coincidence of high backscatter on the survey and the carbonates observed on the seafloor. (D) ALVIN photograph of the carbonate on the SHR pinnacle (photo courtesy of Marta Torres, Oregon State University). Notice the large fracture in the middle of the image.

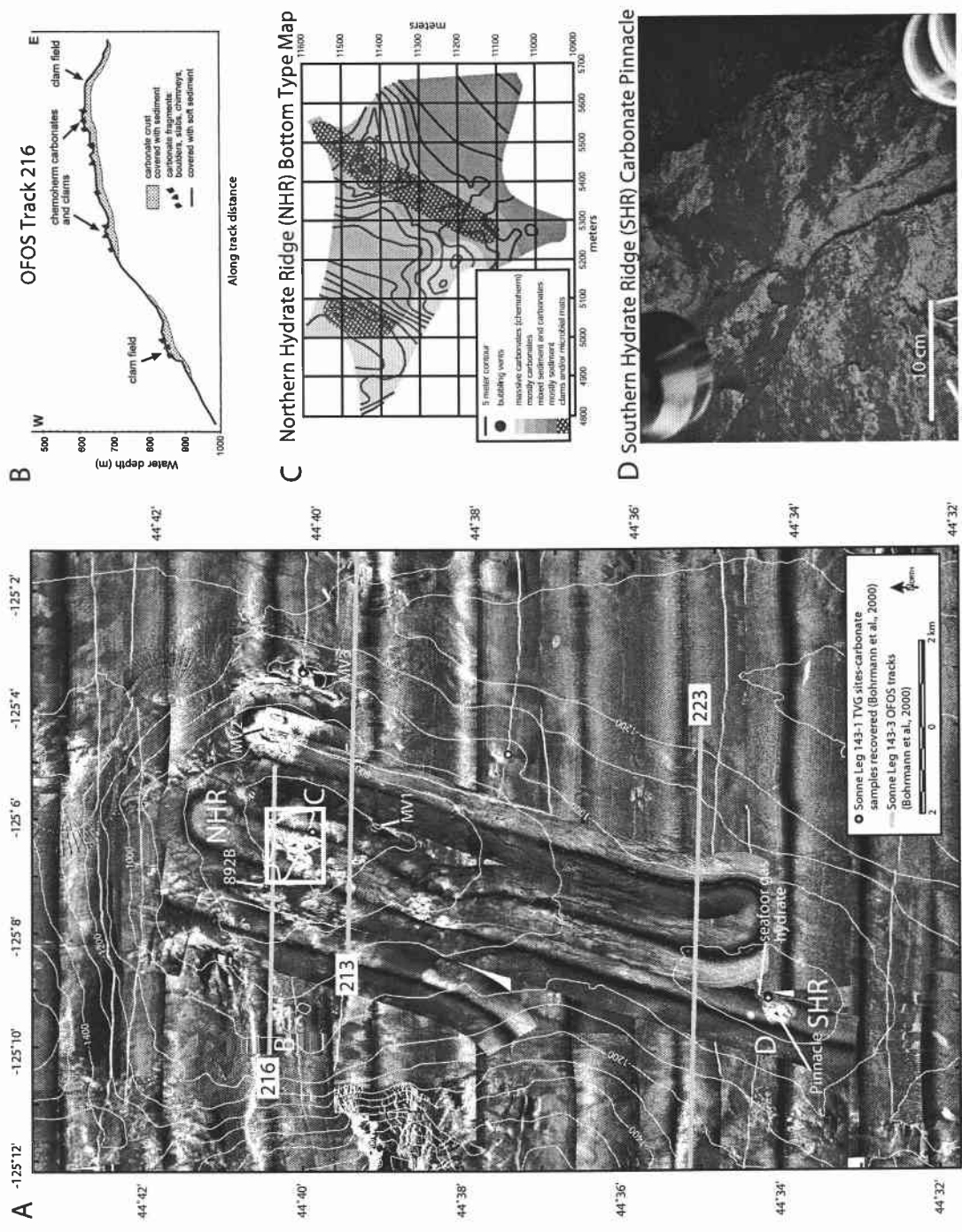


Figure 2-6.

a large TVG (Suess et al., 1999). This suggests the sidescan sonar may have imaged seafloor gas hydrate here and recorded it with intermediate backscatter intensity (Fig. 2-6a), alternatively, the intermediate backscatter could be caused by slightly buried authigenic carbonate not recovered by the TVG. During the same Alvin dives, the small high backscatter circle northwest of the pinnacle was also investigated, however no carbonate or gas hydrate was observed at the seafloor surface (Torres et al., 1999). We suggest sediments cover the authigenic carbonate or hydrate likely responsible for this acoustic signal, as the SM30 has previously imaged objects of high impedance contrast buried by several meters of soft sediment (M. Williamson, personal communication, 1999).

Category II Backscatter-Eastern Slope Basin

Tv-camera tows conducted in 1999 across some of the high reflectivity category II backscatter patches indicated only sediments and bacterial mats at the surface, suggesting carbonates and/or hydrates if present here are buried beneath a thin veneer of sediment (Fig. 2-7a). A tv-camera tow conducted during the R/V Sonne (SO148) cruise in 2000 however, documented bacterial mats, clam fields, and some authigenic carbonates present at the seafloor in this same region (Fig. 2-7a). In addition to the tv-camera tows, three category II circular backscatter patches were cored (by gravity or multicorer) during R/V Sonne cruises SO143 and SO148 (Fig. 2-7a). All of the cored sites showed unusually high methane contents in the sediment compared to a reference site (SO143-63-1A-MUC) in the center of the basin (Fig. 2-7a,b, and c). There appears to be a qualitative relationship between the brightness of the circular patches in the sidescan sonar image and the methane distribution with depth in cores. The highest methane content was recorded at the bright patch at site SO143/35-1-SL with almost 1000 nmol/g within the first 100 cmbsf, whereas the reference site in the center of HRB-E barely exceeds 1 nmol/g (Fig. 2-7b). At the dark patch (sites SO143/32-2-SL and SO143/31-1A-MUC) the methane content gradually increased towards 10 nmol/g in the shallow part, but exceeded 200 nmol/g at >500 cmbsf (Fig. 2-7b and c). The brightest patch (site SO148/75-1B-MUC) showed by far the highest near-surface methane concentration

Figure 2-7. (A) SeaMARC 30 coverage at the western edge of HRB-E. Notice the circular category II high backscatter patches. Tv-camera tow tracks and the gravity and multicorer sites described in the text are shown. (B) Methane distribution in surface sediment multicorer samples taken at some of the backscatter patches shown in (A). Samples taken at a bright backscatter patch (SO148/75-1B-MUC) yielded high methane, at a dark backscatter patch (SO143/31-1A-MUC) lower methane, and at a low backscatter reference site, at the center of HRB-E (SO143/63-1A-MUC), an even lower methane concentration. (C) Methane distribution in two surface sediment gravity core samples (locations shown in A). High methane was found in both gravity core samples; one taken from a dark backscatter patch (SO143/32-2-SL) and a second from a bright backscatter patch (SO143/35-1SL). Gravity core (SO148-76-SL) taken at a very bright backscatter patch recovered carbonates and gas hydrates. Tv-camera tow track SO148/9 also documented authigenic carbonate at the surface (on the same backscatter patch sampled by gravity core SO148/76-SL). The remaining tv-camera tows documented only sediments and bacterial mats at the surface, suggesting that some of the high backscatter patches may be caused by authigenic carbonates and/or gas hydrates slightly buried by hemipelagic sediment.

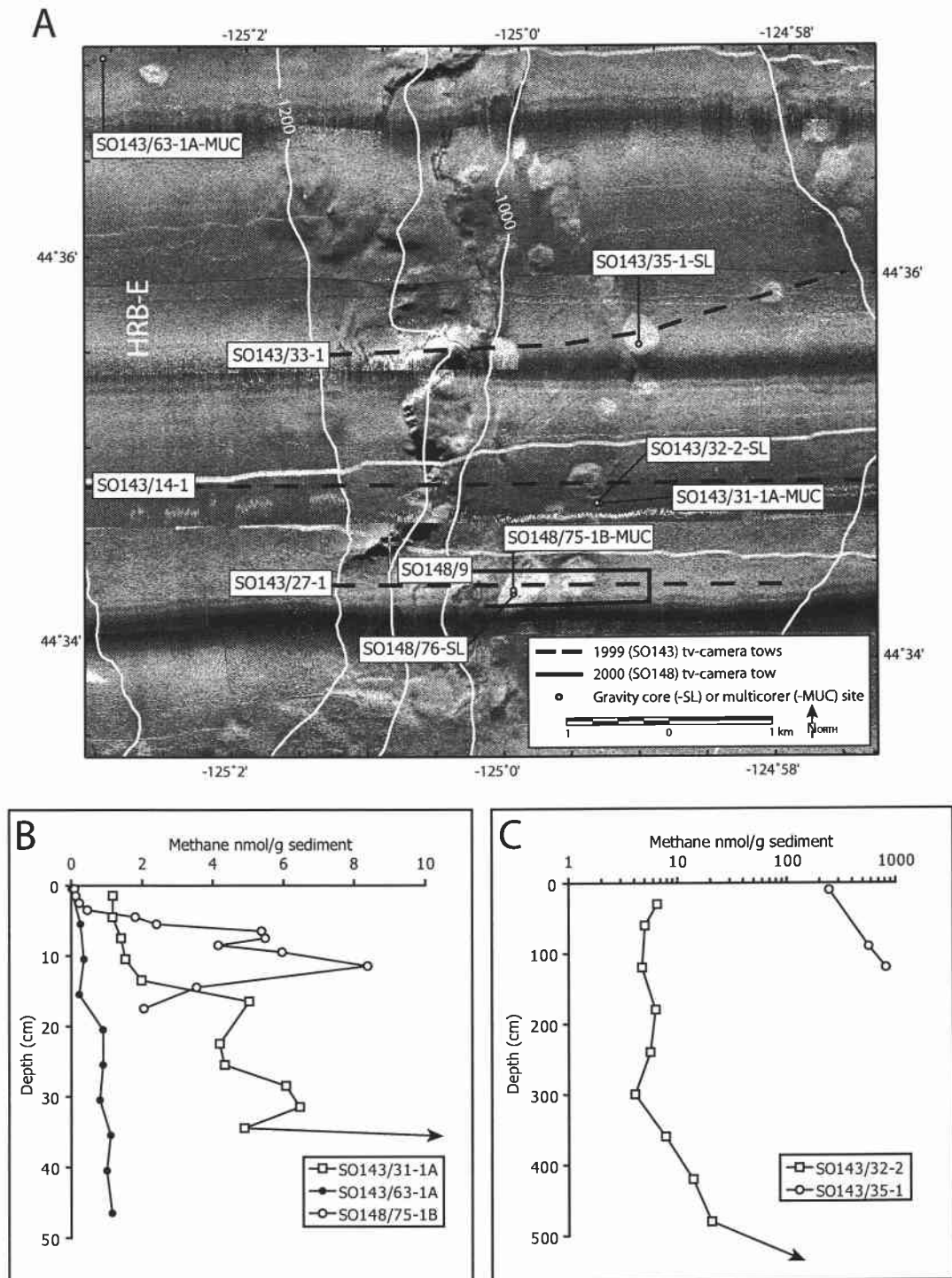


Figure 2-7.

(~8 nmol/g at 10 cmbsf) and at greater depth, reached by gravity coring (SO148/76-SL), contained disseminated gas hydrates and authigenic carbonates. Although limited sampling and seafloor observations have occurred across the entire category II backscatter region (Fig. 2-4 attached foldout), the similar shape and backscatter intensity of the circular patches suggests they may represent authigenic carbonate, as they appear to have the same backscatter strength as the known carbonates on the crest of Hydrate Ridge. The lack of visible surface roughness and blurry nature of the circular patches, however, may indicate many of them are buried by thin drape of hemipelagic sediment. The close association of the authigenic carbonates and gas hydrates recovered in gravity core SO148-76-SL also suggests gas hydrates may be present at many of the category II circular patches.

Category III Backscatter-Daisy Bank

Category III high backscatter sites are coincident with regions of high slope (Figs. 2-4 attached foldout and 2-5), however, a major exception to this occurs on the flat topped ridges associated with the Daisy Bank Fault zone (Fig. 2-4 attached foldout). Seafloor observations by the Delta submersible document abundant carbonate chimneys, doughnuts, and slabs, within 100-150 m of the fault traces and tabular carbonate blocks up to 6 m in length on the top of Daisy Bank (Goldfinger et al., 1996). Recent examination of the 1992 Delta submersible dive videos with the new SM30 sidescan data indicates the extensive high-to-moderate backscatter with apparent surface roughness observed on the top of Daisy Bank is due to cobbles, blocks, and slabs of well-lithified sediments and carbonates (Fig. 2-8). Although the uplifts associated with the Daisy bank fault NW of Daisy Bank have higher backscatter than the top of Daisy Bank, the slope effect due to their steep sided, linear nature, likely enhances some of their backscatter signal, even though lithologically they may be similar to Daisy Bank.

Other Fluid Venting Manifestations

Also present on the crest of Hydrate Ridge and along its northeastern flank are three mud volcanoes, MV1, MV2, and MV3 (Fig. 2-9). The circular craters at the centers

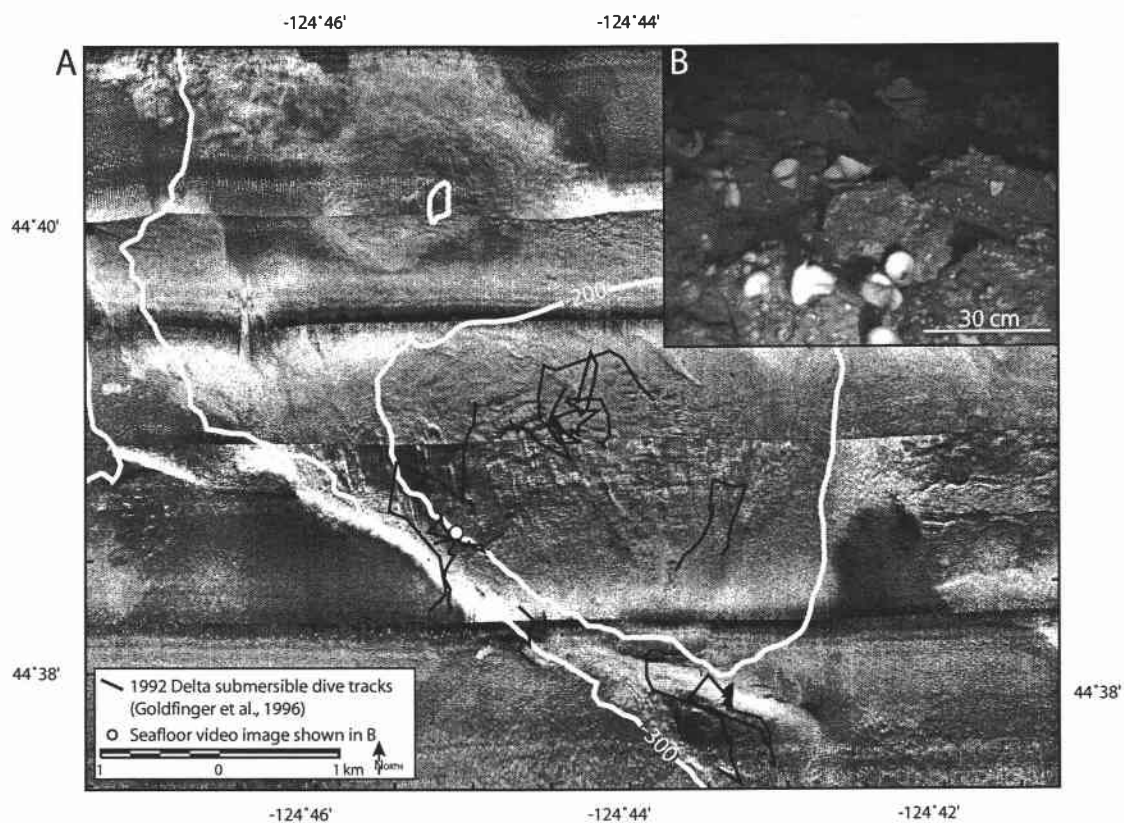


Figure 2-8. (A). SeaMARC 30 coverage across Daisy Bank. 1992 Delta submersible dives tracks are shown. Video observations from the dives document cobbles, blocks, and slabs of well-lithified sediments and carbonates (B, inset) on the nearly flat top of Daisy Bank, coincident with the apparent surface roughness and moderate backscatter observed on the SM30 survey.

of mud volcanoes MV1 and MV3 are clearly visible on the sidescan imagery, however, MV2 is less obvious because of the high backscatter caused by the surrounding carbonates, but a circular crater associated with this high backscatter is visible on high resolution bathymetry (Clague et al., 2001). Mud volcanoes are one of several types of surface expressions of mud intrusions, which occur as overpressured, multiphased pore fluids (methane and water) and sediments are expelled at the seafloor surface (Brown, 1990). The two mud volcanoes present near the crest of Hydrate Ridge (MV1 and MV2) are coincident with the abundant carbonate chemohalms documented on the northern summit of the ridge, while the mud volcano on the eastern flank of the ridge (MV3) has breached the crest of a smaller secondary anticline (Fig. 2-9). The two northern mud volcanoes (MV2 and MV3) show high backscatter on the sidescan imagery, perhaps suggesting methane rich fluids were expelled during their eruption and consequently oxidized to precipitate carbonate (Fig. 2-9). The more southerly mud volcano imaged with more subdued backscatter is coincident with the general decrease in backscatter toward the saddle region of Hydrate Ridge.

Active fluid venting in the form of hydrate-coated bubbles has also been observed on both the northern and southern summits of Hydrate Ridge during Alvin dives (Torres et al., 1999) and tv-camera tows (Suess et al., 1999) and acoustically imaged in 12 and 18 kHz subbottom profiles (Torres et al., 1999; Bohrmann et al., 2000; Heeschen et al., 2003). Methane has also been measured in high concentrations plumes in the water column above Hydrate Ridge (Suess et al., 2001).

Additional evidence for fluid or gas escape, imaged on the SM30 survey, is present in the central to eastern region of the survey as a band of pockmark fields (Fig. 2-10). The pockmark fields are limited on their eastern side by the ~550 m contour and on the western end by the ~1050 m contour. Some of the pockmarks are coincident with the locations of category II high backscatter and others appear to be isolated in lower backscatter sediments.

Figure 2-9. SeaMARC 30 coverage and structures across Hydrate Ridge. The three mud volcanoes (MV1, MV2, and MV3) are present on Northern Hydrate Ridge (NHR). MV2 and MV3 are associated with high backscatter suggesting carbonate precipitation during expulsion. MV2 does not appear to be associated with high backscatter, which is consistent with an overall decrease in patchy backscatter toward the saddle region. Notice MV3 breaches the crest of an anticline on the eastern flank of Hydrate Ridge and MV1 and MV2 exist near the crest of NHR. The acoustic shadow of the Southern Hydrate Ridge (SHR) pinnacle is visible as a black speck in the middle of the largest backscatter patch on SHR. The saddle region between NHR and SHR appears highly fractured, perhaps a result of extension at the crest of Hydrate Ridge.

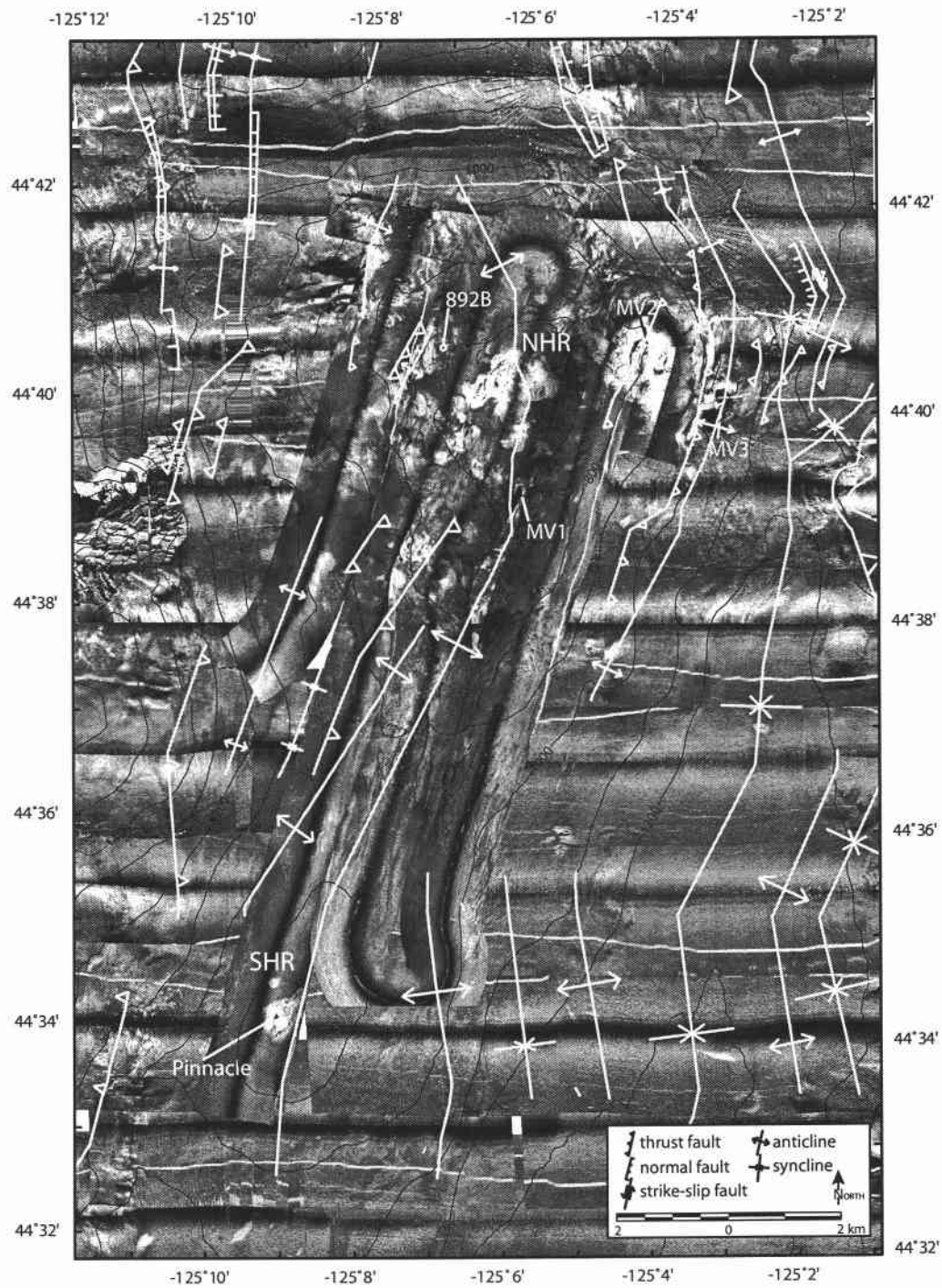


Figure 2-9.

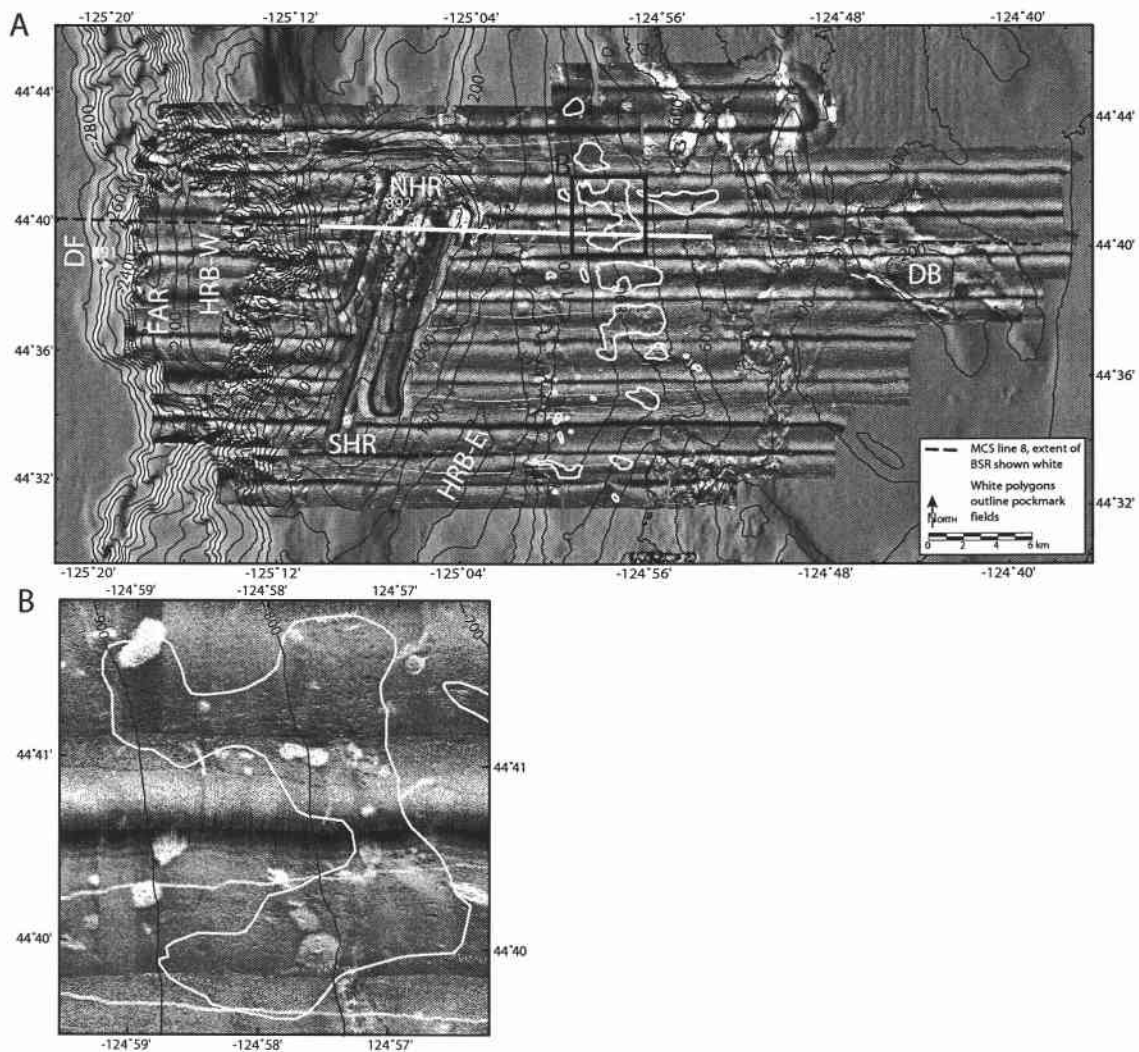


Figure 2-10. (A) SeaMARC 30 complete survey coverage. The pockmark fields and the extent of the BSR are shown. The easternmost pockmark field extends to the ~550 m contour and is coincident with the termination of the BSR at nearly the same depth. This suggests the pockmark fields may represent the gas hydrate stability limit near the eastern part of the survey. Also notice the abrupt termination of most of the pockmark fields and Category II backscatter patches at the 700 m contour (see *Landward Limit of Gas Hydrate Stability* for discussion). (B) Close up image of one of the pockmark fields (location shown in A).

Discussion

Backscatter Distribution

Confirmation of the backscatter patterns on Hydrate Ridge by abundant seafloor observations makes them the most well-constrained features in the survey. In addition, the highest level of detail can be seen by looking at the 1.5 km swaths, which only cover the top of Hydrate Ridge (Fig. 2-4 attached foldout). Examination of this imagery in particular reveals the variations in backscatter strength and seafloor features from the northern to the southern summit of the ridge. The northern summit is characterized by extensive authigenic carbonate chemohierms and gas hydrates of high to intermediate backscatter intensity and the surface of the ridge appears to break apart toward the saddle region, between the two summits, coincident with a dramatic decrease in large carbonate chemohierms. The carbonates appear to become reestablished, to a much lesser degree, toward the southern summit and result in the large pinnacle structure (Fig. 2-4 attached foldout).

Category I and II high backscatter patterns are both blotchy to circular and only differ in their apparent surface roughness. They are both also only present in the regions of the survey where gas hydrate is either inferred by the presence of the BSR (Tréhu et al., 1999; Tréhu and Flueh, 2001) or confirmed by recovered samples (Hovland et al., 1995; Suess et al., 2001). On Hydrate Ridge the apparent surface roughness of the category I high backscatter has been groundtruthed by Alvin, deep towed video observations, and seafloor samples and is likely due to the fresh exposure of the authigenic carbonates and gas hydrates on the seafloor. In contrast to the erosional environment of Hydrate Ridge, the eastern slope basin and region to the east likely have a higher sedimentation rate, which may tend to bury authigenic carbonates and hydrates precipitated near the seafloor surface. This could explain the smooth texture and the variable backscatter intensity of the category II high backscatter sites in these regions. Seafloor observations and core also suggests at least some of the category II high backscatter sites contain authigenic carbonate and gas hydrate buried by hemipelagic sediments. The similar nature of the category II backscatter

patches across the survey suggests they may all have this same composition, however, with only a few of the category II backscatter sites investigated at the seafloor, further groundtruthing in the central and eastern part of the survey is needed to truly verify their compositions.

Relationship to Geologic Structures

Hydrate Ridge Region

The pattern of extensive authigenic carbonates, the presence of three mud volcanoes, and observed seafloor gas discharge suggests fluid venting is highly concentrated on northern Hydrate Ridge. Structurally, the northern summit is shallower, at a ~600 m depth, than the southern summit, at ~800 m. This difference in bathymetry suggests the ridge is effectively plunging to the southwest creating a structural trap at the northern summit for any fluids and gases to migrate toward and accumulate. A large accumulation of free gas is inferred beneath the northern summit of Hydrate Ridge based on seismic velocity and attenuation (Tréhu and Flueh, 2001) and it is this pool of gas, which likely supplies the gas hydrate-authigenic carbonate system in the near surface sediments. The extensive occurrence of authigenic carbonates on the northern summit suggests it has either recorded a longer history or a higher rate of methane expulsion than that recorded by the southern summit. U/Th ages from northern summit authigenic carbonates may indicate a long history of methane expulsion is more likely, as samples of the carbonate carapace there yield ages between 68,700 and 71,700 years, while samples from the southern summit pinnacle range in age from 7,300 to 11,400 years (Teichert et al., in press). The conduits for methane expulsion at the northern end of the ridge could be faults and fractures, similar to those imaged on the 1.5 km swath sidescan data in the saddle between the northern and southern summits of Hydrate Ridge (Fig. 2-9). Perhaps, some of these conduits are bending moment normal faults created during flexure at the crest of Hydrate Ridge. Bedding parallel faults created during flexural slip folding, out of sequence thrust faults, or high porosity stratigraphic horizons could also serve as conduits. Unfortunately, details of the shallow subsurface structure at the crest of

Hydrate Ridge cannot be resolved on the existing seismic reflection data, so the true nature of the conduits can only be speculated at this time. The important observation, however, is that the carbonates appear to be well developed at the northern summit of Hydrate Ridge, where concentrated structural deformation is likely. The first accretionary anticline just west of Hydrate Ridge shows abundant evidence for fluid expulsion at its crest (Kulm and Suess, 1990) and the location of the mud volcano (MV3) on the eastern flank of the northern summit of Hydrate Ridge also coincides with the crest of a smaller anticline (Fig. 2-9). These associations suggest anticlinal folding may help to focus fluids until faults or fractures, potentially caused by the folding, or exposed high porosity stratigraphic horizons create the conduits needed for subsequent fluid expulsion. Future correlation of the high backscatter sites on Hydrate Ridge with higher resolution seismic reflection data, however, will ultimately yield better insight to these processes.

Daisy Bank Fault Zone

Most of the category III high backscatter sites are coincident with high slope, however a major exception to this occurs on the flat topped ridges associated with the Daisy Bank Fault zone (Fig. 2-4 attached foldout). High backscatter along the fault scarp and uplifts along the fault zone suggest either authigenic carbonate presence or an older more lithified and uplifted section of the stratigraphy capable of high backscatter, or a combination of the two. Seafloor observations in the *Delta* submersible document abundant carbonate chimneys, doughnuts, and slabs, within 100-150 m of the fault traces and tabular carbonate blocks up to 6 m in length on the top of Daisy Bank (Goldfinger et al., 1996). Authigenic carbonates have also been observed at the Wecoma left-lateral strike-slip fault to the north and isotopic measurements on them suggest the fluid source is deep within the sedimentary section (Sample et al., 1993). The high backscatter at Daisy Bank is shallower (200 m) than the predicted hydrate stability zone (~450-500 m; Tréhu et al., 2002), and like the Wecoma fault, it likely taps a deeper methane source to precipitate the carbonates present near the seafloor surface. A long-term history of structurally

controlled deep fluid venting along the Daisy Bank Fault is also suspected due to the pervasive high backscatter present along its length. Such a large active fault conduit is likely to deliver a significant volume of fluid to the seafloor surface, perhaps accommodating much of the regional dewatering of the accretionary wedge. These focused fluids, once expelled, result in the significant carbonate precipitation observed on the seafloor and inferred by the high backscatter along the fault zone.

HRB-E and Eastern Slope

Highly focused fluid flow is evident on Hydrate Ridge and along the Daisy Bank Fault, however, in the region between these structures the backscatter pattern is much more diffuse (Fig. 2-4 attached foldout). Category II high backscatter, circular to blotchy with no apparent surface roughness, dominates the region along the eastern edge of HRB-E and eastward toward the Daisy Bank fault zone. The association between the pattern of fluid venting and bathymetry suggests some of the high backscatter patches may be coincident with abrupt changes in slope, perhaps caused by small amplitude folds in the subsurface (similar to those shown in Fig. 2-3). Much of the category II backscatter, however, appears as small, scattered patches in areas of low slope across the region, suggestive of low volume diffuse fluid venting. The coincidence of the category II backscatter with the hydrate stability zone may indicate fluid venting is associated with shallow disruptions in the underlying gas hydrate system. The lack of significant surface roughness on the category II high backscatter, however, and subtle variations in backscatter strength suggests these features may be buried by variable amounts of hemipelagic sediment. This may indicate that either (1) fluid venting is currently not active at some of the sites across the region (where the backscatter is circular but of intermediate reflectivity), (2) fluid venting and carbonate precipitation are continuous, but occur at a slower rate than hemipelagic sedimentation, or (3), there is an episodic nature to the fluid venting, permitting active fluid escape at some sites (e.g. the highest backscatter sites) while abandoning others (e.g. intermediate backscatter patches, possibly covered by hemipelagic sediment since their last activity). We suggest the apparent variability in fluid venting and authigenic carbonate

precipitation across the eastern slope could be attributed to disruptions in the subsurface gas hydrate system. In this region, perhaps larger faults at depth are responsible for the delivery of pore fluids to the gas hydrate stability zone within the upper seafloor sediments. Once there, the fluids only escape by (1) direct fault conduits to the seafloor, which seem unlikely here since there are few linear manifestations of fluid venting, (2) rapid fluid expulsion, resulting in pockmarks on the seafloor, or (3) diffuse fluid flow, through high porosity conduits or microfractures. We suggest the latter two processes occur across this region, as circular high backscatter patches can be seen associated with pockmarks (Fig. 2-10) and high porosity conduits are likely in a wedge characterized by turbidite sedimentation (Kulm and Fowler, 1974).

Landward Limit of Gas Hydrate Stability

Pockmarks terminate near the eastern end of the survey area at ~550 m, coincident with the eastern extent of the BSR, as interpreted on the only multichannel seismic reflection profile (line 8) that extends this far east from the ODP Leg 146 site survey (Fig. 2-10). This suggests the pockmarks may represent the surface manifestation of gas hydrate dissociation near the landward limit of gas hydrate stability in this region. Because pockmarks typically result from rapid fluid or gas escape through a relatively thin sedimentary section (Brown, 1990) the shallow source of methane in gas hydrate near its stability boundary may be a likely source for this fluid expulsion. The ~550 m contour corresponds with only the easternmost pockmark field on the survey. Most of the pockmark fields appear to terminate at the ~700 m contour to the west, coincident with the abrupt termination of category II backscatter (Fig. 2-10). The coincidence of the termination of the BSR on seismic line 8 with the easternmost pockmark field and the other pockmark fields suggests the hydrate stability limit extends to the ~550 m depth near seismic line 8, but lies deeper to the west, at 700 m, across the rest of the survey (Fig. 2-10). We suggest the distribution of pockmarks and category II backscatter patches and their eastern termination serves to delineate the landward limit of gas hydrate stability, and thus fluid venting related to gas hydrate destabilization in this region.

Backscatter Patterns and Fluid Flow

Schematic diagrams describing the possible environments responsible for the three categories of backscatter and the potential pathways for the fluids are shown in Figure 2-11. Fluid flow, driven by compaction and dewatering of the wedge, in the Hydrate Ridge region supplies fluids to the hydrate stability zone via faults and fractures, dipping stratigraphic horizons, or during diffuse intergranular fluid flow. Authigenic carbonates can precipitate from the methane in these fluids as they interact directly with seawater in the shallow subsurface and/or as methane is released during the destabilization of gas hydrate. The distribution of high backscatter across the Hydrate Ridge region suggests fluids pond in anticlinal structures like Hydrate Ridge and the first accretionary ridge (FAR), while migrating away from or completely abandoning more undeformed portions of the wedge (e.g. HRB-E, where there is only one high backscatter patch, Fig. 2-4 attached foldout). The crests of anticlinal structures like Hydrate Ridge are under local tension and it is likely that fractures and faults serve as the major vertical fluid flow conduits to the seafloor. However, because Hydrate Ridge lies within the hydrate stability zone and carbonates derived from destabilized gas hydrate have been identified there (Bohrmann et al., 1998; Greinert et al., 2001) it is likely that both structurally influenced fluid migration and the destabilization of gas hydrate contribute to the authigenic carbonates imaged on the sidescan imagery. Therefore we classify the category I backscatter environment as structurally influenced and gas hydrate related (Fig. 2-11). Category II backscatter occurs in a mildly deformed portion of the wedge within the region of gas hydrate stability. The hydrate system here is likely fed by up dip fluid flow along porous stratigraphic horizons or deeper faults out of HRB-E (evidenced by the abundant backscatter on the eastern edge of HRB-E and on Hydrate Ridge, both up dip of HRB-E). In the middle portion of the survey (HRB-E to the Daisy Bank fault) the bathymetric expression of major subsurface structures is minimal, suggesting the subsurface is only mildly deformed (Fig. 2-1). The high backscatter patterns in the category II region suggest fluid pathways to the surface are diffuse or fluids advect at slower rates. Variable backscatter intensity, due to buried authigenic carbonates may also suggest a sporadic history of fluid venting, although

Figure 2-11. Schematic diagrams depicting the environments likely responsible for each of the backscatter categories. Suggested pathways responsible for the delivery of fluids to the shallow subsurface and gas hydrate stability zone (BSR labeled) are shown in the lower block diagram. Fluids migrate and accumulate at structural highs like Hydrate Ridge and the first accretionary ridge (FAR) and to a lesser extent on the eastern slope east of HRB-E. The structural highs are local sites of tension and it is likely faults and fractures permeate their crests. Category I backscatter occurs in this environment and, in the presence of abundant gas hydrate, fluid flow responsible for the carbonate precipitation at the surface is characterized as structurally influenced and gas hydrate related. Category II backscatter occurs on the eastern slope, east of HRB-E. It is characterized by variable intensity and a patchy distribution of backscatter patterns, suggestive of sporadic seafloor venting. It also lies in a region of the wedge that is mildly deformed, thus structural control on fluid expulsion sites is unlikely. Fluid flow responsible for this backscatter is likely diffuse and related to disruptions in the underlying gas hydrate. Category III backscatter across the Daisy Bank fault zone suggests long-term deep-seated fluid flow. Its location above the hydrate stability zone and the linear backscatter patterns suggest this region is dominated by structurally controlled non-gas hydrate related fluid flow.

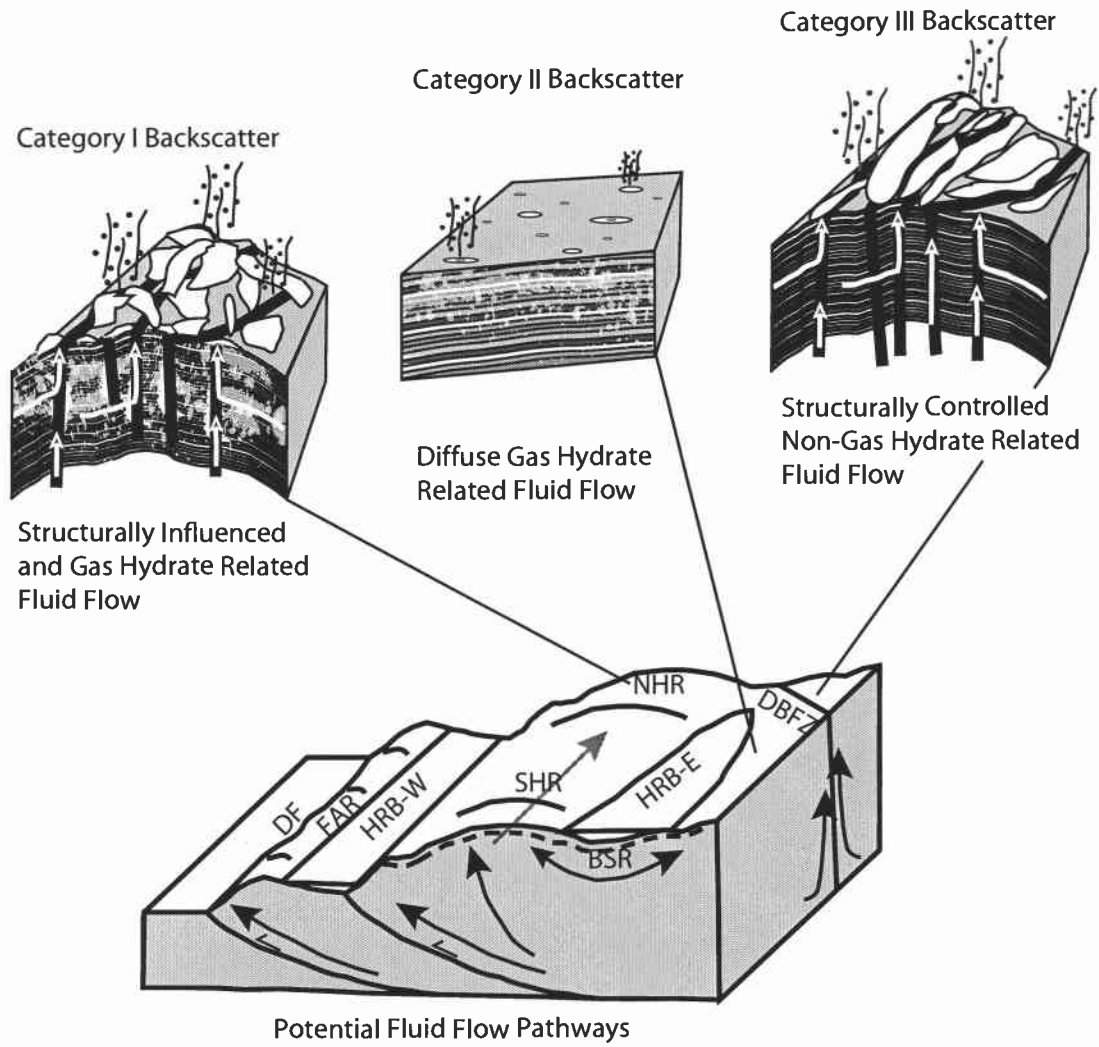


Figure 2-11.

high methane content in the near-surface sediments suggests active upward fluid flow. The lack of significant subsurface structure in the category II backscatter region and its location within the hydrate stability zone, suggests authigenic carbonate precipitation is most likely related to the destabilization of gas hydrate in this region. The category II backscatter environment is thus characterized as diffuse and gas hydrate related (Fig. 2-11). Category III backscatter, not related to major slope changes, occurs along the Daisy Bank Fault Zone. Here, high backscatter patterns suggest fluid flow has been continuous and likely deep-seated. In addition most of the Daisy Bank Fault Zone lies above the eastern hydrate stability limit (~550 at the shallowest). The environment responsible for the Daisy Bank category III backscatter is thus classified as structurally controlled and non-gas hydrate related (Fig. 2-11).

Conclusions

Based on seafloor mapping using high resolution SeaMARC 30 sidescan sonar data coupled with seafloor observations, samples, and subsurface geologic mapping the following conclusion can be made: (1) the blotchy to circular category I high backscatter present on Hydrate Ridge is indeed authigenic carbonate, (2) the category II high backscatter present along the eastern side of the survey is likely authigenic carbonate, with some gas hydrate, slightly buried by hemipelagic sediment, (3) both category I and II high backscatter sites represent carbonates that may have precipitated from destabilized gas hydrate and show an intimately linked gas hydrate carbonate system, however on Hydrate Ridge, direct fluid migration from depth also likely contributes to the carbonate precipitation, (4) breached anticlines serve not only to trap and aid in the migration of fluids and gases through the sediment column, but also serve as escape pathways, providing a local extensional environment at their crests for fluid expulsion, (5) diffuse gas hydrate related fluid flow is likely responsible for the category II high backscatter on the eastern slope, east of HRB-E, (6) category III backscatter associated with the Daisy Bank fault zone is likely derived from deep seated fluids that have a long history of escape along the fault and are likely unrelated to the destabilization of gas hydrate, and

(7) the abrupt decrease of pockmark fields and category II backscatter patches on the eastern edge of the survey area may serve to delineate the landward limit of gas hydrate stability across this region.

Acknowledgements

We thank the 1999 R/V New Horizon crew, the shipboard scientific party, and Williamson and Associates of Seattle, WA for their hard work during the SeaMARC 30 data acquisition and processing phase. We also thank Gerhard Bohrmann (GEOMAR), for helpful comments and suggestions during the sidescan sonar cruise and use of the R/V Sonne Leg 143 data, Peter Linke (GEOMAR) for use of the R/V Sonne SO148 OFOS data, and Marta Torres (OSU) for use of her ALVIN observations on Hydrate Ridge. Additional thanks to Jason Chaytor (OSU) for compiling the 50 m bathymetric grid used to make the slope map and Anne Tréhu and Matt Arsenault (OSU) for assistance with the 1989 Digicon seismic data. This manuscript also benefited from very thorough and thoughtful reviews by Nathan Bangs, David Piper, and an anonymous reviewer. GEOMAR collaborators on cruises SO143 and SO148 were funded through the TECFLUX projects by the Federal Ministry of Science and Technology (BMBF; grants 03GO/143/148). Funding for the TECFLUX project at OSU for the data collection and processing of the SM30 data was provided by NSF Award #9731023. Acknowledgement is also made to the Donors of The Petroleum Research Fund, administered by the American Chemical Society, for partial support of this research.

References

- Blondel, P. and Murton, B.J., 1997. Handbook of Seafloor Sonar Imagery. Wiley-Praxis Series in Remote Sensing. John Wiley & Sons Ltd. in association with Praxis Publishing Ltd., West Sussex, England, 314 p.
- Bohrmann, G., Greinert, J., Suess, E. and Torres, M., 1998. Authigenic carbonates from the Cascadia subduction zone and their relation to gas hydrate stability. *Geology*, 26 (7), 647-650.
- Bohrmann, G., Linke, P., Suess, E. and Pfannkuche, O., 2000. RV SONNE Cruise Report SO143 TECFLUX-I-1999. GEOMAR Report 93.
- Brown, K.M., 1990. The nature and hydrogeologic significance of mud diapirs and diatremes for accretionary systems. *J. Geophys. Res.*, 95 (B6), 8969-8982.
- Carson, B., Seke, E., Paskevich, V. and Holmes, M.L., 1994. Fluid expulsion sites on the Cascadia accretionary prism: Mapping diagenetic deposits with processed GLORIA imagery. *J. Geophys. Res.*, 99 (B6), 11,959-11,969.
- Clague, D.A., Maher, N., and Paull, C.K., 2001. High-resolution multibeam survey of Hydrate Ridge, offshore Oregon. In: Paull, C.K. and Dillon, W.P. (Eds.), *Natural Gas Hydrates: Occurrence, Distribution, and Detection*. Geophysical Monograph 124. American Geophysical Union, Washington, D.C., 297-303.
- Fleming, S.W. and Tréhu, A., 1999. Crustal structure beneath the central Oregon convergent margin from potential-field modeling: Evidence for a buried basement ridge in local contact with a seaward dipping backstop. *J. Geophys. Res.*, 104 (B9), 20,431-20,447.
- Goldfinger, C., Kulm, L.D., Yeats, R.S., Appelgate, B., MacKay, M.E., Moore, G.F., 1992. Transverse structural trends along the Oregon convergent margin: Implications for Cascadia earthquake potential and crustal rotations. *Geology*, 20, 141-144.
- Goldfinger, C., Kulm, L.D., Yeats, R.S., Hummon, C., Huftile, G.J., Niem, A.R., McNeill, L.C., 1996. Oblique strike-slip faulting of the Cascadia submarine forearc: The Daisy Bank fault zone off central Oregon. In: Bebout, G.E., Scholl, D.W., Kirby, S.H., Platt, J.P. (Eds.), *Subduction: Top to Bottom*. Geophysical Monograph 96. American Geophysical Union, Washington, D.C., 65-74.
- Goldfinger, C., Kulm, L.D., Yeats, R.S., McNeill, L. and Hummon, C., 1997. Oblique strike-slip faulting of the central Cascadia submarine forearc. *J. Geophys. Res.*, 102 (B4), 8217-8243.
- Greinert, J., Bohrmann, G. and Suess, E., 2001. Gas hydrate-associated carbonates and methane-venting at Hydrate Ridge: Classification, distribution, and origin of authigenic lithologies. In: Paull, C.K., Dillon, W.P. (Eds.), *Natural Gas Hydrates: Occurrence, Distribution, and Detection*. Geophysical Monograph 124. American Geophysical Union, Washington D.C., 99-113.

- Haugerud, R.A., 1999. Digital elevation model (DEM) of Cascadia, latitude 39N-53N, longitude 116W-133W. U.S. Geological Survey Open-file Report 99-369.
- Heeschen, K.U., Tréhu, A.M., Collier, R.W., Suess, E., and Rehder, G., 2003. Distribution and height of methane bubble plumes on the Cascadia margin characterized by acoustic imaging. *Geophys. Res. Letts.* v. 30, 1643-1646.
- Henry, P., Lallemand, S.J., Le Pichon, X. and Lallemand, S.E., 1989. Fluid venting along Japanese trenches: Tectonic context and thermal modeling. *Tectonophysics*, 160, 277-291.
- Hovland, M., Lysne, D. and Whiticar, M., 1995. Gas hydrate and sediment gas composition, Hole 892A. In: Carson, B., Westbrook, G.K., Musgrave, R.J., Suess, E. (Eds.), *Proceedings of the Ocean Drilling Program, Scientific Results. Ocean Drilling Program, College Station, Texas*, 151-161.
- Hyndman, R.D. and Spence, G.D., 1992. A seismic study of methane hydrate marine bottom simulating reflectors. *J. Geophys. Res.*, 97 (B5), 6683-6698.
- Johnson, J.E., Goldfinger, C., and Tréhu, A.M., 2000, Structural development and deformation styles of the Hydrate Ridge region, Cascadia accretionary prism. *Geol. Soc. Am. Abstracts with Programs*, 32 (7), A36.
- Johnson, H.P. and Helferty, M., 1990. The geological interpretation of side-scan sonar. *Rev. Geophys.*, 28 (4), 357-380.
- Kopf, A.J., 2002, Significance of Mud Volcanism. *Rev. Geophys.*, 40, B1-B49.
- Kulm, L.D. and Fowler, G.A., 1974. Cenozoic sedimentary framework of the Gorda-Juan de Fuca Plate and adjacent continental margin- A Review. In: Dott, R.H. Jr., Shaver, R.H. (Eds.), *Modern and Ancient Geosynclinal Sedimentation. Society of Economic Paleontologists and Mineralogists, Special Publication 19*, 212-229.
- Kulm, L.D. and Suess, E., 1990. Relationship between carbonate deposits and fluid venting: Oregon accretionary prism. *J. Geophys. Res.*, 95 (B6), 8899-8915.
- Kulm, L.D., Suess, E., Moore, J.C., Carson, B., Lewis, B.T., Ritger, S.D., Kadko, D.C., Thornburg, T.M., Embley, R.W., Rugh, W.D., Massoth, G.J., Langseth, M.G., Cochrane, G.R., Scamman, R.L., 1986. Oregon subduction zone: Venting, fauna, and carbonates. *Science*, 231, 561-566.
- Kvenvolden, K.A., 1993. Gas hydrates - Geological perspective and global change. *Rev. Geophys.*, 31 (2), 173-187.
- Linke, P. and Suess, E., 2001. RV SONNE Cruise Report SO148 TECFLUX-II-2000. GEOMAR Report 98.
- Le Pichon, X., Kobayashi, K. and Crew, K.-N.S., 1992. Fluid venting activity within the eastern Nankai Trough accretionary wedge: A summary of the 1989 Kaiko-Nankai results. *Earth Planet Sc. Lett.*, 109, 303-318.

- Lewis, B.T.R. and Cochrane, G.C., 1990. Relationship between the location of chemosynthetic benthic communities and geologic structure on the Cascadia subduction zone. *J. Geophys. Res.*, 95 (B6), 8783-8793.
- MacKay, M.E., 1995. Structural variation and landward vergence at the toe of the Oregon accretionary prism. *Tectonics*, 14 (5), 1309-1320.
- MacKay, M.E., Jarrard, R.D., Westbrook, G.K., Hyndman, R.D., Shipboard Scientific Party of Ocean Drilling Program Leg 146, 1994. Origin of bottom-simulating reflectors: Geophysical evidence from the Cascadia accretionary prism. *Geology*, 22, 459-462.
- MacKay, M.E., Moore, G.F., Cochrane, G.R., Moore, G.F. and Kulm, L.D., 1992. Landward vergence and oblique structural trends in the Oregon margin accretionary prism: Implications and effect on fluid flow. *Earth Planet Sc. Lett.*, 109, 477-491.
- McNeill, L.C., Goldfinger, C., Kulm, L.D., and Yeats, R.S., 2000. Tectonics of the Neogene Cascadia forearc basin: Investigations of a deformed late Miocene unconformity. *Geol. Soc. Am. Bull.*, 112 (8), 1209-1224.
- Moore, J.C. and Vrolijk, P., 1992. Fluids in accretionary prisms. *Rev. Geophys.*, 30, 113-135.
- Ohta, S. and Laubier, L., 1987. Deep biological communities in the subduction zone of Japan from bottom photographs taken during "Nautile" dives in the Kaiko project. *Earth Planet Sc. Lett.*, 83, 329-342.
- Ritger, S.D., Carson, B. and Suess, E., 1987. Methane-derived authigenic carbonates formed by subduction-induced-pore-water expulsion along the Oregon/Washington margin. *Geol. Soc. Am. Bull.*, 98, 147-156.
- Sample, J.C., 1996. Isotopic evidence from authigenic carbonates for rapid upward fluid flow in accretionary wedges. *Geology*, 24 (10), 897-900.
- Sample, J.C. and Reid, M.R., 1998. Contrasting hydrogeologic regimes along strike-slip and thrust faults in the Oregon convergent margin: Evidence from the chemistry of syntectonic carbonate cements and veins. *Geol. Soc. Am. Bull.*, 110 (1), 48-59.
- Sample, J.C., Reid, M.R., Tobin, H.J. and Moore, J.C., 1993. Carbonate cements indicate channeled fluid flow along a zone of vertical faults at the deformation front of the Cascadia accretionary wedge (northwest U.S. coast). *Geology*, 21, 507-510.
- Seely, D.R., 1977. The significance of landward vergence and oblique structural trends on trench inner slopes. In: Talwani, M., Pitman, W.C. (Eds.), *Islands Arcs, Deep Sea Trenches, and Back-Arc Basins*, Maurice Ewing Series. American Geophysical Union, Washington, D.C., 187-198.
- Snavely, P.D. Jr., 1987. Tertiary Geologic Framework, Neotectonics, and Petroleum Potential of the Oregon-Washington Continental Margin. In Scholl, D.W., Grantz, A., and Vedder, J.G. (Eds.), *Geology and resource potential of the*

- continental margin of western North America and adjacent Ocean - Beaufort Sea to Baja California. Circum-Pacific Council for Energy and Mineral Resources, Earth Science Series 6, 305-335.
- Suess, E., Carson, B., Ritger, S., Moore, J.C., Jones, M.L., Kulm, L.D., Cochrane, G.R., 1985. Biological communities at vent sites along the subduction zone off Oregon. The hydrothermal vents of the eastern Pacific: An overview. *Biological Society of Washington Bulletin*, 6, 474-484.
- Suess, E., Torres, M.E., Bohrmann, G., Collier, R.W., Greinert, J., Linke, P., Rehder, G., Tréhu, A., Wallmann, K., Winckler, G., Zuleger, 1999. Gas hydrate destabilization: Enhanced dewatering, benthic material turnover and large methane plumes at the Cascadia convergent margin. *Earth Planet Sc. Lett.*, 170, 1-15.
- Suess, E., Torres, M.E., Bohrmann, G., Collier, R.W., Rickert, D., Goldfinger, C., Linke, P., Heuser, A., Sahling, H., Heeschen, K., Jung, C., Nakamura, K., Greinert, J., Pfannkuche, P., Tréhu, A., Klinkhammer, G., Whiticar, M.J., Eisenhauer, A., Teichert, B., Elvert, M., 2001. Sea floor methane hydrates at Hydrate Ridge, Cascadia Margin. In: Paull, C.K. and Dillon, W.P. (Eds.), *Natural Gas Hydrates Occurrence, Distribution, and Detection*. American Geophysical Union. *Geophysical Monograph* 124, 87-98.
- Suppe, J., 1983. Geometry and kinematics of fault-bend folding. *American Journal of Science* 283, 684-721.
- Teichert, B.M.A., Eisenhauer, A., Haase-Schramm, A., Bock, B. and Linke, P., 2003. U/Th systematics and ages of authigenic carbonates from Hydrate Ridge, Cascadia convergent margin: Records of fluid composition and sealevel changes. *Geochim. Cosmochim. Ac.* in press.
- Torres, M.E., Bohrmann, G., Brown, K., deAngelis, M., Hammond, D., Klinkhammer, G., McManus, J., Suess, E., Tréhu, A., 1999. Geochemical observations on Hydrate Ridge, Cascadia margin, July 99. Reference 99-3, Oregon State University Data Report 174.
- Tréhu, A.M., Bangs, N.L., Arsenault, M.A., Bohrmann, G., Goldfinger, C., Johnson, J.E., Nakamura, Y., Torres, 2002. Complex Subsurface Plumbing Beneath Southern Hydrate Ridge, Oregon Continental Margin, from High-resolution 3D Seismic Reflection and OBS Data. *Proceedings of the Fourth International Conference on Gas Hydrates*, Yokohama, Japan, 90-96.
- Tréhu, A.M. and Flueh, E.R., 2001. Estimating the thickness of the free gas zone beneath Hydrate Ridge, Oregon continental margin, from seismic velocities and attenuation. *J. Geophys. Res.*, 106 (B2), 2035-2045.
- Tréhu, A.M., Torres, M.E., Moore, G.F., Suess, E. and Bohrmann, G., 1999. Temporal and spatial evolution of a gas hydrate-bearing accretionary ridge on the Oregon continental margin. *Geology*, 27 (10), 939-942.

Westbrook, G., Carson, B., Musgrave, R., and Shipboard Scientific Party, 1994. Initial reports of the Ocean Drilling Program, 146. Ocean Drilling Program, College Station, Texas, 630 p.

Chapter III

Structural Vergence Variation and Clockwise Block Rotation in the Hydrate Ridge Region, Cascadia Accretionary Wedge

Joel E. Johnson¹, Chris Goldfinger¹, Nathan L. B. Bangs², Anne M. Tréhu¹,
and Johanna Chevallier¹

1. Oregon State University, College of Oceanic and Atmospheric Sciences, 104
Ocean Admin. Bldg. Corvallis, Oregon 97331

2. University of Texas, Institute for Geophysics, 4412 Spicewood Springs Rd. Austin,
Texas 78759

To be submitted to *Tectonics*

Abstract

Along the Cascadia accretionary margin offshore Oregon, the structural vergence at the toe of the accretionary wedge varies from landward vergent offshore northern Oregon to seaward vergent across the southern Oregon margin. A transition zone between these vergence domains occurs along the central Oregon portion of the wedge, centered on the Hydrate Ridge region. In this paper we identify past variability in structural vergence across the Hydrate Ridge region through detailed structural mapping using multichannel seismic reflection data and gridded bathymetry. These data are coupled to biostratigraphic age constraints obtained from drilling to constrain the timing of accretionary wedge growth since the early Pleistocene (<1.7 Ma). Our results indicate that the wedge in the Hydrate Ridge region advanced in three structural phases during the Quaternary: an early Pleistocene seaward vergent phase (~ 1.7 - 1.2 Ma), an early to middle Pleistocene (~ 1.2 - 0.3 Ma) landward vergent phase, and a late Pleistocene-Holocene (~ 0.3 - 0.25 Ma to present) seaward vergent phase. Age constraints on the timing of landward vergent deformation suggest coincidence with the deposition of the Astoria fan. High pore fluid pressures due to rapid fan deposition are the likely cause of landward vergence for the northern Oregon and Washington margins. The large bathymetric expression of northern Hydrate Ridge is likely due to its history of continued seaward vergence, which permitted some sediment subduction, likely underplating and observed thrust duplexing, all resulting in an increase in the thickness of the accretionary wedge (more uplift) beneath this region. Superimposed on the accretionary wedge growth in the Hydrate Ridge region, two transverse strike-slip faults have affected wedge development. Evidence of clockwise block rotation of the Hydrate Ridge tectonic block between the two transverse strike-slip faults appears most pronounced in the older portion of the wedge, and decreases toward the west. Kinematic constraints onshore from GPS and other evidence for northward migration of the forearc suggests a more southerly location of the strike slip faults after the accretion of the early Pleistocene seaward vergent phase (~ 1.7 - 1.2 Ma) and their subsequent migration north to their present location and orientation, suggesting their continued presence during the accretion of this portion of the

wedge. Constraints on the timing of propagation of the basement strike-slip faults into the abyssal plain section near the deformation front indicate that the early-middle Pleistocene landward vergent phase (~1.2-0.3 Ma) may have been terminated by this faulting, which released pore pressure on the décollement. This local reduction in pore pressure near the deformation front likely served to increase structural coupling at the décollement in this region, resulting in the formation of the modern seaward vergent frontal thrust.

Introduction

Accretionary wedge deformation along active margins has been well documented at many of the world's subduction zones (e.g. Moore et al., 1988; MacKay et al., 1992; von Huene et al., 1996; Gulick et al., 2004). Clues to the geometry and structural configuration of modern accretionary wedges come primarily from swath bathymetry and seismic reflection profiles. DSDP (Deep Sea Drilling Project) and ODP (Ocean Drilling Program) coring have added details of the stratigraphy and physical properties within the wedges, helping to reconstruct their geologic evolution along several margins (e.g. Moore et al., 1988; von Huene et al., 1988; Underwood et al., 2003). Because accretionary wedges develop over long timescales, geophysical methods provide only a snapshot in time of the longer term behavior and development of the wedge. Sandbox and other physical models of subduction zone accretion have been used to recreate wedge growth from inception to full development and have contributed to our understanding of how wedges deform (e.g. Seely, 1977; Gutscher et al., 1996; 2001; Burbridge and Braun, 1998; Byrne et al, 1993; Smit et al., 2003). In addition, structural mapping of fold-and-thrust belts preserved in geologic records onshore (e.g. Price, 1981; Marshak, 1986; Echavarría et al., 2003) and critical taper theory (Davis et al., 1983) have enhanced our understanding of the geologic and geometric controls on accretionary wedge development.

Along the Cascadia subduction zone of western North America, where the Juan de Fuca-Gorda plate system subducts obliquely beneath North America (Fig. 3-1), much of the accretionary wedge is imaged by seismic reflection and swath bathymetric surveys.

Figure 3-1. Bathymetric map of the offshore portion of the Cascadia subduction zone. Bathymetric contours (100 m interval). Along strike structural vergence variations within the accretionary wedge discussed in the text are shown. Note the transition zone or mixed vergence (MV) between landward vergence (LV) to the north and seaward vergence (SV) to the south of the Hydrate Ridge region (boxed). The nine WNW trending left-lateral strike slip faults of Goldfinger et al., 1997 are also shown. The central Oregon faults are labeled (W) Wecoma fault, (DB) Daisy Bank fault, and (AC) Alvin Canyon fault. The extents of the Nitinat and Astoria fans on the abyssal plain are from Carlson and Nelson, 1987. Deep Sea Drilling Program (DSDP) and Ocean Drilling Program (ODP) sites discussed in the text are shown. Juan de Fuca-North America relative plate motion at 45° N, 125.5° W (location shown as black dot with white outline) directed 051.36°, was calculated by Miller et al., 2001.

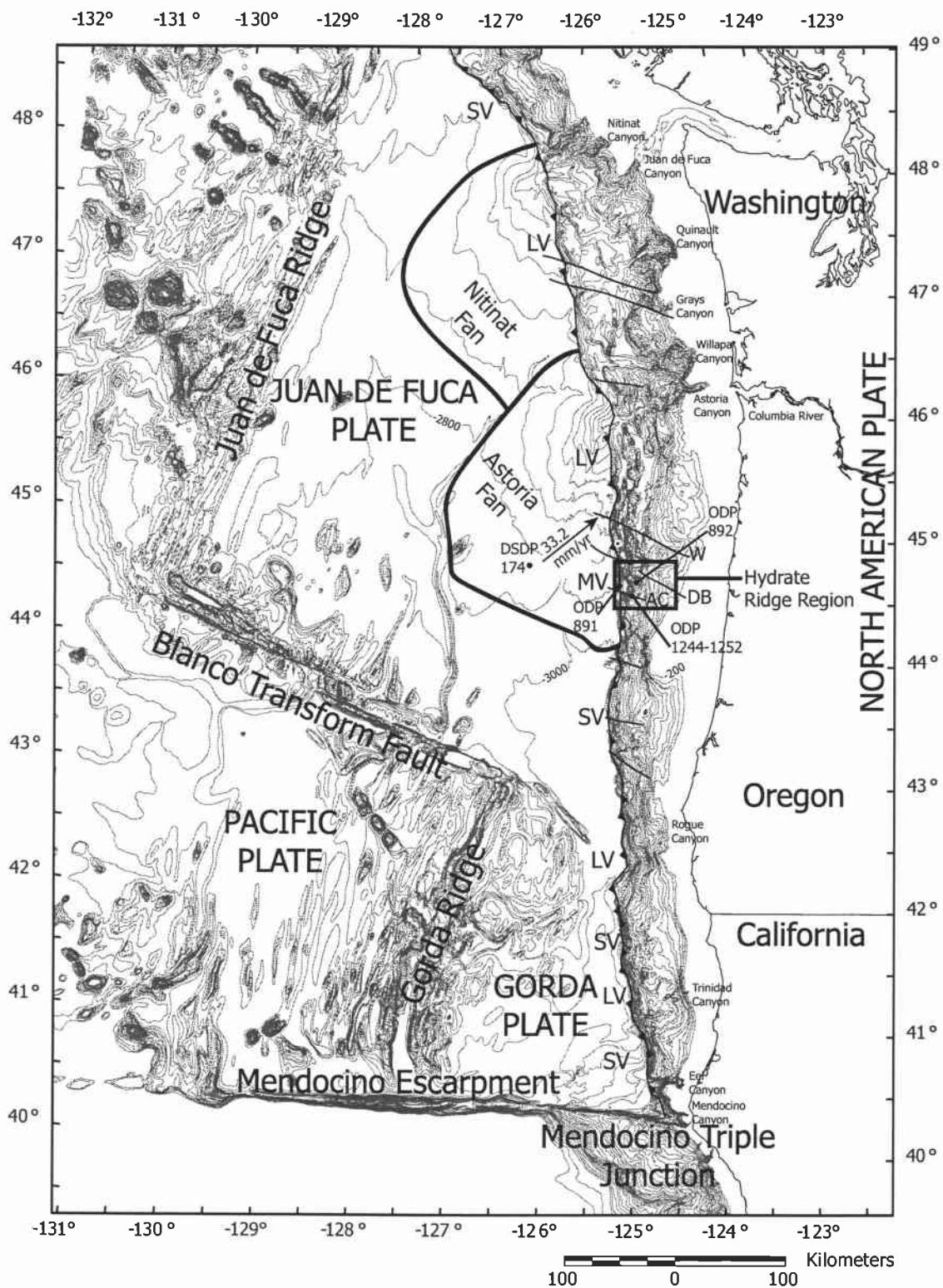


Figure 3-1.

These data sets document the subsurface structure and resultant surface bathymetric expression of many of the structures within the wedge and document along-strike (N-S) variations in structural vergence (Fig. 3-1). Offshore Vancouver Island, the structural vergence is dominantly seaward (Davis and Hyndman, 1989; Hyndman et al., 1994). Offshore Washington and northern Oregon, the structural vergence is dominantly landward (Seely, 1977; MacKay et al., 1992; MacKay, 1995; Flueh et al., 1998). Offshore central and southern Oregon, the vergence of structures is dominantly seaward (MacKay et al., 1992; MacKay, 1995; Goldfinger et al., 2000), with a small local region of landward vergence offshore the Rogue River region (Goldfinger et al., 2000). Offshore northern California, the structural vergence changes more frequently along strike (north to south) from dominantly seaward vergent to landward vergent back to seaward vergent (Gulick et al., 1998). In addition to the seaward and landward thrust faults and folds that comprise the Cascadia accretionary wedge, nine WNW-striking left-lateral strike slip faults (Goldfinger et al., 1997) also cut across the lower slope of the wedge (Fig. 3-1). These faults form in the lower plate as a result of dextral shear of the forearc, due to the oblique subduction, and propagate upward into the wedge.

In the central Oregon portion of the margin discussed here (the Hydrate Ridge region), a transition zone exists between the northern landward vergent province and the southern seaward vergent province, yielding a narrow zone of mixed vergence, both along and across strike, which is coincident with the location of two of the nine left-lateral strike slip faults. DSDP Leg 18 and ODP Legs 146 and 204 drilling results provide insight to the abyssal plain and lower slope accretionary wedge sedimentology and stratigraphy in this region and biostratigraphy from all three legs helps to constrain the ages of the sediments and timing of deformation throughout the region (Kulm and von Huene et al., 1973; Westbrook, Carson, Musgrave et al. 1994; Tréhu, Bohrmann, Rack, Torres et al., 2003).

In this paper, we use multichannel seismic reflection data coupled with 100 m gridded swath bathymetry and core biostratigraphy across the Hydrate Ridge region (Fig. 3-2) to (1) document the faults and folds in the subsurface, (2) determine the interaction

and relative timing of seaward and landward vergent thrusting and (3) investigate the influence of left-lateral strike slip faulting on the deformation history of the lower slope of the wedge. Our results reveal that the wedge advanced westward in a series of three structural phases since the late Pliocene-early Pleistocene: a seaward vergent phase, a landward vergent phase, and a seaward vergent phase. Superimposed on this structural vergence variation with time is the influence of left-lateral strike-slip faulting, which appears to have resulted in the clockwise rotation of structures during and likely since their accretion.

Geologic Setting: Washington and Oregon Margin

The Juan de Fuca and Gorda plates are currently subducting obliquely beneath the North American Plate along the Washington, Oregon, and Northern California continental margins (Fig. 3-1). The Cascadia accretionary wedge evolved in response to the oblique subduction and is composed of folded and faulted abyssal plain turbidites and hemipelagic clays as well as the recycled products of these uplifted sediments as slope basin fills (Kulm and Fowler, 1974; Westbrook, Carson, Musgrave et al. 1994; Tréhu, Bohrmann, Rack, Torres et al., 2003). The oblique convergence also creates a right-lateral shear couple within the forearc region and, off the Washington and Oregon margins, nine WNW striking left-lateral strike-slip faults, antithetic to the shear couple, have been identified on the continental slope and abyssal plain (Goldfinger et al., 1992; 1997). The Quaternary portion of the accretionary wedge is widest off the Washington and northern Oregon margins, coincident with the accretion of the thick Pleistocene Astoria and Nitinat Fans (Carlson and Nelson, 1987; Fig. 3-1), and narrows to the south. Off the central Oregon margin, the incoming abyssal plain stratigraphic section at ODP Site 174 consists of 284 m of late Pleistocene Astoria Fan sandy turbidites, with a Columbia River provenance, underlain by 595 m of Pliocene to early Pleistocene silt turbidites, with a Vancouver Island or Klamath Mountain (southern Oregon) provenance (Kulm and von Huene et al., 1973; Scheidegger et al., 1973). This change in provenance is estimated to have occurred at 1.3 -1.4 Ma as shelf and slope basins, previously

catchments for these sediments, were filled and breached, marking the initial phase of Astoria Fan deposition and progradation onto the abyssal plain (McNeill et al., 2000).

The active accretionary thrust faults and folds of the lower slope are characterized by mostly landward vergent thrusts on the Washington and northern Oregon margins and seaward vergent thrusts on the central and southern Oregon margin (Seely, 1977; Goldfinger et al., 1992; MacKay et al., 1992; MacKay, 1995). The origin of the landward vergent province offshore Washington and northern Oregon may be related to the accretion of rapidly deposited and overpressured sediment from the Astoria and Nitinat submarine fans, which resulted in high pore fluid pressure on the incipient décollement (Seely, 1977; MacKay, 1995). Virtually all of the incoming section in the landward vergent province is accreted to the margin above a deep décollement, whereas a shallower décollement in the seaward vergent portion of the margin at Hydrate Ridge results in accretion of the upper two-thirds of the incoming stratigraphic section and subduction and/or underplating of the lower one-third (MacKay et al., 1992). The outermost accretionary wedge abuts a steep slope break that separates it from the Eocene oceanic basalt Siletz terrane that underlies the continental shelf off the central Oregon to southern Washington margins (Snively, 1987; Tréhu et al., 1994). Above this oceanic basement terrane is a modestly deformed Eocene through Holocene forearc basin sequence (Snively, 1987; McNeill et al., 2000). Goldfinger et al. (1992) document a change in the strike of structures of the accretionary wedge seaward of the Eocene oceanic Siletzia terrane, from NE-SW driven compression within the wedge east of Siletzia to E-W driven compression (resulting in margin parallel structures) to the west. McNeill et al., 2000 suggest that this boundary may mark the backstop for the younger Quaternary accretionary wedge to the west.

Data and Methods

To map the subsurface structures in the region, we used multichannel seismic reflection profiles from an ODP site survey conducted in 1989 (Fig. 3-2). These data were collected using a 4560 in³ air gun array and 144 channel streamer and processed through time migration as described in MacKay et al. (1992). The seismic data shown in

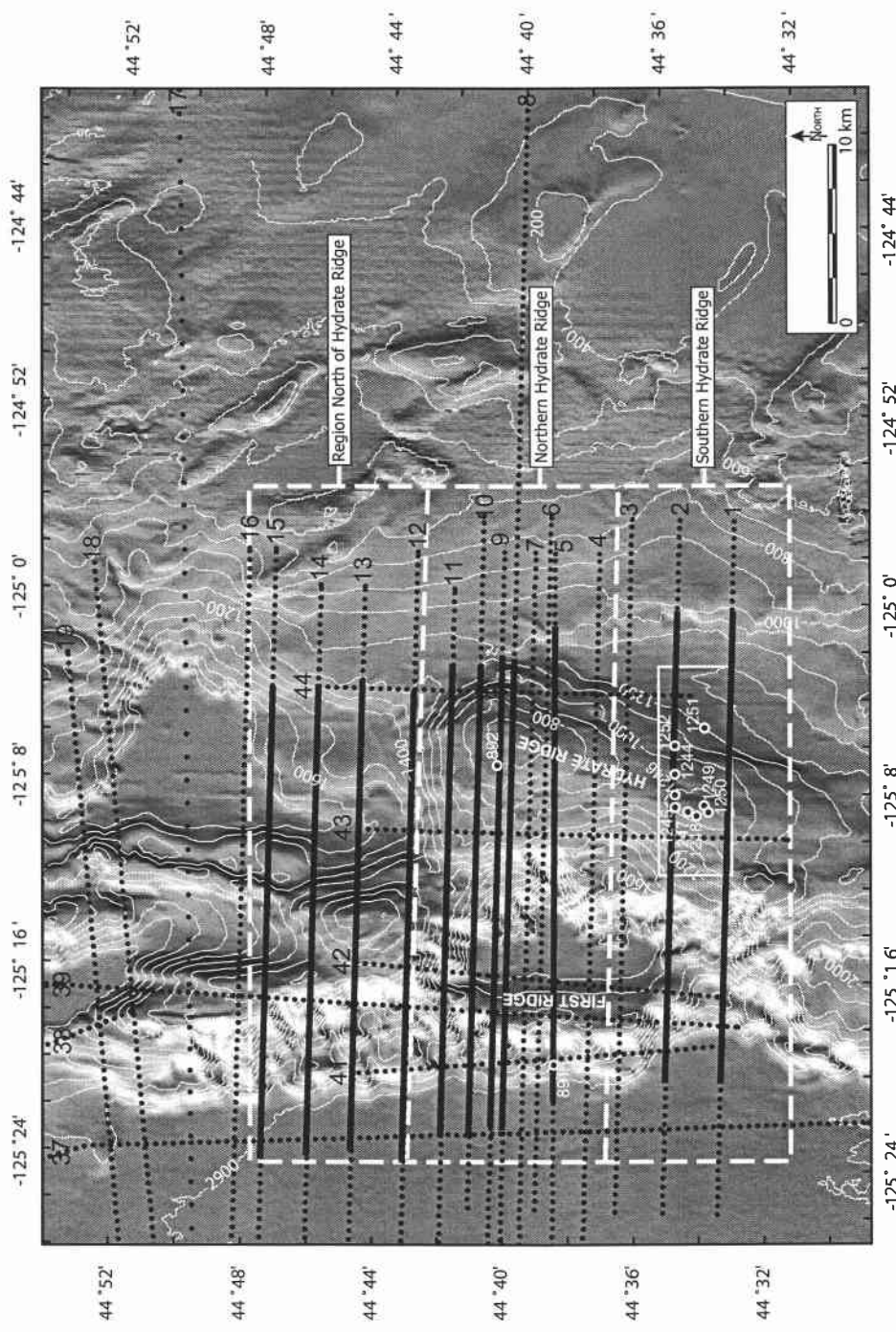


Figure 3-2. Shaded relief bathymetry (100 m pixel) of the Hydrate Ridge region. Digicon multichannel seismic survey tracklines are shown (black dots). Portions of the lines shown in Figures 3-4- through 3-9 are shown as overlain solid black lines. The three geographic regions discussed in the text are also shown (dashed white boxes). ODP drill sites are shown (Leg 204 sites 1244-1252; Leg 146 Sites 891-892). White solid box outlines the 3-D seismic survey which the Leg 204 drill sites were located.

this paper are time migrated and no additional changes to the initial processing have been performed. Although portions of profiles from the survey have been presented in several previous publications (e.g. MacKay et al., 1992; MacKay, 1995; Goldfinger et al., 1997; Westbrook, Carson, Musgrave et al. 1994; Tréhu et al., 1999; Johnson et al., 2003), discussion has been limited to the major structures nearest the deformation front and to shallower structures related to gas hydrate. In this paper, we include the structures that lie between the core of Hydrate Ridge and the deformation front. The bathymetric data used here were compiled from various swath bathymetric surveys conducted in the early 1990's by Oregon State University investigators, National Oceanic and Atmospheric Association (NOAA) EEZ SeaBeam 16 data, and National Ocean Service hydrographic soundings. These data were gridded at 100 m pixel resolution (Goldfinger et al., 1997). Insight was also gained from examination of data from a 3-d seismic survey conducted across southern Hydrate Ridge (Tréhu et al., 2003 and Chevallier, 2004) and unpublished 2-d seismic reflection profiles collected in 2000 by Anne Tréhu (Oregon State University).

The major faults and folds in the Hydrate Ridge region were initially mapped by Goldfinger et al. (1992; 1997), MacKay, et al. (1992) and MacKay (1995) and document the landward to seaward structural vergence change across the region as well as the presence of two deep-seated left-lateral strike slip faults (the Daisy Bank and Alvin Canyon faults of Goldfinger et al., 1997). Here we have reexamined the 1989 ODP site survey seismic data to create a regional structure map that includes previously identified large scale structures and the smaller scale folds and faults. Construction of the regional structure map was completed to identify and correlate structures across the region in order to reconstruct the history of deformation. To obtain the surface expression of the structures that do not intersect the seafloor, the tip lines of the faults and axes of the folds were projected vertically onto the bathymetric surface.

Results

Structural Vergence Variation

Hydrate Ridge is the second accretionary thrust ridge from the deformation front and lies within the younger margin-parallel structural province. Both seaward and

landward vergent structures are present (Fig. 3-3), as well as two left-lateral strike-slip faults (the Daisy Bank and Alvin Canyon faults of Goldfinger et al., 1997; Fig. 3-3). The faults and folds of the region were initially mapped by Goldfinger et al. (1992; 1997) and MacKay et al. (1992) and MacKay (1995) and document the landward to seaward structural vergence change that occurs at the deformation front near the Daisy Bank fault; south of the Daisy Bank fault, the frontal thrust is seaward vergent and north of the DBF the frontal thrust is landward vergent. Although the vergence of the frontal thrust changes abruptly from landward to seaward vergent across the Daisy Bank fault (MacKay et al., 1992), three additional landward vergent structures (discussed below) exist east of the deformation front in the previously defined seaward vergent region south of the Daisy Bank fault. This zone of mixed vergence exists between the Daisy Bank and Alvin Canyon left-lateral strike-slip faults and across the accretionary wedge from the deformation front to Hydrate Ridge, and is the focus of this study.

The along and across-strike structural vergence changes in the Hydrate Ridge region are shown on a series of E-W seismic reflection profiles (Figs. 3-4 through 3-9) located in Fig. 3-2. In addition to the major structures interpreted on each profile we also show the approximate position of the seaward vergent décollement horizon as mapped by MacKay (1995). Using the same seismic reflection data set presented here, MacKay (1995) documented a more shallowly located décollement near the deformation front in the seaward vergent portion of the wedge (which is the décollement surface shown on the seismic lines here) than in the landward vergent portion of the wedge to the north (not discussed in detail here). Because of poor deep seismic imaging within the wedge away from the deformation front, identification of the intersection between the bases of the thrust faults and the décollement horizons are best identified near the deformation front. For this reason, we can only infer that the décollement surface lies deeper in the landward vergent portions of the Hydrate Ridge region (discussed below) based on its deeper position where identified by MacKay (1995) near the deformation front to the north. We have divided the regions of similar structural style and stratigraphy in the Hydrate Ridge region into three zones across the wedge from Hydrate Ridge to the deformation

Figure 3-3. Geologic structures of the Hydrate Ridge region. Mapping of structures based on interpretation and correlation of structures observed on the multichannel seismic reflection survey lines (Fig. 3-2). Specific structures (e.g. seaward vergent thrust 1a) discussed in the text and labeled in Figs. 3-4 through 3-9 are also shown here. The mapped portions of the Daisy Bank and Alvin Canyon faults near the deformation front shown here are from (Goldfinger et al., 1997). The eastern traces of the Daisy Bank fault near Daisy Bank are also from Goldfinger et al., 1997. To the northeast to about -125° longitude, the Daisy Bank fault splays shown here are based on the surface fault expression interpreted on deep towed sidescan sonar (Johnson et al., 2003). The Daisy Bank fault splays with apparent offset features north of the region north of Hydrate Ridge, interpreted between seismic lines, are based on offset seafloor features. The eastern extent of the Alvin Canyon fault (Goldfinger et al., 1997) is off the map to the southeast here, but is shown in Figure 3-1. ODP sites shown as filled black circles (site labels as in Fig. 3-2). Extent of the ODP Leg 204 3-D seismic site survey on southern Hydrate Ridge shown as black box. The three geographic regions discussed in the text are also shown and are separated by the dashed black lines. Inset shows clockwise block rotation model discussed in the text.

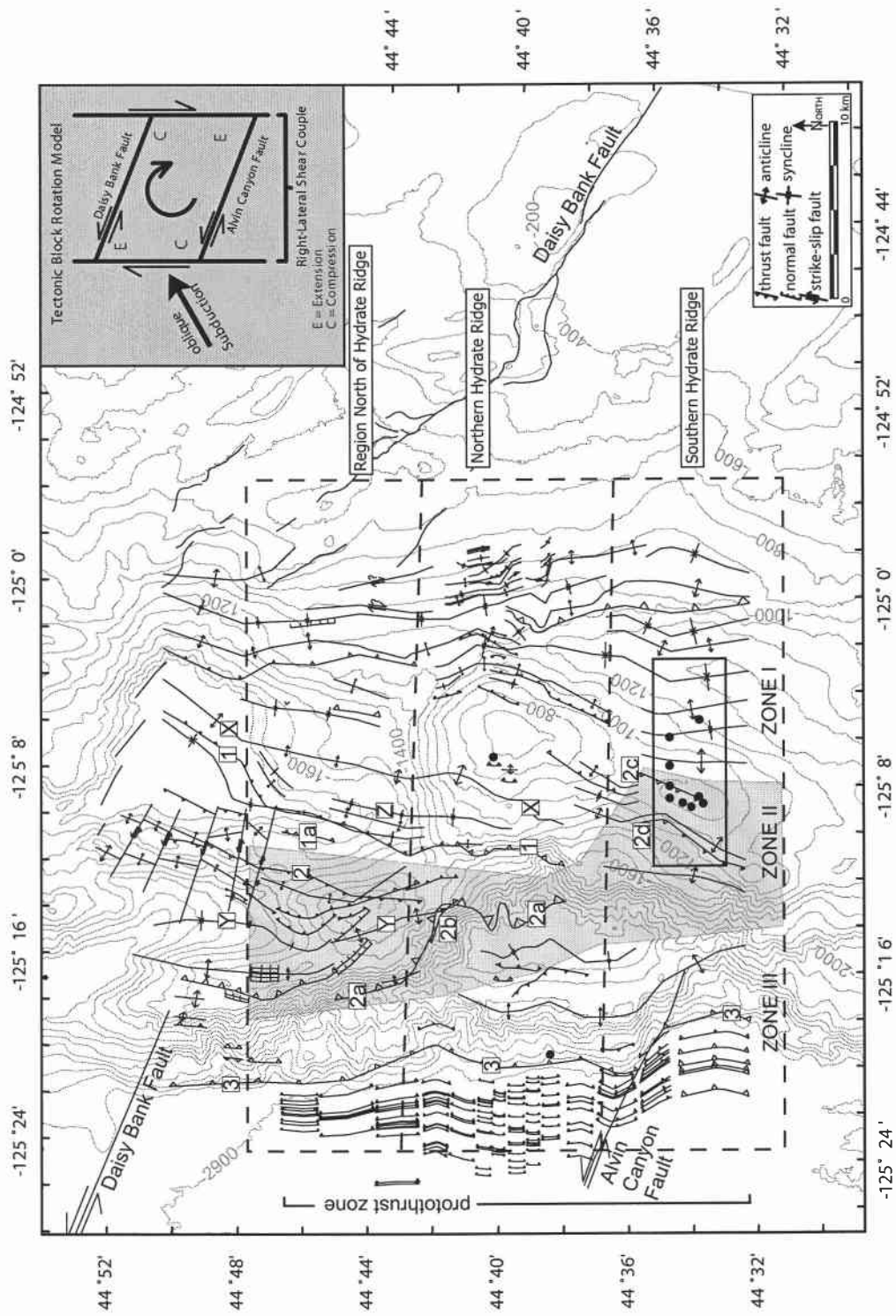


Figure 3-3.

front. Zones I, II, and III also indicate relative timing of major accretionary wedge growth (Age of major Zone I deformation > Zone II > Zone III) as the wedge advanced westward through time. Because we observe that deformation on structures across the wedge has continued throughout the Pleistocene, position in the wedge as an indication of the relative timing of thrusting can be misleading. For this reason, we use the geometries and timing constraints of the major faults and the common stratigraphic packages associated with each fault (see *Relative Timing of Major Tectonic Events*) to infer the relative order of thrusting through time.

North of Hydrate Ridge

In the region north of Hydrate Ridge (Figs. 3-2, 3-4 and 3-5), the primary structure in Zone I is a seaward vergent thrust fault (1) and its associated thrust anticline (X). In addition to this structure, a second seaward vergent thrust (1a) is well imaged on seismic lines OR89-Lines 14 and 13 directly beneath the 1-X structure. The stacked nature of these two seaward vergent thrust faults suggests that thrust duplexing is a common mechanism for shortening in this portion of the wedge (see *Northern Hydrate Ridge*).

The Zone II structural regime differs from that of Zone I by the presence of a landward vergent thrust fault (fault 2, shown in Figs. 3-4 and 3-5). On OR-89 Line 15 and to the north (on lines 16 and 17) there is also an additional landward vergent thrust fault east of fault 2 (Figs. 3-3 and 3-4a), but because this fault is absent south of OR89-line 15 (which was the main focus area for this paper) it is not discussed in detail. Although seaward vergent structures are also present in Zone II, most appear to be related to continued slip and splaying of fault 1a of Zone I (see Figs. 3-4b and 3-5). A possible exception to this pattern is the seaward vergent fault of Zone II, west of the landward vergent thrust (fault 2) observed on OR89-Lines 15 and 14, which may be a separate structure not related to fault 1a. This structure is not observed on any seismic profiles south of OR89-Line 14. The geometry of the surrounding stratigraphy (Y) suggests that slip along the landward vergent thrust (fault 2) was most prominent on OR89-Lines 14 and 13 (Figs. 3-4 and 3-5), as evidenced by folding of the strata (Y). On these two lines

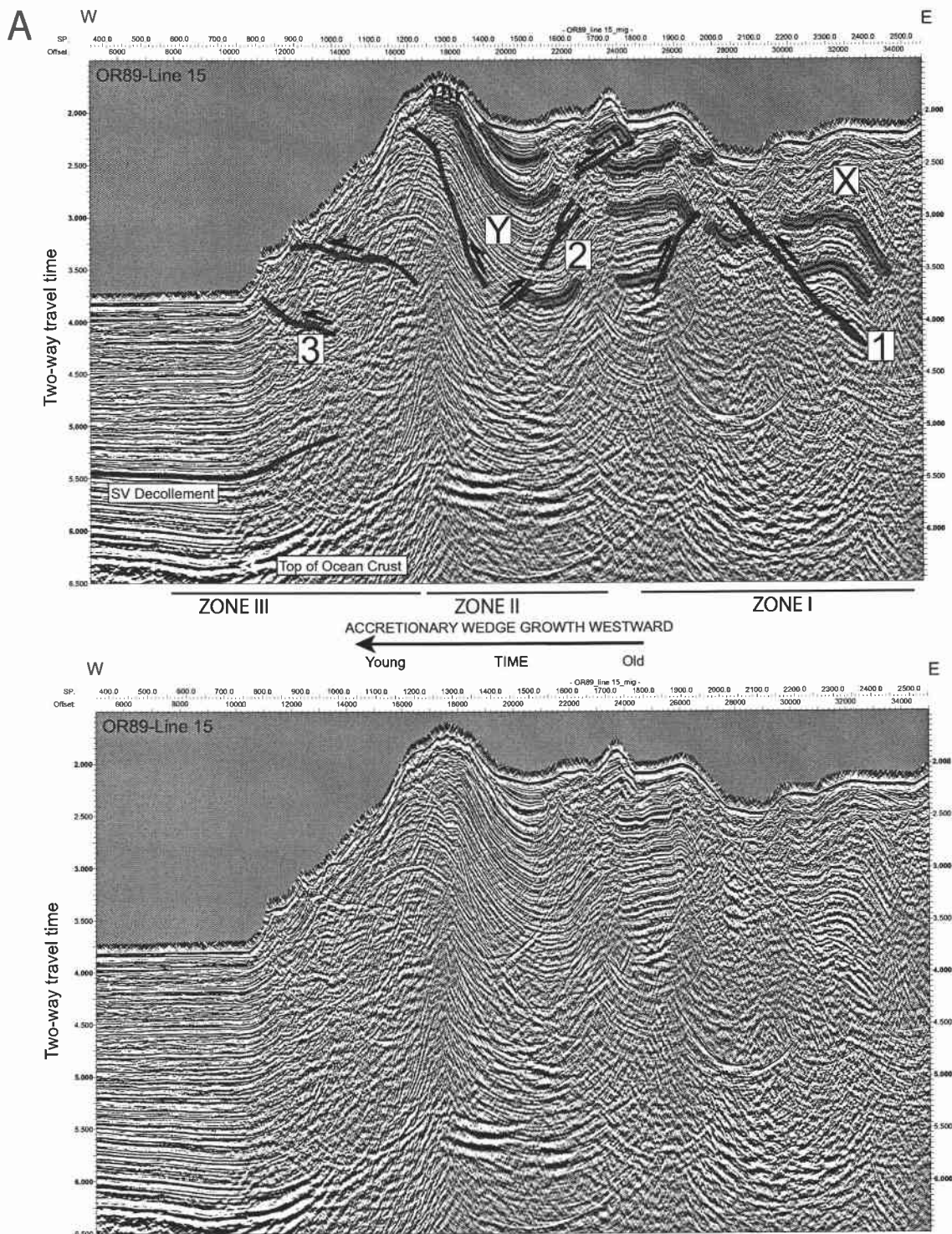


Figure 3-4. A. OR89 Line 15 (interpreted and uninterpreted). B. (next page) OR89 Line 14 (interpreted and uninterpreted).

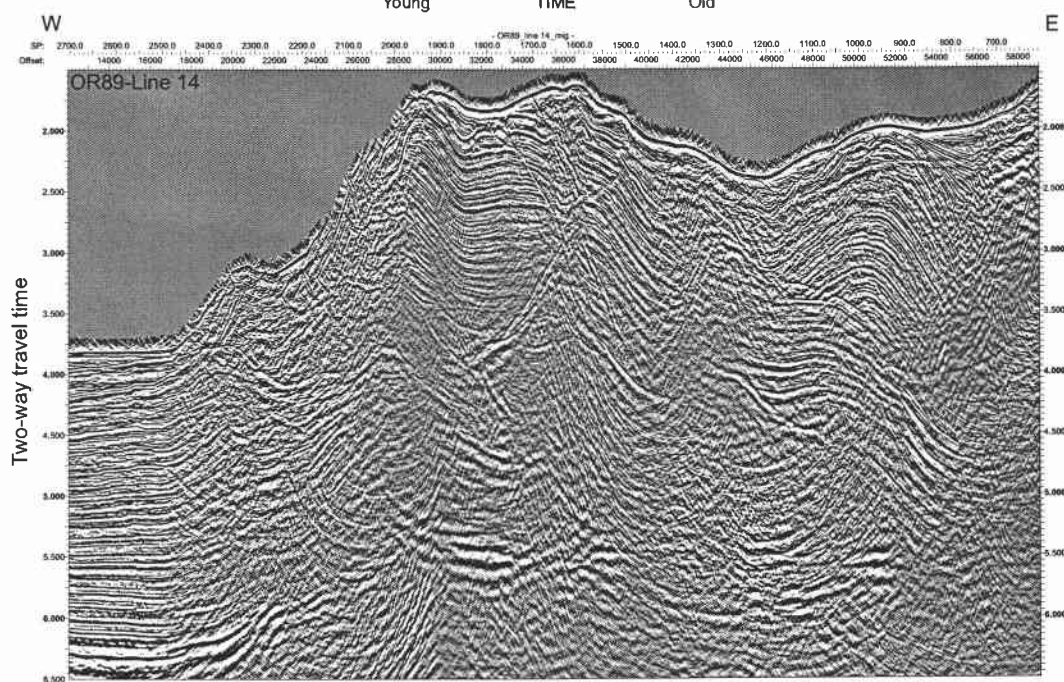
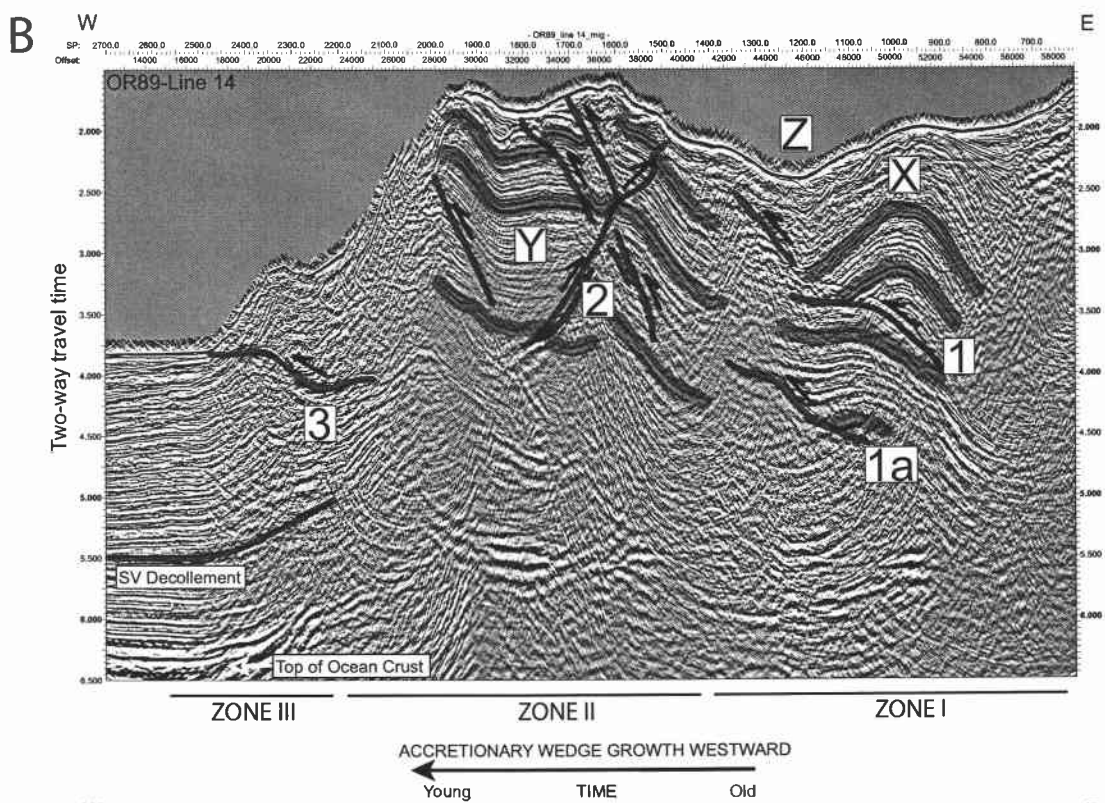


Figure 3-4 (Continued).

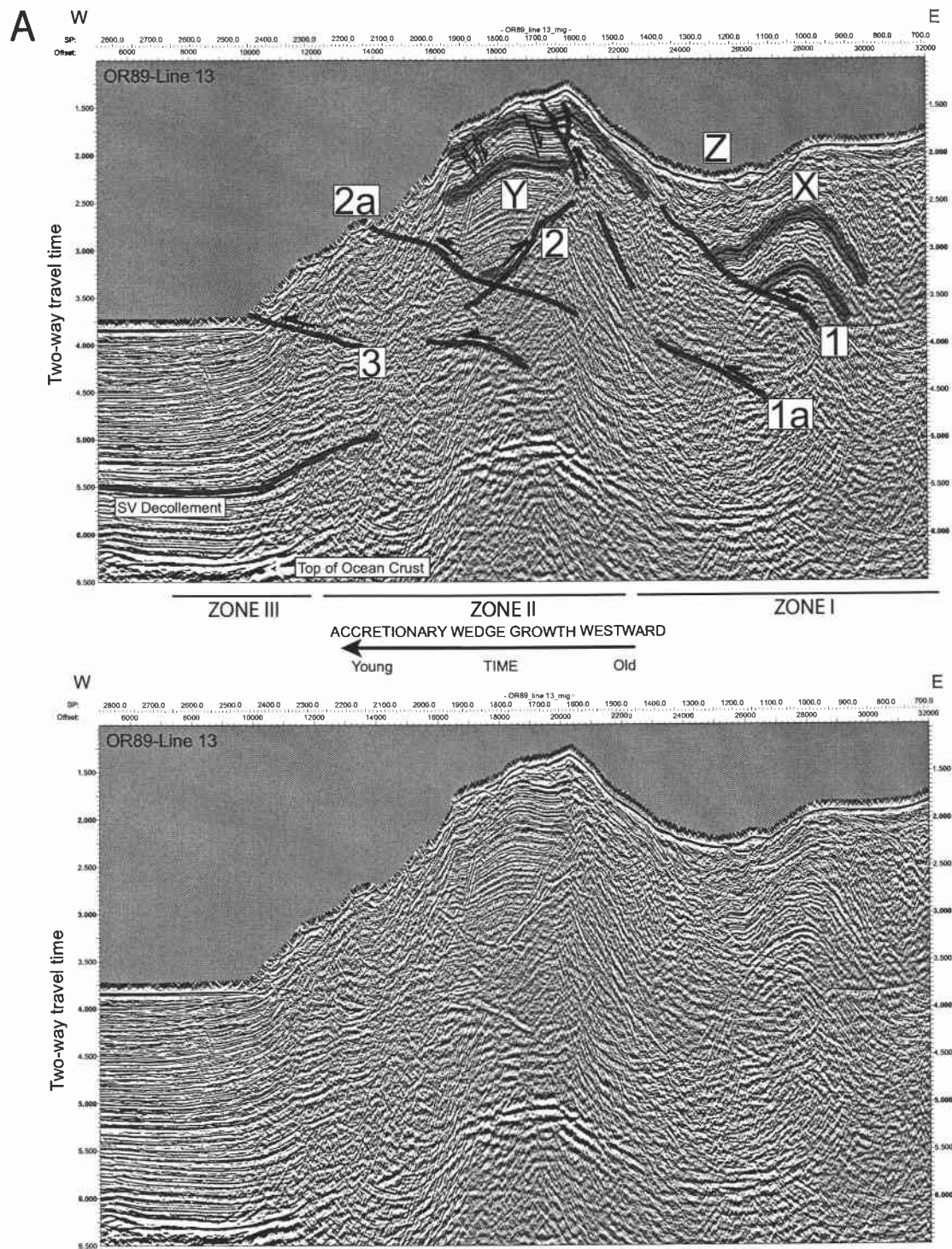


Figure 3-5. A. OR89 Line 13 (interpreted and uninterpreted). B. (next page) OR89 Line 12 (interpreted and uninterpreted).

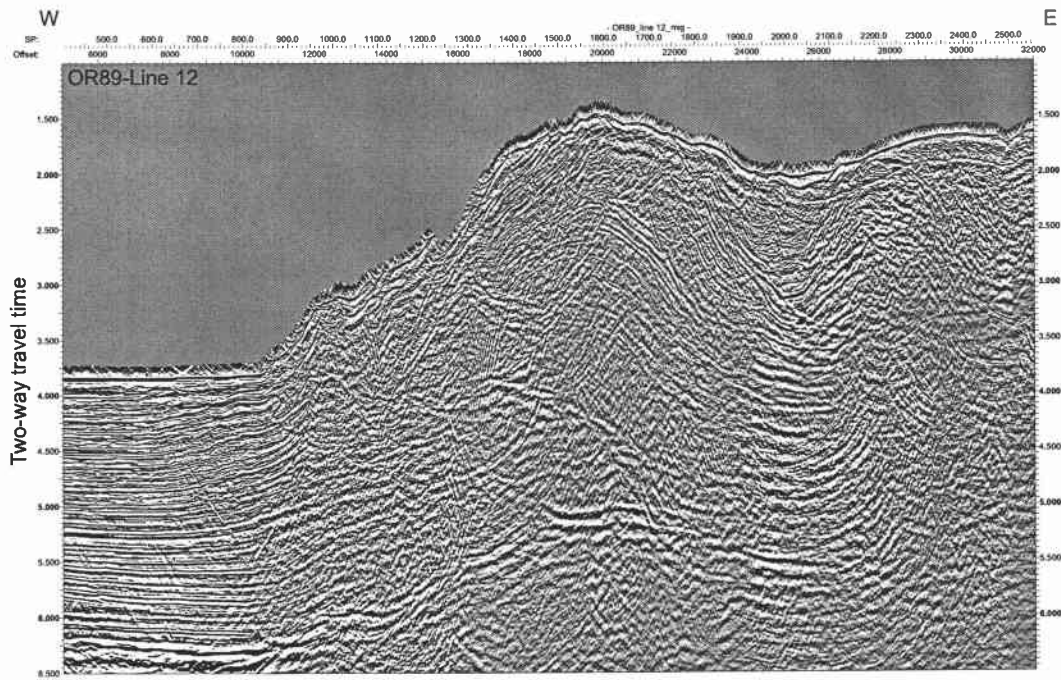
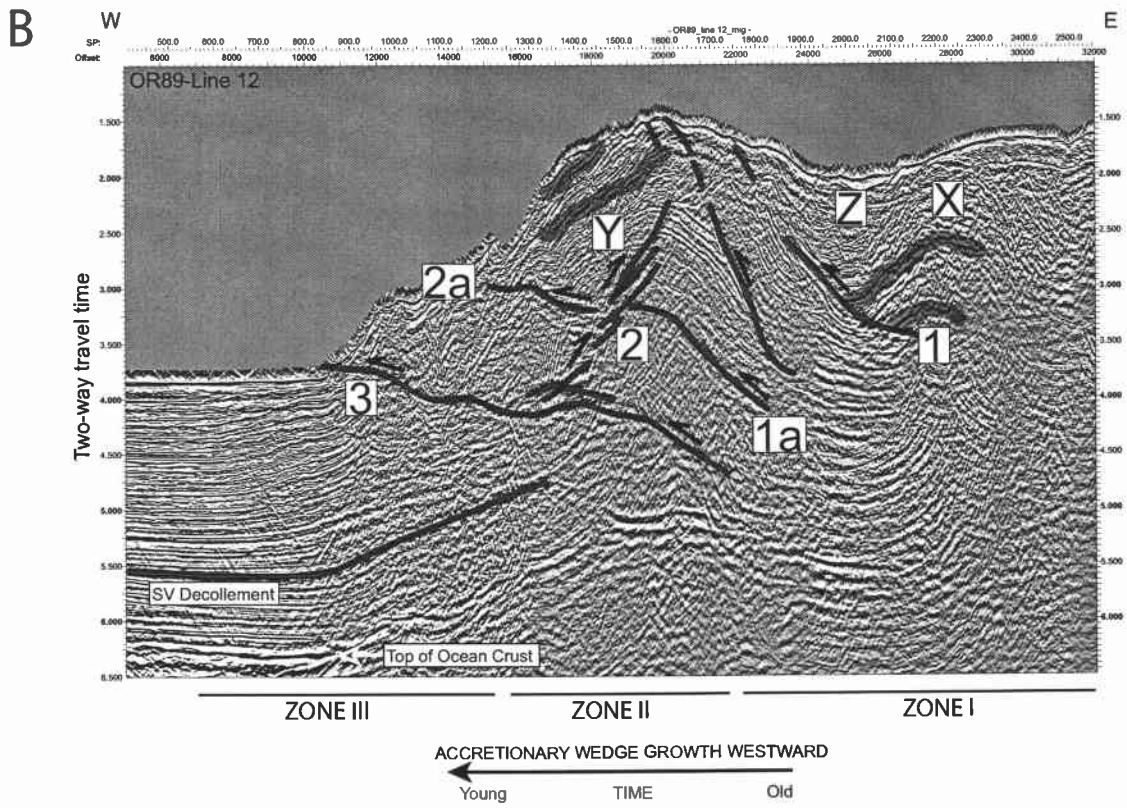


Figure 3-5 (Continued).

(Figs. 3-4 and 3-5) the strata (Y) are deformed first subtly, just beyond horizontal (Line 14) then become folded convex upward (Line 13). The effects of slip along the landward vergent thrust (fault 2) are less pronounced to the south on OR89-Line 12, where the structure dies out and is last observed (Figs. 3-4a and 3-5b) and the folded strata (Y) begins to respond mainly to slip along the seaward vergent splay of fault 1a (labeled fault 2a; Fig. 3-5).

Zone III deformation is marked by a seaward vergent thrust (3) (Figs. 3-4 and 3-5). The dominant structure in this region is the seaward vergent frontal thrust fault (3), which persists across the entire Hydrate Ridge region (Figs. 3-4 through 3-9). Although relative offsets of seaward and landward vergent thrust faults are difficult to ascertain from the data, examination of the progression of structures from north to south across the region north of Hydrate Ridge suggests the accretionary wedge advanced westward first by seaward vergent thrusting (Zone I), then by landward vergent thrusting (Zone II) with continued activity of Zone I structure splays (fault 2a) in the southern part of this region (OR89-Lines 13 and 12), and finally through modern seaward vergent thrusting at the deformation front (Zone III).

Northern Hydrate Ridge

Identification of the deeper structures of northern Hydrate Ridge is somewhat inhibited by the presence of a large free gas pool beneath northern Hydrate Ridge (Tréhu and Flueh, 2001) which results in high attenuation and a seismically incoherent zone (Figs. 3-6 through 3-8). Correlation of stratigraphy and structures from the region north of Hydrate Ridge to northern Hydrate Ridge, however, is possible by close examination of the Zone I structures and stratigraphy in both regions. The upper seaward vergent thrust (1) and anticline (X) and syncline (Z) pair observed in Zone I on all the seismic profiles shown from the northern region (Figs. 3-4 and 3-5) are observed on northern Hydrate Ridge as well (Fig. 3-6). Although the crest of the seaward vergent thrust anticline (X) is much more deformed and/or eroded in the northern Hydrate Ridge region, the limbs of the fold are apparent (Fig. 3-6). In addition to fault (1), folded strata in the syncline (Z)

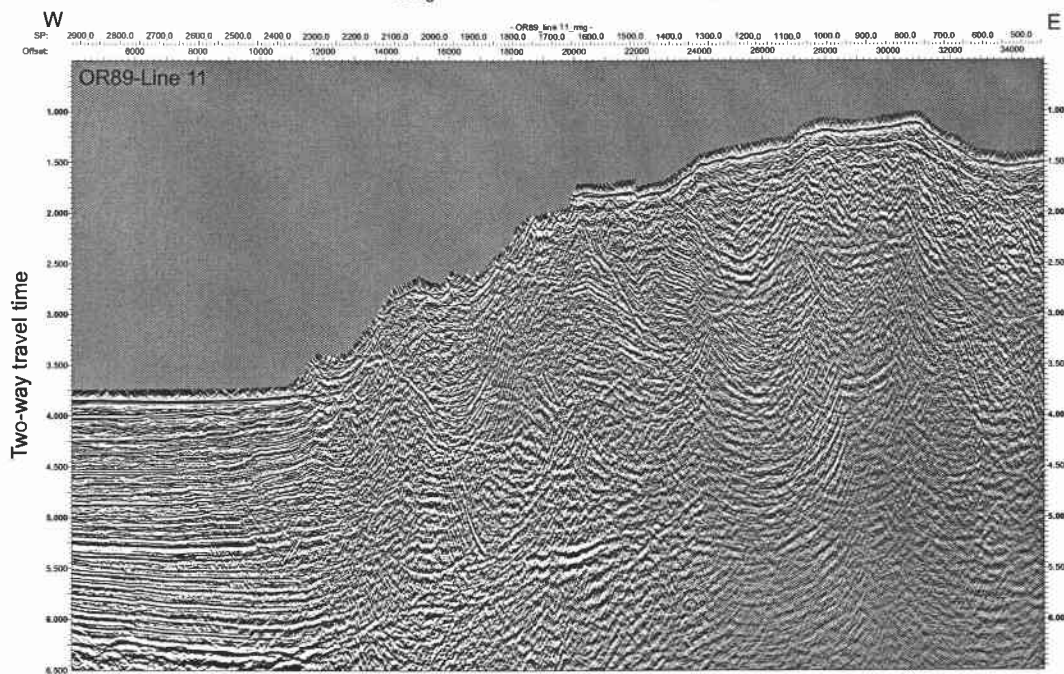
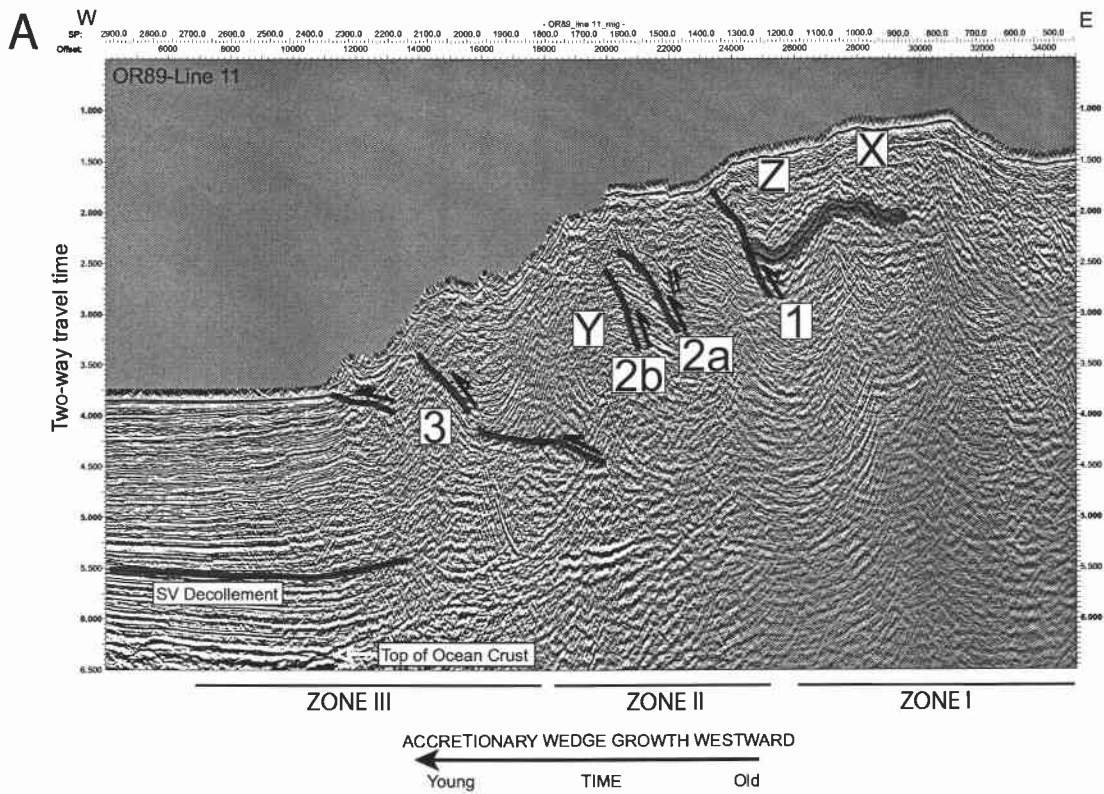


Figure 3-6. A. OR89 Line 11(interpreted and uninterpreted). B. (next page) OR89 Line 10 (interpreted and uninterpreted).

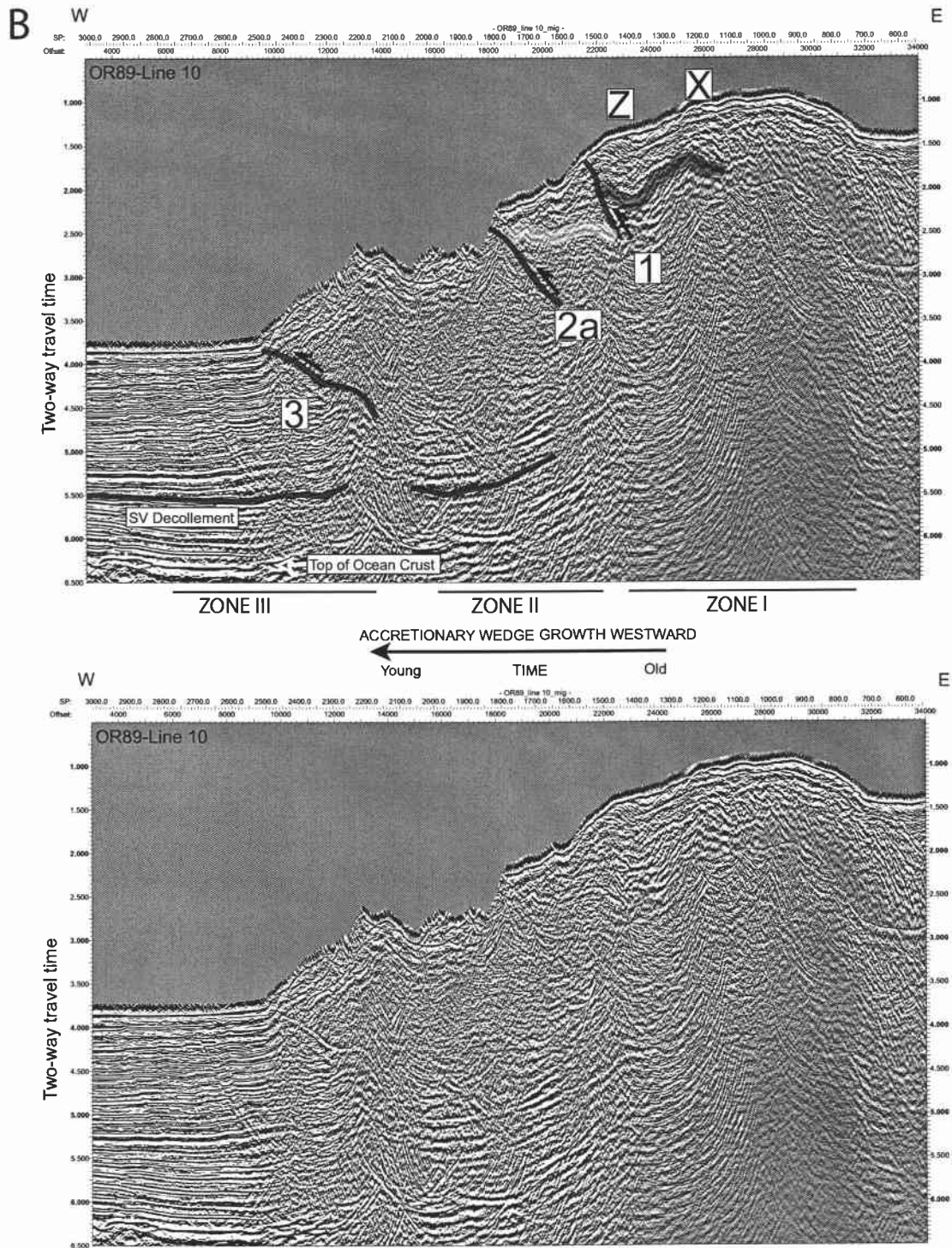


Figure 3-6 (Continued).

provides a good tie point from OR89-Line 12, in the northern region, to OR89-Lines 11 and 10 in the northern Hydrate Ridge region (Figs. 3-5 and 3-6).

Although the Zone I structural style of seaward vergence is correlative from the region north of Hydrate Ridge to northern Hydrate Ridge, a change in structural style occurs in Zone II across this region. Although the strata (Y) appears to be correlative in Zone II on seismic lines OR89-12 and 11, the landward vergent thrust fault observed in Zone II to the north (Figs. 3-4 and 3-5) is absent from northern Hydrate Ridge (Fig. 3-6). Lacking a landward vergent thrust fault to accommodate the shortening and growth of the accretionary wedge westward during the time of Zone II deformation observed to the north, at northern Hydrate Ridge slip was accommodated by at least two seaward vergent thrust faults (faults 2a and 2b; Figs. 3-6 and 3-7). These two faults are likely the western ends of the fault 1a splays imaged on OR-89 Lines 14, 13, and 12 to the north (Figs. 3-4 and 3-5). Examination of the contrast in folded strata surrounding these two faults from the anticline (Y) on OR-89 Line 12 to the faulted and folded geometry of the same strata shown on OR-89 Line 11 reveals the importance of these seaward structures in accommodating shortening across northern Hydrate Ridge. In addition to the seaward vergent thrust faults (2a and 2b) two additional asymmetric folds are developed west of these structures, beneath the slope basin sediments on seismic line OR-89 Line 8 (Fig. 3-7). The asymmetry of these two structures suggest that they are also seaward vergent thrust folds, thus providing additional evidence of shortening along seaward vergent structures during the general period of Zone II deformation on northern Hydrate Ridge. These two small folds developing beneath a younger slope basin yield insight into the processes responsible for the uplift and deformation of slope basin stratigraphy into large thrust folds in the wedge. The results of this type of process are observed on southern Hydrate Ridge where the crest of the ridge is composed of uplifted and deformed slope basin stratigraphic sequences (Tréhu et al., 2003; Chevallier, 2004).

In addition to the accommodation of shortening along the seaward vergent structures discussed above, it is also likely that seaward vergent thrust duplexes, perhaps

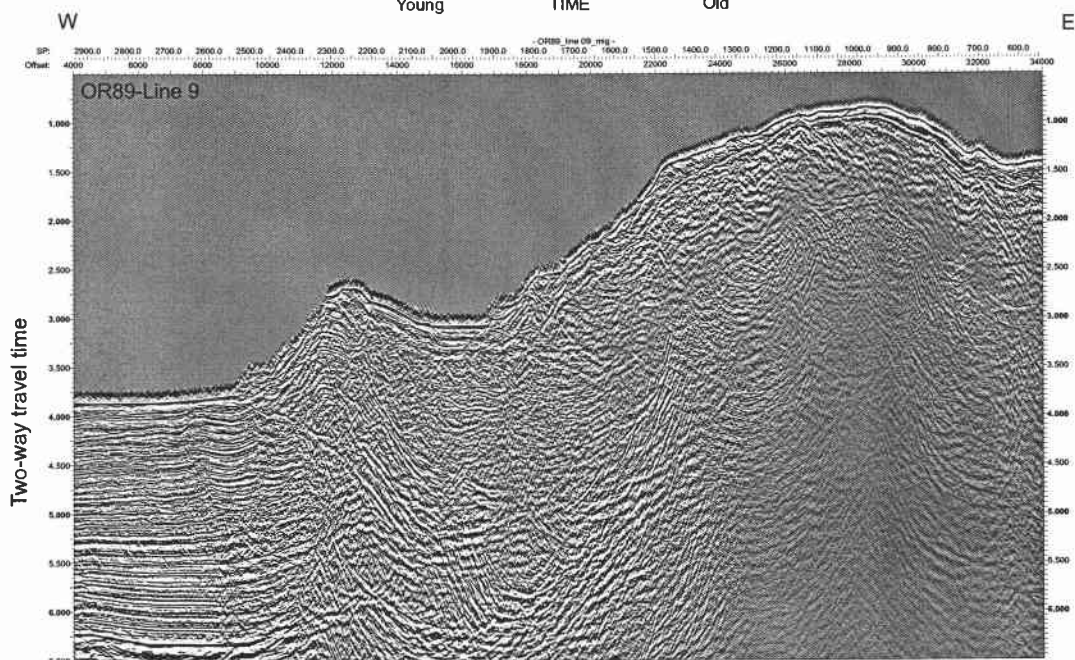
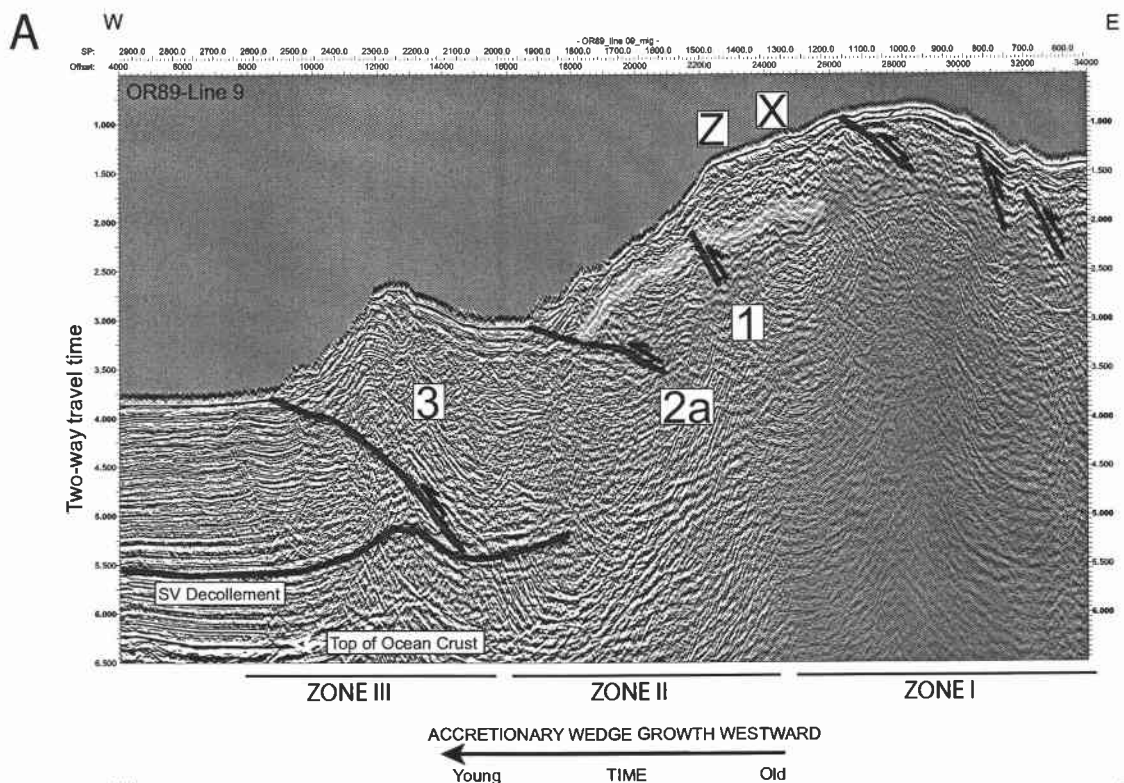


Figure 3-7. A. OR89 Line 9 (interpreted and uninterpreted). B. (next page) OR89 Line 8 (interpreted and uninterpreted).

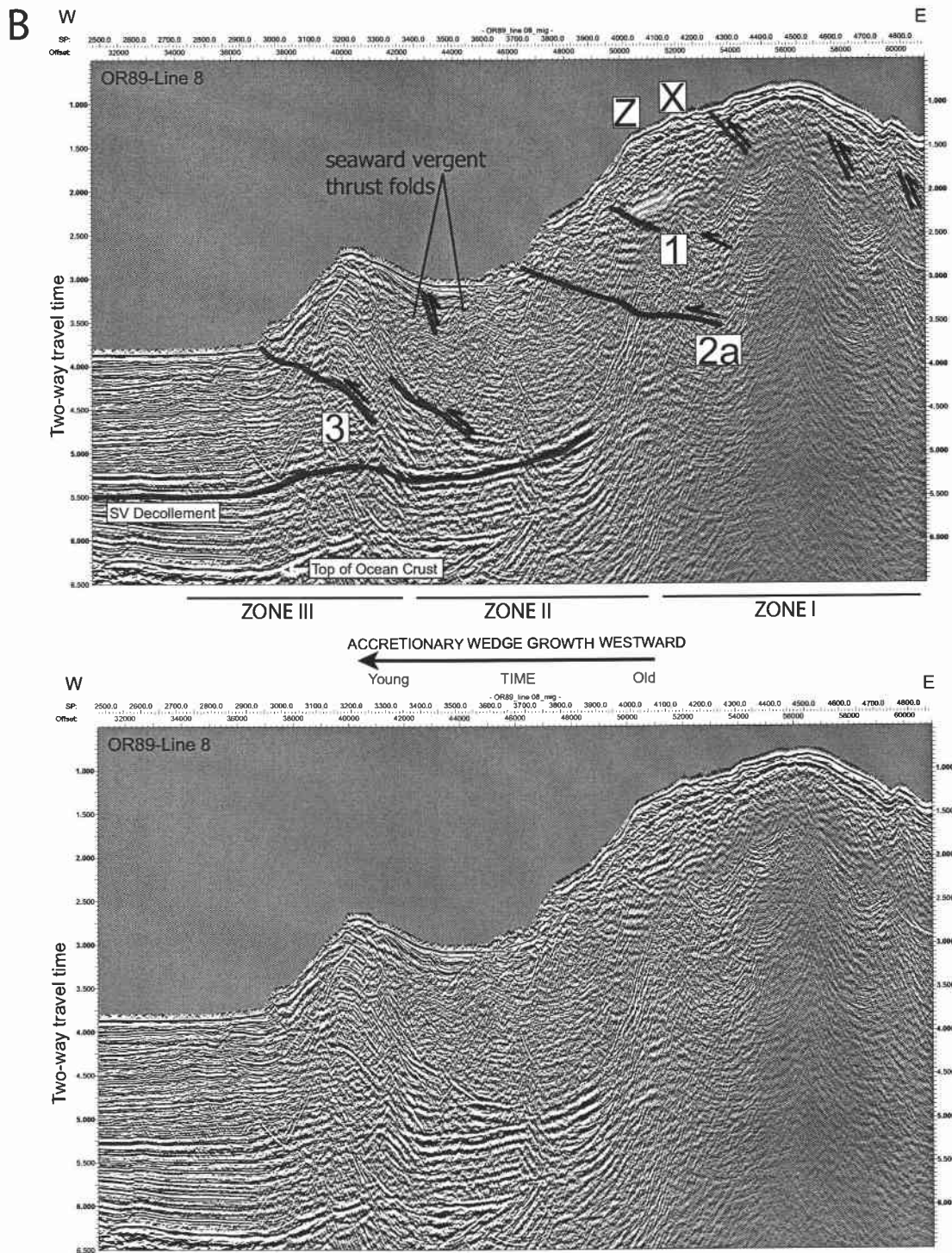


Figure 3-7 (Continued).

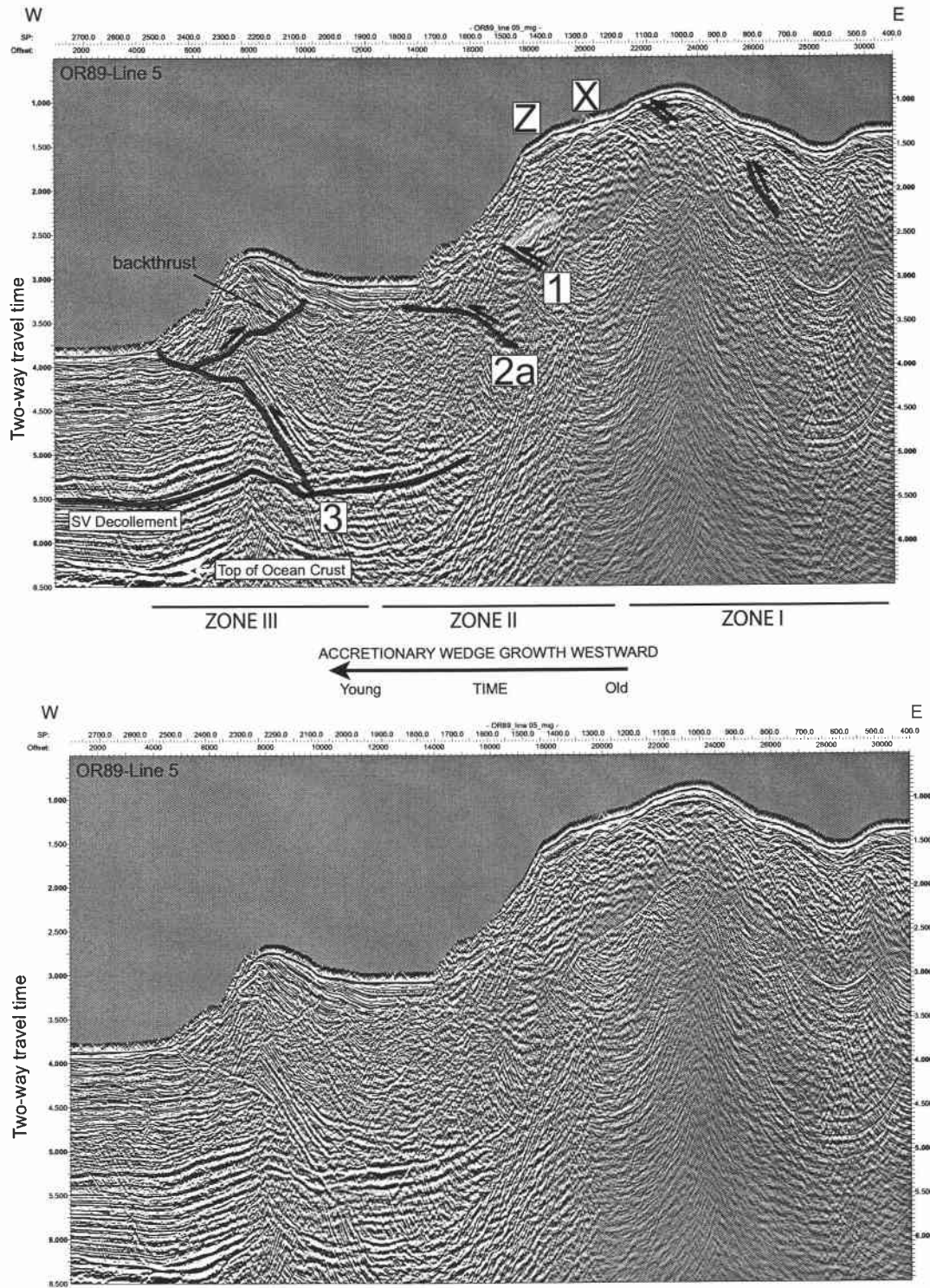


Figure 3-8. OR89 Line 5 (interpreted and uninterpreted)

formed from slip along the stacked couplet of faults (faults 1 and 1a) imaged to the north (Fig. 3-4 and 3-5) and additional unimaged structures, are responsible for the abrupt change in bathymetric relief of fold X seen on OR-89 Lines 15-12 to Lines 11-8 (Figs. 3-4 through 3-7). Additional evidence for the growth of northern Hydrate Ridge through thrust duplexing beneath the crest and even toward the eastern flank of the ridge is seen through the apparent rotation (about a horizontal axis) of faults 1 and 2 in a counterclockwise direction with progression to the south (Figs. 3-6, 3-7, 3-8) and the uplift of an asymmetric thrust anticline on the eastern flank of Hydrate Ridge. The cause of the decrease in the relief and decrease in growth of northern Hydrate Ridge with progression to the south is discussed below. The above observations suggest, that although the structural styles of Zone II deformation differ from north of Hydrate Ridge (landward vergent thrust) to northern Hydrate Ridge (no landward vergent thrust and several seaward vergent thrusts), the timing of Zone II deformation in both regions was approximately the same. Zone III deformation of northern Hydrate Ridge is similar to that observed to the north (Figs. 3-4 through 3-9), where the frontal thrust is seaward vergent.

We interpret three main phases of seaward vergent thrusting at Northern Hydrate Ridge, first in Zone I, then in Zone II, with continued activity of Zone I structures likely, and finally though modern seaward vergent thrusting at the deformation front (Zone III).

Southern Hydrate Ridge

A recent 3-D seismic survey and ODP Leg 204 drilling (Tréhu et al., 2003; Chevallier, 2004) have shown that early Pleistocene to recent (<1.6 Ma) slope basin sediments overlie a core of late Pliocene-early Pleistocene (2.78-1.6 Ma) accretionary wedge material in the southern Hydrate Ridge region (Fig. 3-2). This differs from northern Hydrate Ridge, where the drilling results from ODP Leg 146 show this older core of late Pliocene-early Pleistocene (1.7-1.6 Ma, as determined at ODP Site 892) accretionary wedge material is exposed near the surface (i.e., there are no overlying, younger Pleistocene to recent slope basin sediments in the north). Although the deeper structures responsible for uplift of the core of late Pliocene-early Pleistocene material at

southern Hydrate Ridge are not well imaged on the 3-D survey or in the 1989 2-D seismic data across southern Hydrate Ridge they are imaged in the region north of Hydrate Ridge (Figs. 3-4 and 3-5; Zone I) and beneath northern Hydrate Ridge (Figs. 3-6 and 3-7; Zone I). In these regions they are dominated by seaward vergent structures that result in the uplift and deformation of the late Pliocene-early Pleistocene (perhaps even younger in the region north of Hydrate Ridge) strata there. For this reason, and because the geometry of the Pliocene core at southern Hydrate Ridge resembles in shape the asymmetric thrust fold complex to the north (Tréhu et al., 2003), it seems likely that the Zone I region of southern Hydrate Ridge is dominated by seaward vergent structures as well (Fig. 3-9). We infer less overall slip, thus less uplift, has accumulated across the structures at southern Hydrate Ridge, however, because of its subdued bathymetric expression compared to northern Hydrate Ridge, and because of the preservation of the overlying Pleistocene slope basin deposits, which are eroded away to the north. Southern Hydrate Ridge is composed of a small Zone I seaward vergent core (with overlying slope basin sediments) opposed by two Zone II landward vergent structures (Fig. 3-9), similar to the region north of Hydrate Ridge. In both of these regions observed uplift, and thus inferred fault slip, are less in the Zone I seaward vergent portion of the wedge than in the adjoining landward vergent Zone II regions. If the net shortening across the wedge is roughly constant along strike, the variability in observed uplift and inferred fault slip coupled with the documented structural vergence, suggests slip could be more easily accommodated on landward vergent structures compared to seaward vergent structures (see Structural Vergence and Hydrate Ridge Morphology). Zone III deformation of southern Hydrate Ridge is similar to that observed to the north (Fig. 3-4 through 3-9), the frontal thrust is seaward vergent.

Based on the observations above, it appears that the accretionary wedge advanced westward at southern Hydrate Ridge first by seaward vergent thrusting (Zone I), then by landward vergent thrusting (Zone II), and finally though modern seaward vergent thrusting at the deformation front (Zone III).

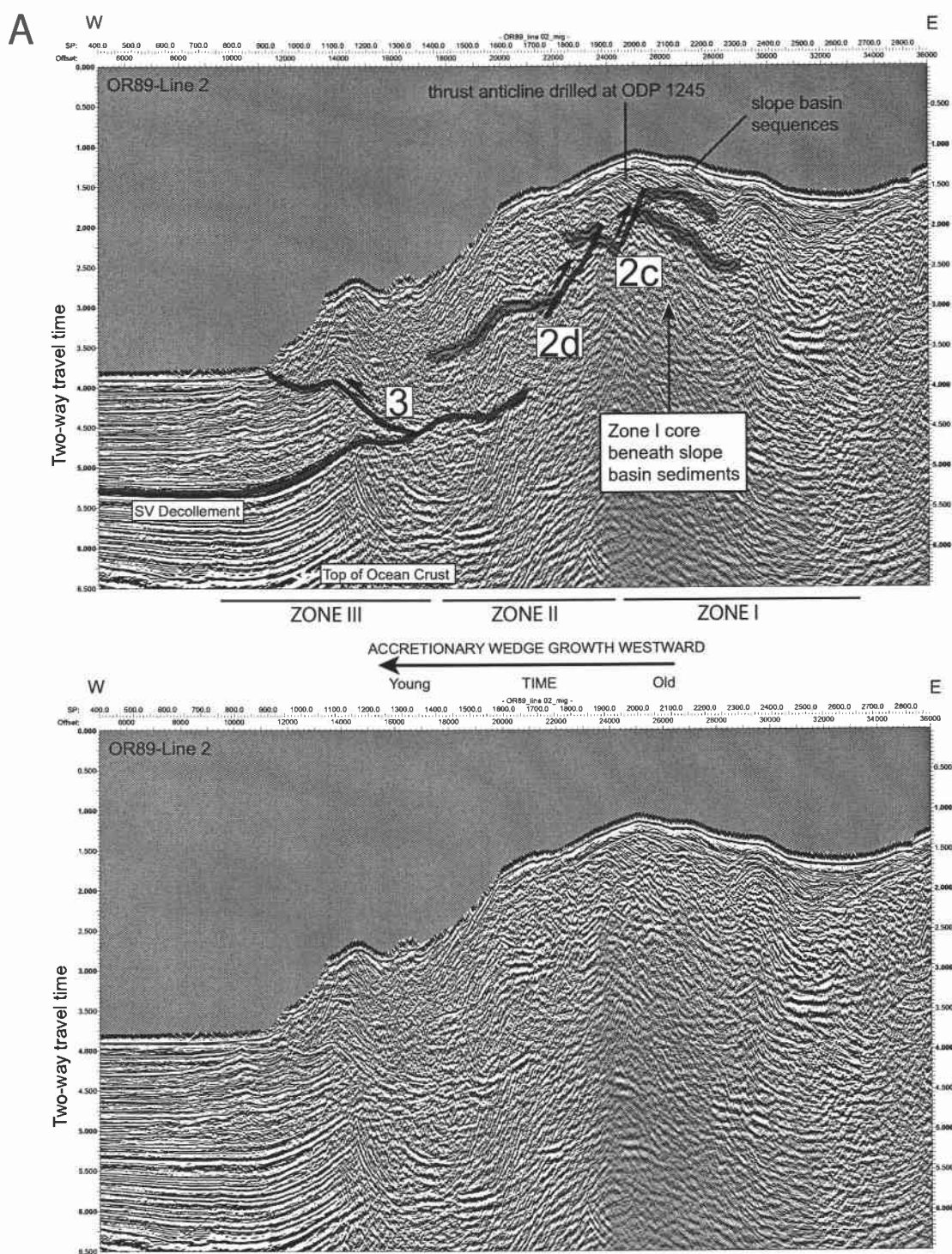


Figure 3-9. A. OR89 Line 2 (interpreted and uninterpreted). B. (next page) OR89 Line 1 (interpreted and uninterpreted).

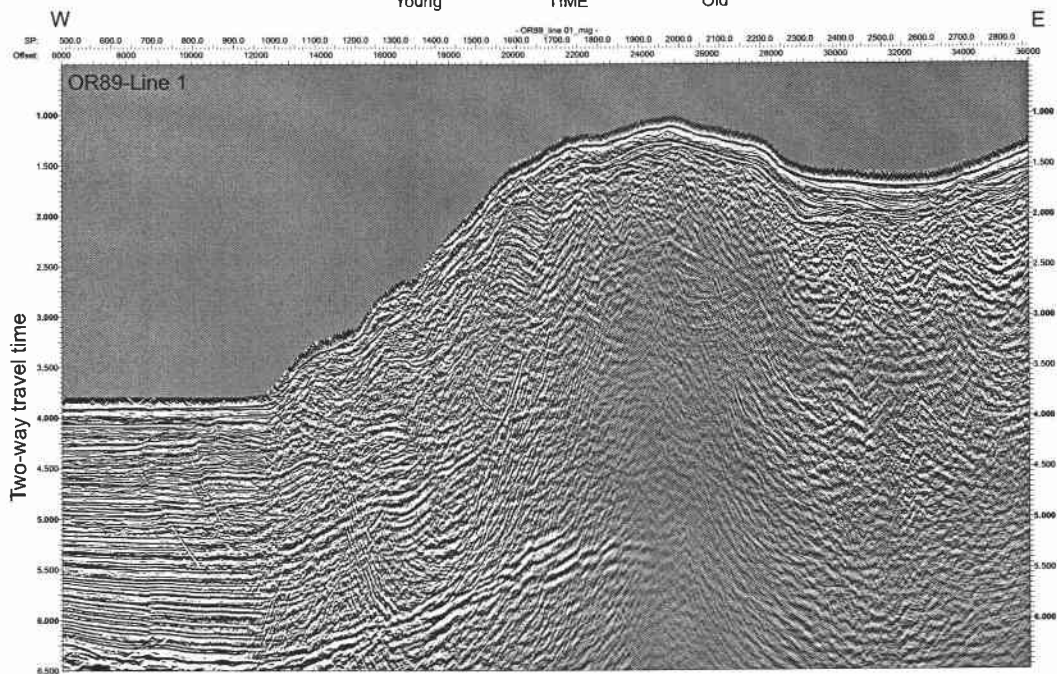
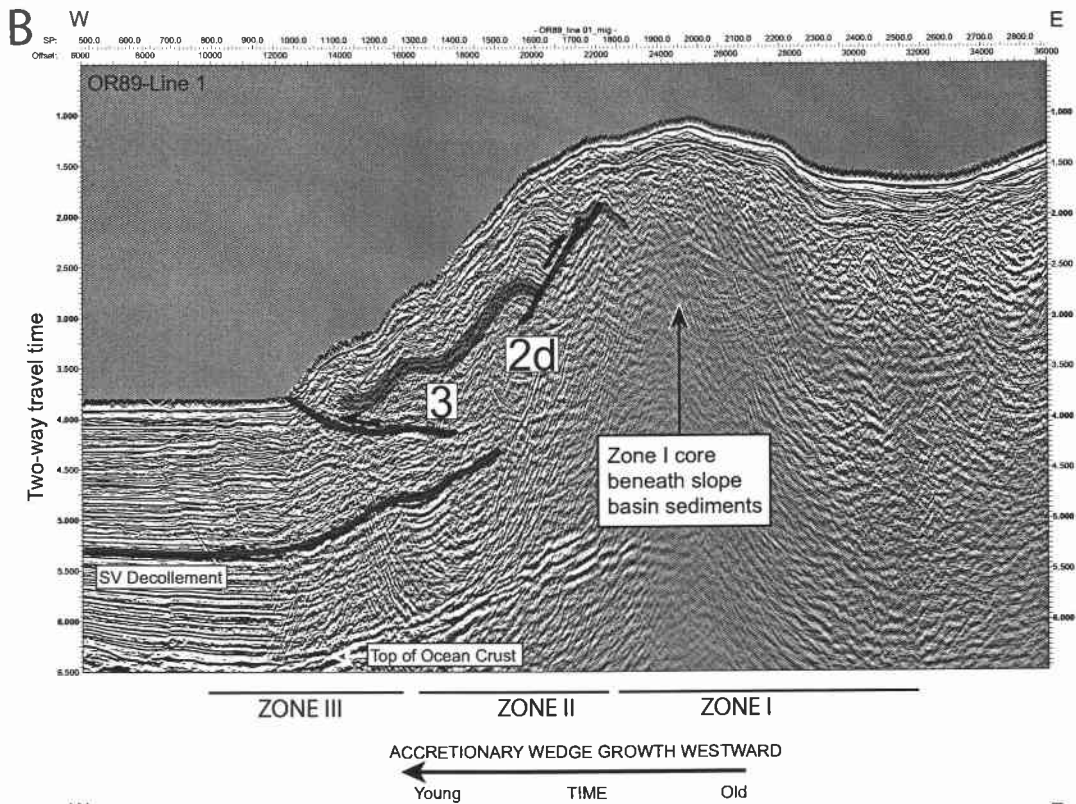


Figure 3-9 (Continued).

Structural Vergence and Hydrate Ridge Region Morphology

A summary of the structural vergence variation and the corresponding bathymetry across the Hydrate Ridge region is shown in Figure 3-10. Examination of the bathymetry and expression of the structural vergence across the Hydrate Ridge region suggests slip on seaward vergent structures is reduced, yielding a subdued bathymetric expression, when they are opposed by landward vergent structures. This appears to explain the low bathymetric relief of the Zone I seaward vergent structures compared to the Zone II structures in the region north of Hydrate Ridge and at southern Hydrate Ridge (Fig. 3-10). The largest bathymetric feature is northern Hydrate Ridge, which is not opposed by any landward vergent structures in all three regions (Fig. 3-10). These observations suggest that if the same amount of net shortening occurs across strike, then regions with both landward and seaward vergent structures will accommodate more slip on the landward vergent structures than on the seaward vergent ones. It also becomes apparent that northern Hydrate Ridge has such high bathymetric relief because it has accumulated the total shortening that occurred across Zones I and II on only seaward vergent structures through accretion, and likely duplexing at depth, while to the north and south the total shortening that occurred across Zones I and II was distributed across both landward and seaward vergent structures, with the landward vergent structures apparently accommodating a greater portion of the total shortening.

A more shallowly located décollement within seaward vergent portions of the wedge in this region (MacKay, 1995; Figs. 3-4 through 3-9), compared to a deeper décollement in the landward vergent region (north of the Hydrate Ridge region discussed here), permits subduction of more of the abyssal plain stratigraphy in seaward vergent portions of the wedge than in landward vergent portions, and thus, the potential for underplating and duplexing might be greater in seaward vergent portions of the wedge. In the Hydrate Ridge region, the longest history of continued seaward vergence (across strike; in all three zones) occurs at northern Hydrate Ridge, which is also the bathymetric region with the highest relief (uplift). Here the seismic data show evidence for thrust duplexing at depth and the seaward vergent (shallow décollement) structural style permits

Figure 3-10. Summary of structural vergence variation within the three regions (Region north of Hydrate Ridge, Northern Hydrate Ridge, and Southern Hydrate Ridge) and the three structural zones (I-II-III) discussed in the text. Region and zone boundaries are shown as dashed white lines. Structural vergence within each region-zone corridor is shown by black boxes labeled SV (seaward vergence) and LV (landward vergence). Locations of the seismic profiles shown in Figures 3-4 through 3-9 are shown in thin black and labeled by line number. The region at southern Hydrate Ridge where the 3-D seismic survey was collected is shown as a black box. Inset shows schematic composite cross sections from each region (locations of each profile shown as solid black lines (A-C) crossing the black SV and LV boxes on the map.

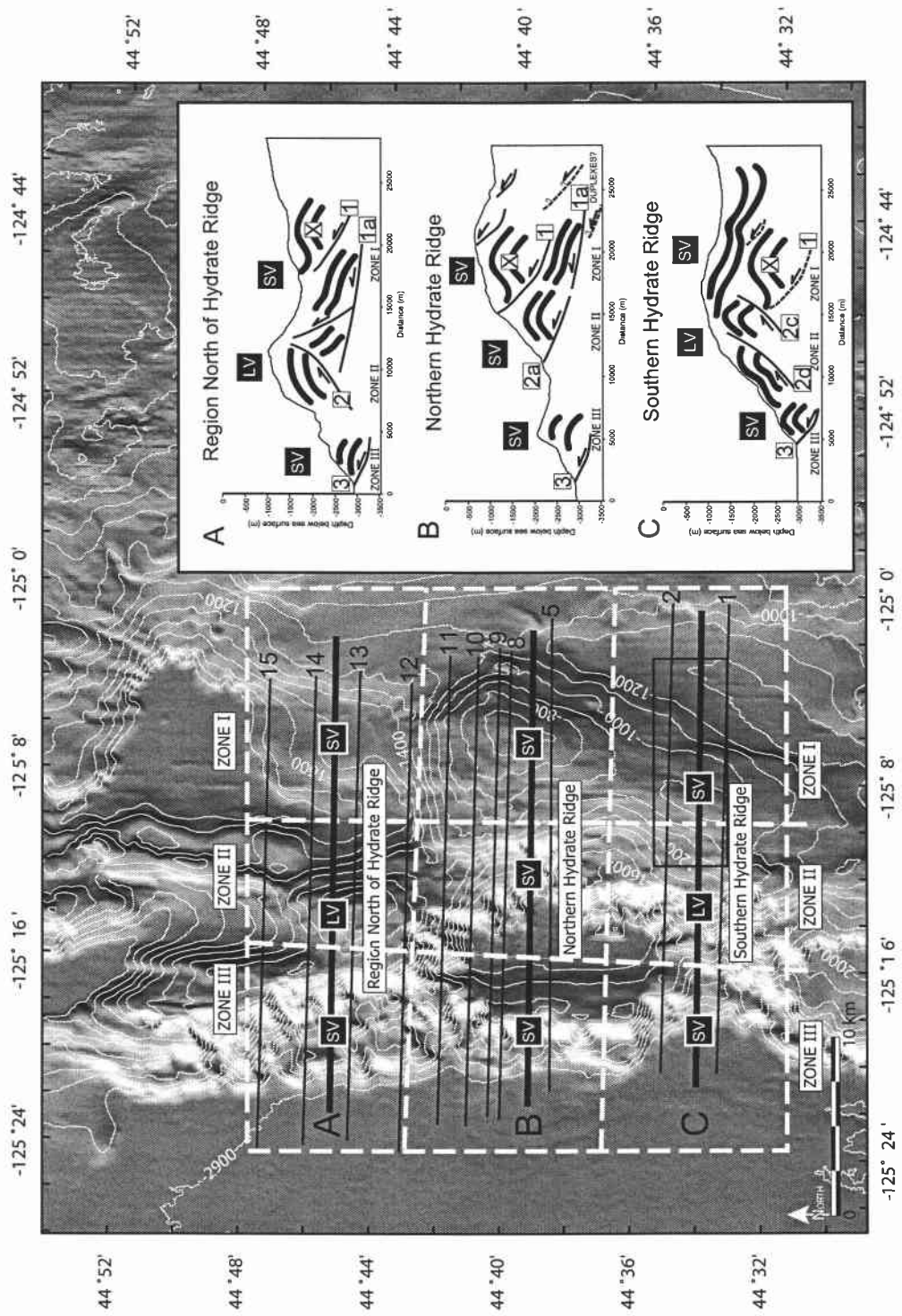


Figure 3-10.

some sediment subduction. The continued subduction of some abyssal plain stratigraphy (beneath the seaward vergent décollement horizon) in the northern Hydrate Ridge region during the accretion of zones I-III increases the potential for underplating of abyssal plain strata and likely promotes the observed deep duplex formation. Both underplating and duplex formation result in thickening of the wedge and are likely the explanation for the observed high relief of northern Hydrate Ridge. The high relief of northern Hydrate Ridge is in contrast to the correlative lower bathymetric relief observed at southern Hydrate Ridge and in the region north of Hydrate Ridge, which as discussed above, are both opposed by Zone II landward vergent structures. In these landward vergent regions, the décollement although not well imaged across the region, likely lies deeper and thus, does not permit abundant abyssal plain sediment subduction.

Daisy Bank and Alvin Canyon Strike-Slip Faults

In addition to the deformation and growth of the accretionary wedge through thrust faults and folds, the Hydrate Ridge region is also affected by two left-lateral strike-slip faults (Fig. 3-3). These faults, initially identified by Goldfinger et al. (1992 and 1997), MacKay et al. (1992) and MacKay (1995) are basement involved structures crossing the Juan de Fuca plate and the wedge at a high angle. They are inferred to be R' Riedel shears in the basement initiated by a right lateral shear couple that is driven by oblique subduction. Because the propagation of the strike slip faults from the basement upward into the accretionary wedge is a function of the coupling across the décollement and the strength of the wedge, they are best identified in seismic reflection profiles and reflected by the bathymetry on the abyssal plain near the deformation front and farther back in the wedge, where older and more dewatered sediments exist. The décollement beneath the lower slope is inferred to be too poorly coupled (evidenced by landward vergence) for the strike slip faults to propagate up through to the seafloor, thus their surface traces are unidentified or broadly distributed (along several splays; e.g. Daisy Bank fault trace, Fig. 3-3) in these regions. The upward propagation of the strike-slip faults from the basement into the accretionary wedge from the abyssal plain to the shelf is shown schematically in Fig. 3-11. Goldfinger et al. (1997) estimated an age of initiation

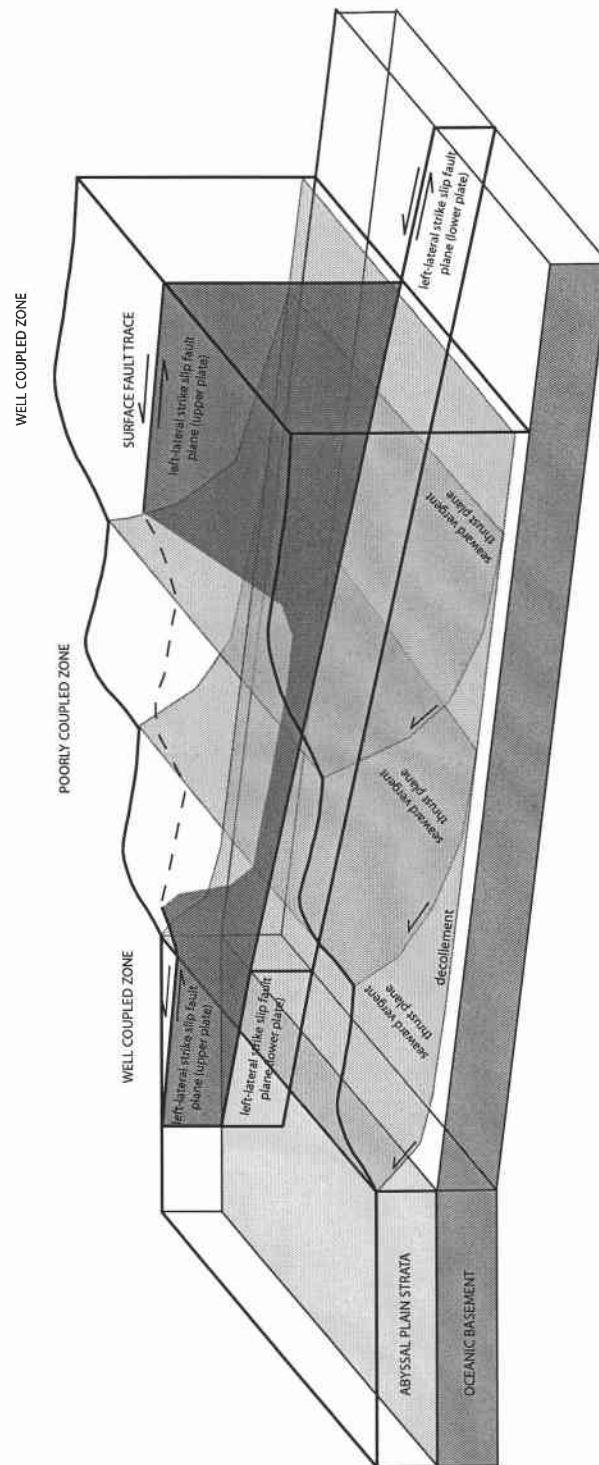


Figure 3-11. Schematic diagram showing the interaction of left lateral strike-slip faults with the accretionary wedge. Notice the successful propagation of the strike slip faults into the upper plate is a function of wedge coupling and strength (as described in the text). Mapped surface traces of the left lateral strike slip faults on the seafloor at the abyssal plain and upper slope (Goldfinger et al., 1997) and diffuse traces on the lower slope support this schematic illustration.

of upper plate motion near the abyssal plain/deformation front boundary for both the Daisy Bank and Alvin Canyon faults of 0.38 ± 0.05 Ma. The strike slip fault surface traces across the wedge and submersible observations of Holocene slip of the Daisy Bank fault at Daisy Bank, east of Hydrate Ridge (Goldfinger et al., 1996b) suggests that these faults are active and likely long lived.

Evidence for Clockwise Block Rotation

Based on the mapped structures, the Hydrate Ridge region appears to be bound at its north and south end by the left lateral strike slip Daisy Bank and Alvin Canyon faults, respectively (Fig. 3-3). The geometry and slip direction of these faults imply clockwise rotation of the block contained between them within an overall right lateral shear couple (Goldfinger et al., 1997). Right-lateral shear, driven by oblique subduction, of the Hydrate Ridge block could be responsible for the apparent clockwise rotation of Hydrate Ridge. The eastern edge of the block likely occurs near the backstop for the Quaternary wedge, which may occur at the contact with the Eocene oceanic Siletzia terrane (Fleming and Tréhu, 1999) or the outer arc high (McNeill et al., 2000). The boundary with the Siletz terrane may be a more likely position of the backstop, however, as its western edge is cut by a right lateral strike-slip fault (Fulmar Fault; Snavely et al., 1980), which could serve as the eastern edge of the right-lateral shear couple responsible for the left lateral Daisy Bank and Alvin Canyon strike slip faults. West of this backstop boundary, the trends of folds within the wedge are N-S (Goldfinger et al., 1992; 1997) suggested a maximum principal stress orientation of east-west. Given this stress orientation, the strike of Hydrate Ridge ought to be approximately N-S. Instead, the strike of Hydrate Ridge (or Zone I deformation) is rotated 020° . This apparent deviation in the strike orientation of Zone I structures is consistent with that predicted during clockwise block rotation between the two left-lateral strike slip faults within an overall right lateral shear couple. The concentration of tightly spaced structures at the north end of the eastern slope basin adjoining Hydrate Ridge and the wider spacing of structures at the south end of this basin serve as additional evidence for clockwise block rotation. Continued mapping of the Zone II landward vergent fault in the region north of Hydrate Ridge (fault

2; Figs. 3-4 and 3-5) to the north also shows its strike is rotated slightly to the NE (Fig. 3-3). Near the deformation front, the bulge in the abyssal plain proto-thrusts SW of Hydrate Ridge and their decrease to the north (Fig. 3-3) provide additional evidence for clockwise block rotation of the Hydrate Ridge region during the accretion of the Zone III structures as well.

Relative Timing of Major Tectonic Events

Northern Hydrate Ridge and the First Accretionary Ridge

The ages of the sediments at northern Hydrate Ridge and the first accretionary ridge (to the west) are constrained by ODP Leg 146 biostratigraphy. At ODP Site 892A on the crest of northern Hydrate Ridge (Fig. 3-2) the ages of the upper 176.5 m of stratigraphy determined from diatom, radiolarian, and foraminifer biostratigraphy range from late Miocene to late Pliocene, (Fournanier, 1995; Caulet, 1995; Zellers, 1995) with a thin cap (upper 3 meters) of early Pleistocene age sediments (deposited sometime between 1.6-0.9 Ma; Fournanier and Caulet, 1995). The sediments at Site 892A are deformed by one or more thrust faults, and several hiatuses in sedimentation were identified from the biostratigraphic work. The lithofacies, in terms of grain size, bulk composition, and sedimentary structures, of the recovered sediments at ODP Site 892A are interpreted to be equivalent to the late Pliocene-early Pleistocene abyssal plain section recovered at DSDP Site 174 (Shipboard Scientific Party, 1994. Site 892). This suggests abyssal plain stratigraphy was uplifted and deformed at Site 892A as it was accreted to the margin. Based on the range of ages possible for the upper 3 m of stratigraphy at Site 892A (1.6-0.9 Ma), the sediments recovered near the seafloor at Site 892A could be as young as 0.9 Ma or as old as 1.6 Ma. If they are indeed 0.9 Ma, they are likely a thin slope basin sequence that was deposited above a growing northern Hydrate Ridge, which has since been mostly eroded away, filling the slope basins to the west and east. Evidence for a thick sequence of slope basin strata deposited over a growing Hydrate Ridge structure is found at southern Hydrate Ridge (Tréhu et al., 2003; Chevallier, 2004), which has preserved this slope basin sequence due to less uplift and erosion than northern Hydrate Ridge. If the upper 3 m of sediments are as old a 1.6 Ma they are consistent with

the age of the youngest underlying abyssal plain stratigraphy (1.7-1.6 Ma; Fourtanier and Caulet, 1995) and no younger slope basin stratigraphy is preserved at northern Hydrate Ridge.

The older sediments at ODP Site 892 are in contrast to the middle-late Pleistocene sediments recovered at ODP Site 891, to the west, on the first accretionary ridge (Fig. 3-2). The age of the sediments at Site 891 is based on foraminifers, radiolarians, and measured normal polarity paleomagnetism and suggests the recovered sediments above the frontal thrust were deposited during the last 0.37 m.y. (Shipboard Scientific Party, 1994 explanatory notes; Zellers, 1995). Comparison of the lithology at ODP site 891 with DSDP Site 174 and the seismic reflection data suggests that the stratigraphic section at Site 891 represents uplifted abyssal plain deposits related to the Astoria fan (Shipboard Scientific Party, 1994; site 891). Because the core recovery and microfossil abundance was low, higher resolution age constraint within the section at ODP Site 891 is not possible. Nevertheless, this implies faulting and folding of the stratigraphy at ODP Site 891 must have occurred sometime after deposition of these sediments or within the middle to late Pleistocene (< 0.37 Ma). Using a separate approach, Westbrook (1994) used the plate convergence rate and critical taper theory to estimate uplift of ridge one at ODP Site 891 and concluded uplift is unlikely to be older than 0.3 Ma and probably initiated about 0.25 Ma, consistent with the estimate based on the biostratigraphy.

Because the sediments at both sites 891 and 892 likely represent uplifted and accreted abyssal plain section, the folding and thrusting at each site must have occurred after the deposition of the youngest preserved abyssal plain sediments that are present at each site. Because there could have been erosion or depositional hiatuses at each site and deposition during the accretion process, the youngest age of the uplifted abyssal plain sediments preserved at each site represents the oldest time the deformation at each site could have began. Because the age of the youngest sediments deformed by the frontal thrust, however, cannot be determined at ODP Site 891, we will use the range of 0.30-0.25 Ma given by Westbrook (1994) for the timing of uplift of ridge one. We interpret

the youngest uplifted abyssal plain deposits at ODP site 892A to be in the range of 1.7-1.6 Ma.

The above age relationships imply that because Hydrate Ridge lies farther east in the accretionary wedge and contains older deformed sediments than the first accretionary ridge, the difference in age of deformed sediments at ODP Site 892 and the timing of uplift of ridge one at ODP Site 891 can be used as a proxy for the maximum difference in timing of accretion into the wedge. This implies northern Hydrate Ridge (Zone I deformation) was incorporated into the wedge sometime after the early Pleistocene (1.7-1.6 Ma) and the major period of uplift was likely completed by the late Pleistocene (0.30-0.25 Ma), when the earliest age of ridge one uplift (Zone III deformation), could have occurred. Because the wedge builds westward with continued accretion, the uplift of ridge one at the deformation front initiates a time when shortening, previously taken up on structures to the east, was beginning to be accommodated on the first ridge frontal thrust. For this reason, we suggest that most of the uplift of Hydrate Ridge (Zone I deformation) was completed by the time ridge one or Zone III deformation was initiated.

Linking Northern and Southern Hydrate Ridge

The similarity in structural origin inferred in this paper between the Zone I seaward vergent part of the wedge at northern Hydrate Ridge and the Zone I core of accretionary material at southern Hydrate Ridge is supported by comparison of the ages of deformed sediments at each location. Diatom and nannofossil biostratigraphy completed during ODP Leg 204 drilling on southern Hydrate Ridge (in particular site 1244; Fig. 3-2) yielded an age range of early Pleistocene (1.7-1.6 Ma) for the upper portion of the older core of accretionary wedge material underlying the younger Pleistocene to recent slope basin stratigraphy at southern Hydrate Ridge (Shipboard Scientific Party, 2003-site 1244). The age of the youngest deformed sediments recovered at Northern Hydrate Ridge (1.7-1.6 Ma) is consistent with the age at the top of the old core of accretionary wedge material at southern Hydrate Ridge (1.7-1.6 Ma). This implies that a similar age stratigraphic sequence is deformed at each location and is consistent with a model of accretion in which the core of southern Hydrate Ridge and

northern Hydrate Ridge were incorporated into the wedge from the abyssal plain at approximately the same time. Currently, the uplift of northern Hydrate Ridge has exposed this older stratigraphic package at the seafloor surface, whereas at southern Hydrate Ridge less uplift results in the burial of the core of 1.7-1.6 Ma and older stratigraphy beneath the younger overlying slope basin sediments (Tréhu et al., 2003).

Southern Hydrate Ridge Landward Vergence

The above age constraints imply that the major period of uplift and seaward vergent slip along Zone I structures in the northern and southern Hydrate Ridge regions occurred sometime after the early Pleistocene (1.7-1.6 Ma) and was mostly completed by the late Pleistocene (0.3-0.25 Ma), which is the estimated age for the initiation of ridge one uplift as described above. Because of the position of Zone II deformation within the wedge (between Zones I and III), the timing of Zone II accretion into the wedge (landward vergence in the region north of Hydrate Ridge and on southern Hydrate Ridge and seaward vergence on northern Hydrate Ridge), must have occurred sometime within this same time window (1.7-1.6 Ma to 0.3-0.25 Ma).

Recent structural mapping within the 3-D seismic survey on southern Hydrate Ridge (Chevallier, 2004), coupled with the ODP Leg 204 biostratigraphic data (Shipboard Scientific Party, 2003- Site 1245), has constrained the timing of the most eastward landward vergent folding, and thus thrusting within Zone II at southern Hydrate Ridge (Fig. 3-9, OR-89 Line 2). Through sequential unfolding of biostratigraphically constrained horizons, Chevallier (2004) suggests that initiation of the most eastward landward vergent fold began 1.2 Ma and was completed by 0.3 Ma. We suggest that the period of landward vergence at southern Hydrate Ridge was coincident with the period of landward vergence in the region north of Hydrate Ridge and seaward vergence at northern Hydrate Ridge, as all three regions appear to lie within the same location along strike within the wedge (the Zone II region). This implies that Zone II deformation throughout the region most likely occurred between 1.2 Ma and 0.3 Ma.

Discussion

Accretionary Wedge Construction

Accretionary wedge growth through time by adding material through continued accretion at the deformation front (via frontal accretion or underplating) is a well documented model for the development of the wedge. However, contemporaneous shortening can occur along major or even minor faults across a range of structures throughout the wedge at any time (via "out of sequence thrusts", internal folding, small scale internal faulting, and ductile deformation at depth (Moore and Silver, 1987). In general, the tectonic activity on thrust faults and folds, however, typically decreases with distance from the deformation front. This is due in part to (1) the rotation of faults from shallow to steeply dipping as the wedge deforms; once fault dips become too steep it is mechanically more efficient to build the wedge outward via a new more shallowly dipping thrust plane than to sustain activity on the older faults and (2) because the strength of the wedge increases with distance from the deformation front due to compaction and pore fluid dewatering processes. The results presented here suggest that the wedge built outward in a series of three main phases (Zones I-III) since the early Pleistocene (<1.7 Ma). As mentioned above, some continued slip on structures within these three zones is expected and observed as the wedge develops through time, for example, on northern Hydrate Ridge some Zone I structures are likely active during Zone II wedge building. However, here we observed three periods of time when three different portions of the wedge were most active, suggesting the three wedge building events.

If we assume wedge construction generally progressed from east to west and occurred through three main phases of deformation, it appears the Zone I structures developed during a time window spanning 1.7-1.2 Ma. (or during a 0.5 m.y. period), the Zone II structures developed over 1.2-0.3 Ma. (during a 0.9 m.y. period), and the Zone III structures developed from 0.3 Ma to the present (during the last 0.3 m.y). The duration of tectonic activity with time within these three regions appears to correlate well with the number of structures and amount of uplift present across the Hydrate Ridge region. The major activity of the Zone II structures occurred over the longest period of time (0.9

m.y.). In the region north of Hydrate Ridge, this corresponds with the greatest bathymetric relief of the wedge in that region, which is cored by one landward vergent thrust fault. In this same zone to the south, at northern Hydrate Ridge, there is also an abrupt increase in the bathymetric relief of the Zone II and the Zone I seaward vergent structures, resulting in large bathymetric relief of northern Hydrate Ridge. To the south, the Zone II structures consist of two landward vergent thrust faults. The bathymetric relief of Zone II at southern Hydrate Ridge is less than that of Zone II in the region north of Hydrate Ridge, even though they are both shortening via landward thrusts. The difference in bathymetric relief is likely due to the presence of the second landward vergent thrust fault at southern Hydrate Ridge, which accommodates some of the slip that to the north is accommodated mostly on a single landward vergent thrust.

Landward Vergence and the Deposition of the Astoria Fan

Possible explanations for the origin of landward vergence in accretionary wedges are (1) a seaward dipping backstop; (e.g. Byrne et al., 1993) and (2) high pore fluid pressure and thus low basal shear stress (Seely, 1977; Byrne et al., 1993). MacKay (1995) also adds to this list (3) an arcward dipping décollement surface and (4) the strength of the backstop. Along the Washington and northern Oregon portion of the Cascadia margin, Seely (1977) proposed the rapid deposition of the Nitinat and Astoria submarine fans onto the abyssal plain during the Pleistocene as the major mechanism responsible for high pore fluid pressure and thus landward vergence (Fig. 3-3). MacKay (1995) added that in addition to the change in pore pressure due to the submarine fans, an arcward dipping décollement and to a lesser degree a strong backstop might also be needed to promote landward vergence. Across the Hydrate Ridge region, where vergence has changed across strike from seaward vergent (Zone I) to landward vergent (Zone II) in the region north of Hydrate Ridge and at southern Hydrate Ridge, but not at northern Hydrate Ridge, an arcward dipping décollement, within the overlying abyssal plain stratigraphy that lies parallel to the dip (4-5°; Tréhu et al., 1994) of the underlying Juan de Fuca plate, and a potentially strong backstop (the Siletz terrane (Fleming and Tréhu, 1999) or the outer forearc high (McNeill et al., 2000) have likely existed and remained

relatively constant boundary conditions for the portion of the accretionary wedge formed during the last ~1.7 Ma (when the Zone I and Zone II structures initiated in the Hydrate Ridge region). The only remaining mechanism for preferred landward vergence that has varied over this time interval is high pore fluid pressure, which likely increased after the rapid deposition of the Pleistocene submarine fans on the abyssal plain. Because southern margin of the Astoria fan extends across the abyssal plain south of the Hydrate Ridge region (Fig. 3-1), perhaps the landward vergent portion of the wedge in the Hydrate Ridge region (Zone II north and south of northern Hydrate Ridge) accreted since the deposition of the fan may have been susceptible to landward vergence through high pore pressure induced by rapid fan deposition.

McNeill et al. (2000) suggest the initiation of major Astoria fan deposition on the abyssal plain was linked to near complete filling of shelf forearc basins and subsequent breaching of the outer arc high that trapped sediments in them about 1.4-1.3 Ma. Slope basins and eventually the trench on the abyssal plain would be the first portions of the margin to fill with sediment during breaching of the outer arc high. Subsequent fan development would propagate the fan westward with time to the location of DSDP site 174 (Fig. 3-1), where the base of the fan sediments is estimated to be 0.76 Ma in age (Goldfinger et al., 1996a; Ingle, 1973). Although accretion of part or most of the earliest version of the Astoria fan with time due to continued subduction of the Juan de Fuca plate occurred, the rate of fan development was greater than the consumption of the fan during this time, resulting in the presence of the modern surviving fan on the abyssal plain. The timing of initiation of the Astoria fan is important as it constrains the timing of any landward vergence that is attributed to rapid deposition of fan sediments to <1.4-1.3 Ma. In this paper, we suggest the landward vergence documented in Zone II of the Hydrate Ridge region initiated ~1.2 Ma and was mostly completed by ~0.3 Ma. This timing is coincident with the presence of Astoria fan on the abyssal plain, and therefore as in Washington and northern Oregon, we suspect rapid deposition of the fan sediments and subsequent high pore fluid pressures and low basal shear stress on the décollement is

likely the cause of the Zone II landward vergence in the region north of Hydrate Ridge and on southern Hydrate Ridge.

Different from the Washington and northern Oregon margins, however, the Zone II landward vergence at Hydrate Ridge is (1) not continuous along strike (e.g. Zone II at northern Hydrate Ridge is seaward vergent) and as discussed below, (2) did not continue with time until the present (the deformation frontal thrust of Zone III is seaward vergent; (see *Cessation of Landward Vergence at the Deformation Front*). North of the Hydrate Ridge region discussed here, the correlative portion of the Zone II wedge remains landward vergent along strike (MacKay et al., 1992). In the correlative Zone II region to the south, the vergence is seaward (Goldfinger et al., 2000) and remains seaward southward to the northern California margin (Goldfinger et al., 2000). This suggests that the along strike mixed vergence zone (Zone II throughout the Hydrate Ridge region) that lies between landward vergent structures in the north and seaward vergent structures to the south is quite narrow. The abrupt along strike change to a seaward vergent wedge south of the Hydrate Ridge region and landward vergent wedge to the north, with a narrow transition zone of mixed, along strike, vergence in between (Zone II at Hydrate Ridge), suggests the effect of the rapid deposition of the Astoria fan as a mechanism for landward vergence was slightly variable in Zone II in the Hydrate Ridge region and not effective south of Hydrate Ridge, where seaward vergence prevails. If rapid fan deposition is the mechanism responsible for at least the landward vergent structures of Zone II, perhaps variability in fan thickness, or more precisely, thinning of the fan stratigraphy on the abyssal plain to the south, is responsible for the variability in along strike structural vergence in the Hydrate Ridge region and the lack of landward vergence south of Hydrate Ridge. In the region farther south of Hydrate Ridge a thinning Astoria fan near its southern terminus may be a possible explanation for the lack of landward vergence, however, in the Hydrate Ridge region and to the north, MacKay (1995) observes, on N-S seismic line OR89-Line 37 across the abyssal plain, that the total sediment thickness on the abyssal plain is locally relatively uniform, suggesting a

thinning Astoria fan is not the likely explanation for the variability in Zone II vergence in the Hydrate Ridge region.

An alternative explanation for the Zone II structural variability may be that the thickness of the abyssal plain stratigraphy above the incipient décollement on the abyssal plain varies in an E-W direction and is modified by slip along the strike slip faults. MacKay (1995) show that the abyssal plain sediments thicken toward the east as they approach the deformation front and where they are offset by the left-lateral strike slip faults, thicker sediments on the north sides of the faults are juxtaposed against thinner ones to the south. This variation in thickness across the strike slip faults results in subtle along strike thickness changes in the abyssal plain stratigraphy above the incipient décollement across the Hydrate Ridge region. The variations in total sediment thickness above the incipient décollement have the effect of changing the lithostatic sediment load at any one location, potentially modifying the pore fluid pressure at the depth of the incipient décollement. A decrease in the thickness of the sediments above the incipient décollement could result in a decrease in the pore fluid pressure, favoring a seaward vergent structure to develop, whereas an increase in the thickness might favor high pore fluid pressures on the décollement, yielding a landward vergent structure. During the accretion of the Zone II portion of the wedge, the same sediment thickness variability observed on the modern abyssal plain outboard of the deformation front by MacKay (1995) was also likely present. We hypothesize that this along-strike sediment thickness variability may have been sufficient to create the Zone II along strike vergence variability documented here, however, a definitive explanation for the Zone II structural variability awaits future work.

Cessation of Landward Vergence at the Deformation Front

Perhaps the most intriguing across-strike vergence change in the Hydrate Ridge region occurs at the deformation front (Zone III), which contains seaward vergent structures throughout the region. This is in contrast to the mixed vergence (landward-seaward-landward) documented along strike in Zone II throughout the region and similar to the seaward vergence documented in Zone I. At the deformation front north of the

Daisy Bank fault, the structural vergence is landward, similar to the rest of the Pleistocene portion of the wedge, and south of the Daisy Bank fault (all the way to the Rogue Canyon region; Fig. 3-1) the frontal thrust is dominated by seaward vergence. If the deposition of the Astoria fan was responsible for the Zone II landward vergence in the region north of Hydrate Ridge and on southern Hydrate Ridge, it would seem likely that landward vergence would continue to prevail in these region during Zone III deformation as well, as it does off of northern Oregon and Washington. Zone III is seaward vergent, however, everywhere in the Hydrate Ridge region.

Similar across strike disruption of landward vergent structures, associated with the rapid deposition of the Astoria fan, does occur locally in the landward vergent region just north of Hydrate Ridge as well, where the left lateral Wecoma strike-slip fault intersects the deformation front (Fig. 3-1). In this region, Tobin et al. (1993) document local seaward vergence of the frontal thrust where the strike slip fault intersects the wedge. Through a series of Alvin dives, abundant chemosynthetic biological communities, pervasive veining and fracturing, and extensive carbonate cementation along splays of the Wecoma fault were observed, documenting its role as an active fluid flow conduit. Based on these observations, Tobin et al. (1993) suggested that the Wecoma fault acts as a drain for overpressured fluids located on the incipient décollement. The escape of highly overpressured fluids from the incipient décollement results in an increase in the effective basal stress, which results in local seaward vergence. The pervasive occurrence of landward vergent structures in the region to the north due to an inferred high pore fluid pressurized décollement caused by the rapid deposition of the Astoria Fan favors this explanation for localized seaward vergence. In the Hydrate Ridge region, the Daisy Bank and Alvin Canyon faults intersect the accretionary wedge in the same manner as the Wecoma fault. In this case, however, the distance between the two strike-slip faults is quite close, and we suggest the deformation frontal thrust (in Zone III) is seaward vergent across the region in the same manner as suggested for the Wecoma fault to the north. Although, active fluid venting near the deformation front associated with the strike-slip faults in the Hydrate Ridge region has not been documented, the Daisy Bank and Alvin

Canyon faults, both similar to the Wecoma fault to the north, offset both the basaltic basement and the abyssal plain sections (Goldfinger et al., 1997), suggesting their probable role as effective fluid conduits.

In addition to the structural similarity between these three strike-slip faults and their apparent effect on the vergence of the frontal thrust, we also have some indication of the timing of frontal thrust uplift and strike-slip fault initiation on the abyssal plain. Here, we suggest that the landward vergence documented on southern Hydrate Ridge (Chevallier, 2004) and inferred across the Hydrate Ridge Zone II region, was most active sometime between ~ 1.2 Ma and was mostly completed by ~ 0.3 Ma. The cessation of landward vergence appears to coincide with the estimate for the uplift of the seaward vergent frontal thrust (0.3-0.25 Ma; Westbrook, 1994). Goldfinger et al. (1997) estimated an age for initiation of motion along both the Daisy Bank and Alvin Canyon faults on the abyssal plain of 0.38 ± 0.05 Ma. The timing of the above events supports the assertion that initiation of motion on the strike slip faults may have served to stop the Zone II landward vergence in the Hydrate Ridge region and be responsible for the seaward vergent frontal thrust fault.

Clockwise Block Rotation

The surface traces of both the Daisy Bank and Alvin Canyon faults are not only observed near the deformation front but also within the older portion of the wedge, east of Hydrate Ridge (Fig. 3-3). The presence of these strike slip fault traces suggests the strike slip faults are long lived. Because the age of the accretionary wedge is younger toward the west, and the strike slip faults remain active away from the deformation front (e.g. Daisy Bank east of Hydrate Ridge has post-12 ka activity; Goldfinger et al., 1997) and likely continually deform the wedge as it builds out westward, the block contained between them, farthest back in the wedge, will have experienced the cumulative effect of rotation through time. This means that between the left lateral strike slip faults, the older structures farther back in the wedge should be more rotated than those closer to the deformation front. The best evidence for block rotation between the strike slip faults comes from the distribution and spacing of structures surrounding Hydrate Ridge and the

apparent $\sim 20^\circ$ clockwise rotation of the ridge from a N-S strike. We suggest that the $\sim 20^\circ$ clockwise rotation of Hydrate Ridge, relative to a N-S strike, was a result of coincident slip along the strike slip faults during and since the accretion of this portion of the wedge (during the last 1.7 Ma). This is in contrast to a model in which original accretion to the margin resulted in structures with a N 20° E strike, which we do not favor because equivalent structures to the north, away from the strike slip faults, strike N-S. In addition, the bulge in abyssal plain protothrusts suggests that a more recent phase of this rotation is in effect, with propagation of frontal thrusts farther toward the west in the southwest corner of the block and dissipation of these structures to the north. These observations suggest that clockwise block rotation between the left-lateral strike-slip faults accompanied east-west thrusting and folding during the tectonic evolution of the entire Hydrate Ridge region. Clockwise block rotation and northward migration of the lower portion of the Cascadia forearc through slip along the nine identified left-lateral strike slip faults is predicted as the basement involved faults propagate up into the wedge with continued convergence (Goldfinger et al., 1997). Although previous direct evidence for block rotation along the lower slope of the margin is lacking, a notable change in the strike of many of the strike-slip fault traces within the older portion of the accretionary wedge exists (Goldfinger et al., 1997), lending support to the block rotation model and northward translation of the forearc with time.

There are two potential explanations for why identification of other clockwise rotated structural blocks within the Cascadia accretionary wedge is difficult off the Washington and northern Oregon margin and off the southern Oregon margin. The first involves the mechanics of the propagation of the strike slip faults into the upper plate. When the wedge is more coupled (high basal shear stress) and strong (dewatered), the strike slip faults are more likely to propagate up into the accretionary wedge (Fig. 3-11; Fig. 3-3, as evidenced by their good expression on the abyssal plain and further back in the wedge; e.g. at Daisy Bank). They then deform the block contained between them, resulting in clockwise block rotation. In the Hydrate Ridge region, there are more seaward vergent than landward vergent thrust faults (Fig. 3-10), suggesting in general

that the region is more coupled (high basal shear stress) at the décollement interface compared to that inferred in a landward vergent dominated (low basal shear stress) portion of the wedge. When the wedge is more coupled, the strike slip faults propagate more easily up into the wedge, thus deforming the structures of the upper plate. This suggests that the deformation associated with the strike-slip faults in regions dominated by landward vergence may be minimized, as the high pore fluid pressure (low basal shear stress) associated with landward vergence may decrease coupling of the wedge. Perhaps future work to identify additional evidence for clockwise block rotation between the other strike slip faults along the margin should focus on the regions of seaward vergence rather than within the landward vergent region of northern Oregon and Washington. To the south, offshore southern Oregon and Northern California, although seaward vergence exists and there are three left-lateral strike slip faults (Goldfinger et al., 1997), giant submarine landslides have sufficiently disrupted the seafloor bathymetry and stratigraphy (Goldfinger et al., 2000), making identification of rotated structural blocks virtually impossible. In addition to the above explanations, limited seismic data equivalent to the survey used here exists in the regions to the north and south of Hydrate Ridge. Perhaps future seismic and high resolution bathymetry surveys will potentially identify additional rotated blocks within the wedge.

Northward Migration of the Cascadia Forearc

If the left lateral strike slip faults are responsible for the clockwise block rotation of the Hydrate Ridge region, their presence within the wedge during the accretion of Hydrate Ridge structures during the last 1.7 Ma is necessary. Oblique subduction of the Juan de Fuca plate beneath North America initiates a right lateral shear couple within the Cascadia forearc region. This oblique subduction and right lateral shear coupled with tectonic block rotation of the forearc likely driven by Basin and Range extension (Humphreys and Hemphill-Haley, 1996; McCaffrey et al., 2000) results in the overall northward translation of the forearc with time. Evidence for the northward translation of the Cascadia forearc is documented onshore through paleomagnetic measurements that show clockwise block rotation in Oregon coast basalts (e.g. Wells and Simpson, 2001)

and GPS measurements (e.g. McCaffrey et al., 2000), on both long and short timescales, respectively. The GPS rates of forearc rotation (about a pole near the Washington-Oregon border at $\sim 131^\circ$ longitude) are consistent with the geologic rates once the elastic component of the GPS signal is removed (McCaffrey et al., 2000). Evidence for the northward translation of the offshore part of the forearc exists by the presence of nine left-lateral strike slip faults (Goldfinger et al., 1997) which formed in response to a right lateral shear couple initiated by oblique subduction. Northward translation of the outer forearc region requires that the western ends of the strike slip faults also translate northward with time. This process is most easily visualized by sliding a stack of books on end between your hands (top and bottom of the books perpendicular to your hands) via right lateral shear, where the boundaries between books are the strike slip faults. This motion with time results in migration of the left side of the books (or left ends of the strike slip faults) with continued right lateral shear. In the Hydrate Ridge region, the northward translation of the forearc could mean that the position of the strike slip faults in the past was south of their current position, perhaps even out of the Hydrate Ridge region entirely. To address this possibility we calculate (below) the position of the strike slip faults at 1.2 Ma. We choose this time, which is just after the accretion of the Zone I deformation, because the best evidence for clockwise block rotation associated with the presence of the strike slip faults occurs within this portion of the wedge, and the wedge must have been mostly accreted for the strike-slip faults to have rotated it.

GPS (Global Positioning System) results at the Newport, central Oregon site suggest the onshore portion of the central Cascadia forearc is moving northward at a rate of about 10 mm/yr (McCaffrey et al., 2000). The GPS measurements record both an elastic (recoverable) subduction zone signal and permanent (non recoverable) deformation component. At the Newport site on the coast, the elastic component of the 10 mm/yr is about 3-6 mm/yr, while the remaining 4-7 mm/yr reflects permanent (non recoverable) deformation. Base on the modeling of McCaffrey et al. (2000), the projected permanent rate of northward migration of the submarine forearc near the deformation front west of Newport is 15 mm/yr. The submarine forearc likely

accommodates this northward component of translation through slip along the left-lateral strike slip faults, slip along right lateral margin parallel strike slip faults (e.g. the Fulmar fault of Snively, 1980), or through oblique slip along the accretionary wedge thrust faults. Goldfinger et al. (1997) calculated slip rates for five of the nine strike slip faults present along the Washington and Oregon margins. To calculate the total amount of the north component of slip that could be accommodated by the strike slip faults near Hydrate Ridge, we use the fault strike and the calculated slip rates (Goldfinger et al., 1997) Alvin Canyon (6.2 mm/yr) fault and the minimum margin wide slip rate of 5.5 mm/yr applied to the three strike slip faults south (for which slip rates have not been determined) to calculate the cumulative north component of slip that could be accommodated along the strike slip faults at the latitude of Hydrate Ridge. The result suggests about 10 mm/yr, northward component of the forearc slip, at the latitude of the Hydrate Ridge region, could be accommodated along the strike slip faults. This is quite similar (given the assumed estimates of slip rate for the 3 strike slip faults to the south of the Alvin Canyon fault) to permanent northward rate of 15 mm/yr projected from the GPS data for this region, suggesting the strike slip faults likely accommodate most of the northward migration of the submarine forearc.

These constraints suggest that if the strike slip faults were present just after the accretion of Zone I structures in the Hydrate Ridge region (~1.2 Ma), they should have migrated northward since that time approximately 12 km, to their present locations. Positioning of the western ends of the Daisy Bank and Alvin Canyon faults 12 km southward from their present location implies that the strike slip faults would have still encompassed Hydrate Ridge. Although evidence in the seismic data examined here for the presence of this potentially older strand of the Daisy Bank fault ~12 km south of its current position is lacking, a northwest oriented flank of a submarine bank about 12 km south of Daisy Bank could be evidence of past left lateral slip on this now abandoned fault strand. Abandoned traces of the strike-slip faults in the upper plate as they are translated northward with time were suggested by Goldfinger et al., 1997, and other examples exist throughout the accretionary wedge.

Structural Control on Dewatering of Wedge at Hydrate Ridge

The fluid venting manifestations on the crest of northern Hydrate Ridge are very extensive, as imaged on deep-towed sidescan sonar data, compared to those on southern Hydrate Ridge (Johnson et al., 2003). The existence of duplexed seaward vergent thrust faults beneath northern Hydrate Ridge have likely aided not only in its uplift but also in providing multiple deep fluid migration pathways to facilitate the massive fluid expulsion observed at the crest. Duplexing is more prevalent in seaward vergent portions of the wedge in the Hydrate Ridge region because the detachment for such thrusts typically lies above the basement cover contact (MacKay, 1995), leaving a portion of the incoming abyssal plain section to be incorporated into the wedge through duplexing from below. In contrast, landward vergent detachments in this region usually lie closer to the basement/cover contact (MacKay, 1995), virtually offscraping all of the incoming section and incorporating it into the wedge through accretion. On the southern summit of Hydrate Ridge, this type of duplexing is less pervasive, as shortening here during zone I and II deformation was accommodated on both the seaward and the landward vergent thrust faults and folds west of the crest. This results in fewer structural pathways for fluid escape. Southern Hydrate Ridge is also capped by younger slope basin sediments, which could act as an impermeable seal that inhibits fluid escape to the surface. Perhaps these two reasons explain the lack of massive authigenic carbonates on the southern summit. Without an abundance of structural conduits, and with an overlying cap of relatively impermeable sediments sealing their outlet toward the seafloor, stratigraphic conduits for fluid flow become important on southern Hydrate Ridge. The significance of stratigraphic conduits for fluid flow was observed during ODP Leg 204 drilling on southern Hydrate Ridge, which revealed the only authigenic carbonate occurrence there was a result of fluid flow through a high porosity and permeable ash rich stratigraphic horizon (Horizon A; Tréhu et al., submitted).

Conclusions

Based on the results presented in this paper, the following conclusions can be made regarding the construction of the accretionary wedge in the Hydrate Ridge region

during the last 1.7 Ma. (1) The wedge consisted of seaward vergent thrust faults and folds in early Pleistocene time (Zone I deformation everywhere) that were most active between 1.7 and 1.2 Ma. (2) An earlier version of the left lateral strike-slip faults was likely present and perhaps initiated clockwise block rotation of Zone I in the Hydrate Ridge region at or just after this time. (3) The rapid deposition of Astoria fan (1.4-1.3 Ma-recent) likely initiated high pore fluid pressure on the incipient décollement in the Hydrate Ridge region and resulted in the accretion of landward vergent structures in Zone II, which were most active between 1.2 and 0.3 Ma. (4) The most recent phase of wedge construction occurred during Zone III seaward vergent faulting at the deformation front and developed from 0.3 Ma to the present in the Hydrate Ridge region. (5) The cessation of landward vergent Zone II structures and the initiation of Zone III seaward vergence was likely controlled by the propagation of the strike slip faults from the basement to the seafloor ~0.38 m.y. ago. These faults may have acted as release valves for the high pore fluid pressures on the incipient décollement and resulted in the cessation of landward vergence (Zone II) and initiation of seaward vergence (Zone III). (6) Progressive clockwise block rotation between vertical propagating and lateral translating left lateral strike slip faults, as the wedge was constructed through time, results in the N 20° E clockwise orientation of Zone I and II structures in the Hydrate Ridge region. More recently (0.38 Ma), propagation of the strike slip faults vertically toward the seafloor in the Zone III region initiated renewed upper plate activity of the strike slip faults and clockwise block rotation during Zone III deformation, resulting in the map view bulge of abyssal plain protothrusts.

Acknowledgements

Funding for was provided by NSF Grant #OC9731023. Acknowledgement is also made to the Donors of The Petroleum Research Fund, administered by the American Chemical Society, for partial support of this research and the COAS Chipman-Downs Fellowship at Oregon State University. Additional thanks to Marta Torres (OSU) for valuable discussions and Matt Arsenault (OSU) for assistance with the seismic data.

References

- Burbidge, D.R., and Braun, J., 1998, Analogue models of obliquely convergent continental plate boundaries: *Journal of Geophysical Research*, 103, 15,221-15,237.
- Byrne, D.E., Wang, W., and Davis, D.M., 1993, Mechanical role of backstops in the growth of forearcs: *Tectonics*, 12, 123-144.
- Carlson, P.R., and Nelson, C.H., 1987, Marine geology and resource potential of Cascadia Basin, *in* Scholl, G., and Vedder, ed., *Geology and Resource Potential of the Continental Margin of Western North America and Adjacent Ocean Basins*, 6: Houston TX, Circum-Pacific Council for Energy and Mineral Resources, Earth Sciences Series, 523-535.
- Caulet, J.-P., 1995, Radiolarians from the Cascadia Margin, leg 146, *in* Carson, B., Westbrook, G.K., Musgrave, R.J., and Suess, E., eds., *Proc. ODP, Sci. Results, Volume 146 (Pt. 1): College Station, TX, Ocean Drilling Program*, 47-61.
- Chevallier, J., 2004, Seismic sequence stratigraphy and tectonic evolution of Southern Hydrate Ridge [M.S. thesis]: Corvallis, OR, Oregon State University, 117 p.
- Davis, D., Suppe, J., and Dahlen, F.A., 1983, Mechanics of Fold-and-Thrust Belts and Accretionary Wedges: *J. of Geophys. Res.*, B2, 1153-1172.
- Davis, E.E., and Hyndman, R.D., 1989, Accretion and recent deformation of sediments along the northern Cascadia subduction zone: *Geol. Soc. Am. Bull.*, 101, 1465-1480.
- Echavarría, L., Hernández, R., Allmendinger, R., and Reynolds, J., 2003, Subandean thrust and fold belt of northwestern Argentina: Geometry and timing of the Andean evolution: *AAGP Bull.*, 87, 965-985.
- Fleming, S.W., and Tréhu, A., 1999, Crustal structure beneath the central Oregon convergent margin from potential-field modeling: Evidence for a buried basement ridge in local contact with a seaward dipping backstop: *J. of Geophys. Res.*, 104, 20,431-20,447.
- Flueh, E.R., Fisher, M.A., Bialas, J., Childs, J.R., Klaeschen, D., Kukowski, N., Parsons, T., Scholl, D.W., ten Brink, U., Tréhu, A.M., and Vidal, N., 1998, New seismic images of the Cascadia subduction zone from cruise SO108-ORWELL: *Tectonophysics*, 293, 69-84.
- Fourtanier, E., 1995, Neogene diatom biostratigraphy of site 892, Cascadia Margin, *in* Carson, B., Westbrook, G.K., Musgrave, R.J., and Suess, E., eds., *Proc. ODP, Sci. Results, Volume 146 (Pt. 1): College Station, TX, Ocean Drilling Program*, 63-77.
- Fourtanier, E., and Caulet, J.-P., 1995, Siliceous microfossil stratigraphic synthesis of site 892, Cascadia Margin, *in* Carson, B., Westbrook, G.K., Musgrave, R.J., and Suess, E., eds., *Proc. ODP, Sci. Results, Volume 146 (Pt. 1): College Station, TX, Ocean Drilling Program*, 369-374.
- Goldfinger, C., Kulm, L.D., McNeill, L.C., and Watts, P., 2000, Super-scale failure of the southern Oregon Cascadia margin: *Pure and Applied Geophysics*, 157, 1189-1226.

- Goldfinger, C., Kulm, L.D., Yeats, R.S., McNeill, L., and Hummon, C., 1997, Oblique strike-slip faulting of the central Cascadia submarine forearc: *J. of Geophys. Res.*, 102, 8217-8243.
- Goldfinger, C., Kulm, L.D., Yeats, R.S., Appelgate, B., MacKay, M.E., and Cochrane, G.R., 1996a, Active strike-slip faulting and folding of the Cascadia subduction-zone plate boundary and forearc in central and northern Oregon, *in* Rogers, A.M., Walsh, T.J., Kockleman, W.J., and Priest, G.R., eds., *Assessing earthquake hazards and reducing risk in the Pacific Northwest, Volume 1: Washington*, United States Government Printing Office.
- Goldfinger, C., Kulm, L.D., Yeats, R.S., Hummon, C., Huftile, G.J., Niem, A.R., and McNeill, L.C., 1996b, Oblique strike-slip faulting of the Cascadia submarine forearc: The Daisy Bank fault zone off central Oregon, *Subduction: Top to Bottom, Geophysical Monograph 96*, American Geophysical Union, 65-74.
- Goldfinger, C., Kulm, L.D., Yeats, R.S., Appelgate, B., MacKay, M.E., and Moore, G.F., 1992, Transverse structural trends along the Oregon convergent margin: Implications for Cascadia earthquake potential and crustal rotations: *Geology*, 20, 41-144.
- Gulick, S.P.S., Bangs, N.L.B., Shipley, T.H., Nakamura, Y., Moore, G., and Kuramoto, S., 2004, Three dimensional architecture of the Nankai accretionary prism's imbricate thrust zone off Cape Muroto, Japan: Prism reconstruction via an echelon thrust propagation: *J. of Geophys. Res.*, 109, doi: 10.1029/2003JB002654.
- Gulick, S.P.S., Meltzer, A.M., and Clarke Jr., S.H., 1998, Seismic structure of the southern Cascadia subduction zone and accretionary prism north of the Mendocino triple junction: *J. of Geophys. Res.*, 103, 27207-27222.
- Gutscher, M.-A., Klaeschen, D., Flueh, E., and Malavielle, J., 2001, Non-Coulomb wedges, wrong-way thrusting, and natural hazards in Cascadia: *Geology*, 29, 379-382.
- Gutscher, M.-A., Kukowski, N., Malavielle, J., and Lallemand, S., 1996, Cyclical behavior of thrust wedges: Insights from high basal friction sandbox experiments: *Geology*, 24, 135-138.
- Humphreys, E. and Hemphill-Haley, M.A., 1996, Causes and characteristics of western U.S. deformation: *Geol. Soc. Am. Abstracts*, 28.
- Hyndman, R.D., Spence, G.D., Yuan, T., and Davis, E.E., 1994, Regional geophysics and structural framework of the Vancouver Island Margin Accretionary Prism, *in* Westbrook, G.K., Carson, B., Musgrave, R.J., and *al., e.*, eds., *Proc. ODP, Init. Repts., Volume 146 (Pt. 1)*: College Station, TX, Ocean Drilling Program, 399-419.
- Ingle, J.C., 1973, Neogene foraminifera from the Northeastern Pacific Ocean, Leg 18, Deep Sea Drilling Project, *in* Kulm, L.D., von Huene, R., et al., *Initial reports of the Deep Sea Drilling Project, Volume 18*: Washington, U.S. Government Printing Office, 517-567.

- Johnson, J.E., Goldfinger, C., and Suess, E., 2003, Geophysical constraints on the surface distribution of authigenic carbonates across the Hydrate Ridge region, Cascadia margin: *Marine Geology*, 202, 79-110.
- Kulm, L.D., and Fowler, G.A., 1974, Cenozoic Sedimentary Framework of the Gorda-Juan de Fuca Plate and Adjacent Continental Margin- A Review, *in* Dott, R.H., and Shaver, R.H., eds., *Modern and Ancient Geosynclinal Sedimentation*, Special Publication, Society of Economic Paleontologists and Mineralogists, 212-229.
- Kulm, L.D. and von Huene, R., et al., 1973, Initial reports of the Deep Sea Drilling Project, Volume 18: Washington, U.S. Government Printing Office.
- MacKay, M.E., Moore, G.F., Cochrane, G.R., Moore, G.F., and Kulm, L.D., 1992, Landward vergence and oblique structural trends in the Oregon margin accretionary prism: Implications and effect on fluid flow: *Earth and Planetary Science Letters*, 109, 477-491.
- MacKay, M.E., Moore, G.F., Klaeschen, D., and von Huene, R., 1995, The case against porosity change: Seismic velocity decrease at the toe of the Oregon accretionary prism: *Geology*, 23, 827-830.
- Marshak, S., 1986, Structure and tectonics of the Hudson Valley fold-thrust belt, eastern New York State: *Geol. Soc. Am. Bull.*, 97, 354-368.
- McCaffrey, R., Long, M.D., Goldfinger, C., Zwick, P.C., Nabelek, J.L., Johnson, C.K., and Smith, C., 2000, Rotation and plate locking at the southern Cascadia subduction zone: *Geophys. Res. Lett.*, 27, 3117-3120.
- McNeill, L.C., Goldfinger, C., Kulm, L.D., and Yeats, R.S., 2000, Tectonics of the Neogene Cascadia forearc basin: Investigations of a deformed late Miocene unconformity: *Geol. Soc. Am. Bull.*, 112, 1209-1224.
- Miller, M.M., Johnson, D.J., Rubin, C.M., Dragert, H., Wang, K., Qamar, A., and Goldfinger, C., 2001, GPS-determination of along-strike variation in Cascadia margin kinematics: Implications for relative plate motion, subduction zone coupling, and permanent deformation: *Tectonics*, 20, 161-176.
- Moore, C., J., Mascle, A., Taylor, E., Andreieff, P., Alvarez, F., Barnes, R., Beck, C., Bhermann, J., Blanc, G., Brown, K., Clark, M., Dolan, J., Fisher, A., Gieskes, J., Hounslow, M., McLellan, P., Moran, K., Ogawa, Y., Sakai, T., Schoonmaker, J., Vrolijk, P., Wilkens, R., and Williams, C., 1988, Tectonics and hydrogeology of the northern Barbados Ridge: Results from Ocean Drilling Program Leg 110: *Geol. Soc. Am. Bull.*, 100, 1578-1593.
- Moore, J.C., and Silver, E.A., 1987, Continental Margin Tectonics: Submarine Accretionary Prisms: Review of *Geophys.*, 25, 1305-1312.
- Price, R.A., 1981, The Cordilleran foreland thrust and fold belt in the southern Canadian Rocky Mountains, *in* McClay, K.R., and Price, N.J., eds., *Thrust and Nappe Tectonics*, Volume 9, Geological Society of London Special Paper, 427-448.
- Scheidegger, K.F., Kulm, L.D., and Piper, D.J.W., 1973, Heavy mineralogy of unconsolidated sands in Northeastern Pacific sediments: Leg 18, Deep Sea Drilling Project, *in* Kulm, L.D., von Huene, R., and *al., e.*, eds., *Initial Reports of*

- the Deep Sea Drilling Project, Volume 18: Washington, U.S. Government Printing Office, 877-887.
- Seely, D.R., 1977, The significance of landward vergence and oblique structural trends on trench inner slopes, *in* Talwani, M., and Pitman, W.C.I., eds., *Island Arcs, Deep Sea Trenches, and Back-Arc Basins*, Maurice Ewing Series, Volume vol. 1: Washington, D.C., American Geophysical Union, 187-198.
- Shipboard Scientific Party, 1994, Explanatory Notes, *in* Westbrook, G.K., Carson, B., Musgrave, R.J., and *al., e.*, eds., *Proc. ODP, Init. Repts.*, Volume 146 (Pt. 1): College Station, TX, Ocean Drilling Program, 15-48.
- , 1994, Site 891, *in* Westbrook, G.K., Carson, B., Musgrave, R.J., et al., *Proc. ODP, Init. Repts.*, Volume 146 (Pt. 1): College Station, TX, Ocean Drilling Program, 241-300.
- , 1994, Site 892, *in* Westbrook, G.K., Carson, B., Musgrave, R.J., et al., *Proc. ODP, Init. Repts.*, Volume 146 (Pt. 1): College Station, TX, Ocean Drilling Program, 301-378.
- , 2003, Site 1244, *in* Tréhu, A.M., Bohrmann, G., Rack, F., Torres, M.E., et al., *Init. Repts. [CD-ROM]*, Volume 204: College Station, TX, Ocean Drilling Program, 1-132.
- , 2003, Site 1245, *in* Tréhu, A.M., Bohrmann, G., Rack, F., Torres, M.E., et al., *Init. Repts. [CD-ROM]*, Volume 204: College Station, TX, Ocean Drilling Program, 1-131.
- Smit, J.H.W., Brun, J.P., and Sokoutis, D., 2003, Deformation of brittle-ductile thrust wedges in experiments and nature: *J. of Geophys. Res.*, 108, doi:10.1029/2002JB002190.
- Snively, P.D., Jr., Wagner, H.C., and Lander, D.L., 1980, Geologic cross section of the central Oregon continental margin: Boulder, CO, Plate Tecton. Group, U.S. Geodyn. Comm., Geol. Soc. of Am.
- Snively, P.D., Jr., 1987, Tertiary Geologic Framework, Neotectonics, and Petroleum Potential of the Oregon-Washington Continental Margin, *in* Scholl, D.W., Grantz, A., and Vedder, J.G., eds., *Geology and resource potential of the continental margin of western North America and adjacent Ocean -Beaufort Sea to Baja California*, Volume 6: Circum-Pacific Council for Energy and Mineral Resources Earth Science Series, 305-335.
- Tobin, H.J., Moore, J.C., MacKay, M.E., Orange, D.L., and Kulm, L.D., 1993, Fluid flow along a strike-slip fault at the toe of the Oregon accretionary prism: Implications for the geometry of frontal accretion: *Geol. Soc. Am. Bull.*, 105, 569-582.
- Tréhu, A., Asudah, I., Brocher, T.M., Luetgert, J.H., Mooney, W.D., Nabelek, J.L., and Nakamura, Y., 1994, Crustal architecture of the Cascadia forearc: *Science*, 266, 237-243.
- Tréhu, A.M., Bohrmann, G., Rack, F.R., Torres, M.E., et al., 2003, *Proc. ODP, Init. Repts. [CD-ROM]*, Volume 204: College Station, TX, Ocean Drilling Program.

- Tréhu, A.M., Flemings, P.B., Bangs, N., Chevallier, J., Gracia, E., Johnson, J.E., Liu, C.-S., Liu, X., Riedel, M., and Torres, M.E., 2004, Feeding methane vents and gas hydrate deposits at south Hydrate Ridge: Science, submitted.
- Tréhu, A.M., and Flueh, E.R., 2001, Estimating the thickness of the free gas zone beneath Hydrate Ridge, Oregon continental margin, from seismic velocities and attenuation: *J. of Geophys. Res.*, 106, 2035-2045.
- Tréhu, A.M., Torres, M.E., Moore, G.F., Suess, E., and Bohrmann, G., 1999, Temporal and spatial evolution of a gas hydrate-bearing accretionary ridge on the Oregon continental margin: *Geology*, 27, 939-942.
- Underwood, M.B., Moore, G.F., Taira, A., Klaus, A., Wilson, M.E.J., Fergusson, C.L., Hirano, S., Steurer, J., and Party, L.S.S., 2003, Sedimentary and Tectonic Evolution of a Trench-Slope Basin in the Nankai Subduction Zone of Southwest Japan: *Sedimentary Geology*, 73, 589-602.
- von Huene, R., Pecher, I.A., and Gutscher, M.-A., 1996, Development of the accretionary prism along Peru and material flux after subduction of Nazca Ridge: *Tectonics*, 15, 19-33.
- von Huene, R., and Suess, E., 1988, Ocean Drilling Program Leg 112, Peru continental margin: Part 1, Tectonic history: *Geology*, 16, 934-938.
- Wells, R.E., and Simpson, R.W., 2001, Northward migration of the Cascadia forearc in the northwestern U.S. and implications for subduction deformation: *Earth, Planets and Space*, 53, 275-283.
- Westbrook, G.K., 1994, Growth of Accretionary Wedges off Vancouver Island and Oregon, in Westbrook, G.K., Carson, B., and Musgrave, R.J., eds., *Proceedings of the Ocean Drilling Program, Initial Reports, Volume 146 (part 1)*: College Station, TX, Ocean Drilling Program, 381-388.
- Westbrook, G.K., Carson, B., Musgrave, R.J., et al., 1994, *Proc. ODP, Init. Repts.*: College Station, TX, Ocean Drilling Program.
- Zellers, S.D., 1995, Foraminiferal Biofacies, paleoenvironments, and biostratigraphy of Neogene-Quaternary sediments, Cascadia Margin, in Carson, B., Westbrook, G.K., Musgrave, R.J., and Suess, E., eds., *Proc. ODP, Sci. Results, Volume 146 (Pt. 1)*: College Station, TX, Ocean Drilling Program, 79-113.

Chapter IV

Holocene Slope Failure in an Active Margin Gas Hydrate Bearing Region, Hydrate Ridge, Cascadia Margin

Joel E. Johnson¹, Chris Goldfinger¹, and C. Hans Nelson²

1. Oregon State University, College of Oceanic and Atmospheric Sciences, 104
Ocean Admin. Bldg. Corvallis, Oregon 97331

2. CSIC Instituto Andaluz de Ciencias de la Tierra Facultad de Ciencias, University
of Granada Campus de Fuentenueva s/n 18002 Granada, Spain

To be submitted to *Earth and Planetary Science Letters*

Abstract

Slope failure in the marine environment within the gas hydrate stability zone along continental margins has been suggested as a probable mechanism for the mobilization of seafloor gas hydrate, allowing its transfer from the seafloor and the release of its enclosed methane to the ocean and even the atmosphere. In this paper, we determine the frequency of slope failure events at a well studied active margin gas hydrate province (Hydrate Ridge) located on the lower slope of the Cascadia accretionary wedge. Our results suggest an average Holocene recurrence interval of 400-500 years for slope failure events in this region. Comparison with a Holocene marine paleoseismic record on the abyssal plain of subduction zone earthquakes suggests between 50-70% of the slope failure events were likely triggered by subduction zone earthquakes; 13 of the total 18 Holocene subduction zone earthquakes are recorded at this site. Because these earthquakes are margin wide events, it is likely that they serve as a dominant trigger for slope failures not only at Hydrate Ridge, but also within the gas hydrate stability zone across the margin. These results suggest the frequency of Cascadia subduction zone earthquakes may influence the frequency of methane flux from the seafloor to the ocean and even the atmosphere by controlling the margin wide frequency of Holocene slope failure events.

Introduction

Current gas hydrate research is focused on the physical, chemical, and biological aspects of gas hydrate systems, the dynamics of gas hydrate stabilization, and perhaps more importantly, factors that influence their destabilization. Although several long time scale and potentially global mechanisms are believed to influence the stability of gas hydrate systems on continental margins worldwide (e.g. changes in bottom water temperature; Kennett et al., 2003; Jung and Vogt, 2004 or eustatic sea level; Paull et al., 1996), the potential role of short time scale cycles, such as the subduction zone earthquake cycle, on the stability of marine gas hydrates has thus far received little attention.

One of the major mechanisms for the nearly instantaneous destabilization of gas hydrate in the marine environment involves the disruption of the seafloor by submarine slope failures (i.e. slides, slumps, debris flows, and turbidites). In regions bearing gas hydrate, the physical disturbance of the seafloor during slope failure could disrupt the hydrated sediment fabric and allow much, if not all, of the buoyant gas hydrate involved in the sediment failure to escape to the water column and even the atmosphere. Recently Brewer et al. (2002) and Paull et al. (2003) documented the ease with which seafloor gas hydrate is dislodged from seafloor sediments at Hydrate Ridge, on the Cascadia continental margin. In their experiment, they disrupted the seafloor sediments using the arm of a ROV, which resulted in dislodged pieces of gas hydrate leaving the seafloor and buoyantly rising toward the sea surface. They captured the small hydrate pieces in a mesh bag and followed their ascent upward, witnessing their partial destabilization along the way and their eventual melting at the sea surface. The methane from the destabilized gas hydrate was released to both the ocean and the atmosphere as a result of this process. If slope failures are a mechanism for destabilizing seafloor and shallow seafloor gas hydrates, determining their frequency of occurrence and understanding their potential triggering mechanism(s) could yield insight into the processes that affect the frequency of gas hydrate destabilization events on the seafloor.

As a mechanism for the mobilization of seafloor gas hydrate, slope failures in the marine environment within the gas hydrate stability zone (water depths >300 m, and bottom water temperatures approaching 0° C) can vary in frequency depending on the frequency of the trigger(s) responsible for the failure. On a long (100 ka) timescale tectonic uplift can result in an increased rate of slope failures in marine settings (e.g. Klein, 1984). On glacial-interglacial timescales, the in situ destabilization of gas hydrate during sealevel lowstands has been speculated as a possible trigger for slope failure (e.g. Paull et al., 1996; Rothwell et al., 1998). At this same timescale, climatically induced variations in sediment flux from terrestrial to marine environments can also result in changes in the slope failure frequency on continental margins (e.g. Nelson, 1976). On a shorter timescale, gas hydrate induced slope failure can also occur during bottom water

warming events at millennial time scales during interstadials on continental margins (Kennett et al., 2003). Also on short timescales, earthquake triggered submarine slope failures can occur on both passive (e.g. Heezen and Ewing, 1952) and active continental margins (e.g. Inouchi et al., 1996; Field et al., 1982). On active margins, a potentially important recurrent trigger for regionally synchronous and large-scale slope failures is subduction zone earthquakes. Subduction zone earthquakes are the largest magnitude seismic events on Earth, and typically have spatially extensive rupture lengths and recurrence intervals of hundreds to thousands of years. These large seismic events could potentially trigger multiple slope failures over broad regions of the seafloor, providing a cyclic, short term mechanism for the mobilization and destabilization of seafloor gas hydrates.

Along the Cascadia subduction zone margin, a Holocene record of submarine slope failures attributed to past subduction zone earthquakes is preserved as synchronously triggered submarine canyon and channel turbidites (Adams, 1990; Goldfinger et al., 2003). In this paper we examine the Holocene (10,000 yr -recent) record of slope failure, preserved as turbidites, shed from a region bearing gas hydrate (Hydrate Ridge) within the accretionary wedge on the Cascadia continental margin (Fig. 4-1) and compare it with the record from one of submarine canyon and channel turbidite sites of Goldfinger et al. (2003). We use physical property data and AMS radiocarbon dates from planktonic foraminifera taken from hemipelagic clay intervals between turbidites to decipher which deposits at Hydrate Ridge can most likely be attributed to past subduction zone earthquakes and which may have resulted from other triggers.

Geologic Setting

Hydrate Ridge is a composite thrust ridge formed from seaward and landward vergent thrust faults (Johnson et al., in prep) and is located within the lower slope of the Cascadia accretionary wedge (Fig. 4-1). It is flanked on both the east and west by slope basins. The isolation of the western slope basin from any canyon or channel system sourced to the east indicates that sedimentation in the slope basin consists of hemipelagic

Figure 4-1. (A) Bathymetric map of the offshore portion of the Cascadia subduction zone. Bathymetric contour interval is 100 m. Locations of the Hydrate Ridge western slope basin (see enlarged view in B) and the Juan de Fuca Canyon (JDF) core sites are shown. Cascadia submarine canyons and channels are also shown (blue). The nine WNW trending basement involved left-lateral strike slip faults of Goldfinger et al., 1997 are also shown (black lines). The central Oregon faults are labeled (W) Wecoma fault, (DB) Daisy Bank fault, and (AC) Alvin Canyon fault. The extents of the Nitinat and Astoria fans on the abyssal plain are from Carlson and Nelson (1987). Juan de Fuca-North America relative plate motion at 45° N, 125.5° W (shown as black dot with white outline) directed 051.36°, was calculated by Miller et al., 2001. (B) Shaded relief bathymetry of the Hydrate Ridge region (location shown in A). Locations of the three core sites within the western slope basin adjoining Hydrate Ridge on the lower slope of the Cascadia accretionary wedge are shown. Ocean Drilling Program (ODP) sites discussed in the text are also shown. A piston core (PC) and companion trigger core (TC) were taken at sites 02 and 56, and a kasten core (KC) was taken at the 01 site.

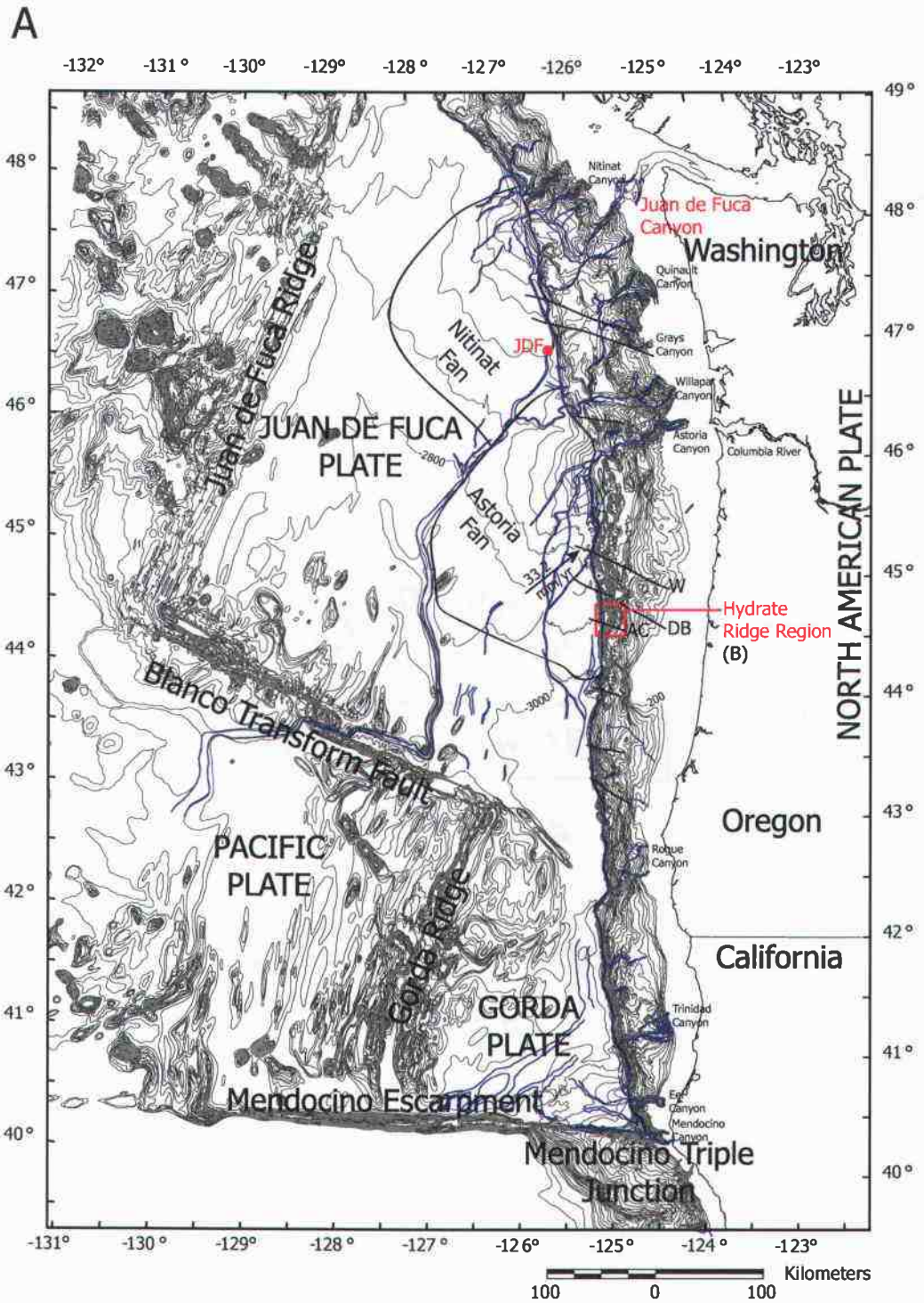


Figure 4-1.

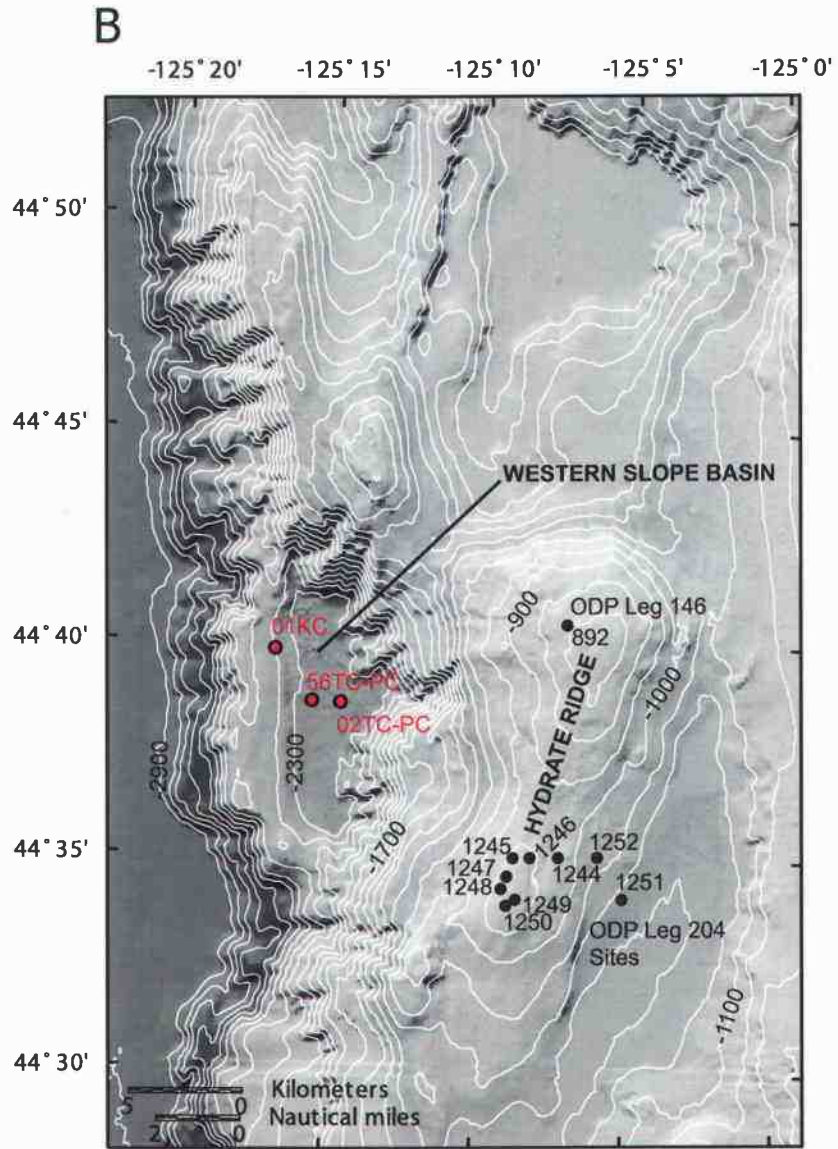


Figure 4-1 (continued).

clay settling out of the water column and local submarine slope failures derived from the surrounding bathymetric highs (i.e. Hydrate Ridge). The most likely sediment transport pathway into the basin is a small submarine canyon that cuts into the western flank of northern Hydrate Ridge (Fig. 4-1b), however, several other smaller potential pathways can also be seen surrounding the basin toward the east and to the north.

Gas hydrates are prevalent in the subsurface and at the surface of Hydrate Ridge, as evidence by the presence of a ubiquitous bottom simulating reflector (BSR) recorded in seismic reflection surveys (Tréhu et al., 1999), and recovered gas hydrate samples from seafloor sampling devices (e.g. Suess et al., 2001; Greinert et al., 2001) and Ocean Drilling Program coring efforts (Westbrook et al., 1994; Tréhu et al., 2003) from both the northern and southern summit regions of the ridge, respectively (Fig. 4-1). In situ and proxy measurements for the amount of gas hydrate present in the subsurface at southern Hydrate Ridge suggest heterogeneous concentrations ranging from 30-40 % of pore space at the summit and up to 20% of pore space at some local patchy zones at the crests of folds along the flanks to only 1-4% of pore space in other regions (Tréhu et al., 2004). Although the concentrations of gas hydrate at the northern summit of Hydrate Ridge are not constrained by extensive drilling, it is likely that similar or even higher concentrations may exist, as the amplitude of the BSR is stronger than at southern Hydrate Ridge and a larger free gas zone is inferred beneath the summit of northern Hydrate Ridge (Tréhu and Flueh, 2001). This suggests that there is the potential for sustaining high gas hydrate concentrations at northern Hydrate Ridge. The more extensive occurrence of authigenic carbonates on the northern summit compared to a small region on the southern summit (Johnson et al., 2003) and older U/Th ages from the carbonates in the north (Teichert et al., 2003), also suggests the fluid venting/gas hydrate system is older and thus more developed at northern Hydrate Ridge.

Paleoseismic records of Cascadia subduction zone earthquakes exists both onshore (e.g. Atwater and Hemphill-Haley, 1997; Kelsey et al., 2002; Witter et al., 2003) and offshore (Adams, 1990; Goldfinger et al., 2003). Onshore, records of subsided

marshes and tsunami deposits associated with past subduction zone earthquakes extend as far back as 6700 years B.P. (Witter et al., 2003). Offshore, the turbidite paleoseismic record spans the entire Holocene (10,000 years B.P.-recent; Goldfinger et al., 2003). The average recurrence interval for these past subduction zone earthquakes is about 600 years. At the Holocene timescale under consideration here, the stratigraphic record of slope failures at Hydrate Ridge can be compared to the offshore turbidite record because they span the same time interval. An event comparison using radiocarbon dates is possible because both records are likely similarly affected by the same radiocarbon reservoirs.

Research Methods

We identify the turbidites preserved in the cores by visual inspection of the sediments, high resolution line scan camera color images, x-rays and gamma density and high resolution point magnetic susceptibility measurements. We determine the approximate age of deposition for turbidites through accelerator mass spectrometry (AMS) radiocarbon dating of a mixed species assemblage of planktonic foraminifera (Table 4-1) collected from the hemipelagic clay intervals between turbidites. In order to obtain enough carbon for dating from the foraminifera tests we typically need 800-1000 individuals (or >2.0 mg), which along the Cascadia margin equates to approximately 3 cm of hemipelagic sediment beneath each turbidite. To obtain the foraminifera, we sieve the hemipelagic clay using a 63 micron mesh, retain the coarse fraction, and pick the individual foraminifera tests. AMS radiocarbon ages were determined at the Lawrence Livermore National Laboratory (LLNL) Center for AMS. Raw AMS ages are reservoir corrected and converted to calendar years using the Calib 4.3 software package (Stuiver and Reimer, 1993) and marine reservoir correction data base (Stuiver et al., 1998). We determined which core tops were preserved from our cores through measurements of ^{210}Pb activity (conducted at Oregon State University).

Turbidite	Core	Planktonic foraminifera species																						
		<i>Globigerina bulloides</i>	<i>G. quinqueloba</i>	<i>Globigerinella aequilateralis</i>	<i>G. calida</i>	<i>Globigerinita glutinata</i>	<i>G. uvula</i>	<i>Globigerinoides ruber</i>	<i>G. trilobus</i>	<i>Globorotalia hexagona</i>	<i>Globorotalia crassaformis</i>	<i>G. inflata</i>	<i>G. scitula</i>	<i>G. truncatulinoides</i>	<i>G. cf. menardii</i>	<i>G. cf. hirsuta</i>	<i>Hasigerina pelagica</i>	<i>Orbulina suturalis</i>	<i>O. universa</i>	<i>O. bilobata</i>	<i>Turborotalia eggeri</i>	<i>T. pachyderma (sins)</i>	<i>T. pachyderma (dex)</i>	
T2	02TC	65	71			19							5						2			1	473	62
T2	56TC	126	45			31						12										5	691	256
T3	02PC	30	88						1			3											197	27
T3	56PC	58	124			2			1			4										1	735	80
T3	56PC	13	27								1											1	99	8
T4	02PC	93	109			9						2	7									4	565	221
T4	56PC	33	26			3		1			5	9							3			7	438	551
T5	02PC	18	20			3						2											173	28
T6	56PC	53	163			6	73					21							4			6	580	223
T7	56PC	58	72			18		13				11			2				6			23	603	212
T10	56PC	52	172			15		2				4										14	429	148
T10	56PC	78	37									34										5	358	56
T11	56PC	21	121			16						7										3	415	86
T11	56PC	30	17			2						3							2			3	351	22
T12	56PC	56	110			18		2				5			1	5						4	480	101
T13	56PC	74	41			10						3			1				1			9	663	197
T14	56PC	75	67			13						4							2			7	689	102
T15	56PC	243	26			18						11										9	603	70
T17	56PC	55	16			6																	266	8
T18	56PC	101	6			6																3	524	274
T19	56PC	143	85			10						11							2			2	654	266
T22	56PC	275	6			6		14				26							12			7	286	286
T23	56PC	427	19			10						27							7			2	141	373
T24	56PC	323	115			62						36							4			3	195	352
T25	56PC	168	71			21						33							2				227	674
base	01KC	1032				20						31											36	
base	01KC	957				5						24											2	1

Table 4-1. Individual foraminifera counts by species for samples taken from hemipelagic sediments beneath turbidites (e.g. T2). Depth intervals within the cores for individual samples are shown in Table 4-3.

Results

Slope Basin Turbidite Stratigraphy

The Holocene stratigraphic record of slope failures, preserved as turbidites in the slope basin west of Hydrate Ridge, was studied at three core sites located west of the submarine canyon cut into the western flank of Hydrate Ridge (Figs. 4-1 and 4-2). The most proximal (furthest east) site to the canyon contains an upper Holocene (~3000 years [B.P. 1950] to modern) record in piston and trigger core RR02-0702PC/TC. The mid-basin site to the west (RR0207-56PC/TC) contains a complete Holocene record (~11,000 years [B.P. 1950] to modern)].

The distal kasten core site (RR02-0701KC) may contain a partial Holocene record, however, radiocarbon dating to confirm Holocene stratigraphy was not possible due to the poor preservation of hemipelagic clay intervals. The only ages obtained from this core are at the base of the section and are late Pleistocene (see below). Evidence for a partial Holocene record above a characteristic color change and change in microfossil fauna (observed in RR0207-01KC at 175 cm; Table 4-2) is consistent with the color change from gray below to green above and the upward shift from foraminifera to radiolarian dominance observed throughout Cascadia basin (Duncan et al., 1970), which typically marks the late Pleistocene to Holocene transition (average age ~12,500 years B.P; Duncan et al., 1970). Although this color change and faunal change is present in the kasten core, radiocarbon ages at the base of the core suggest the turbidites there are late Pleistocene, ~20 ka in radiocarbon years (too old for calendar year calibration) (Fig. 4-2). Because of the proximity of the old radiocarbon ages to the color and faunal shift at ~175 cm in this core, it is unlikely that this boundary represents the 12,500 year B.P. datum. Instead, significant erosion may have occurred near this boundary, disconformably juxtaposing an older (foraminifera-rich) late Pleistocene section against younger (radiolarian-rich) Holocene sediments. Measured excess ^{210}Pb activity at the top of the kasten core confirms the most recent (< ~100 years) sediments are preserved. Therefore it is likely that some portion of the Holocene (evidence by radiolarian rich stratigraphy) is recorded at this site between the top of the core to a depth of 175 cm. However, whether

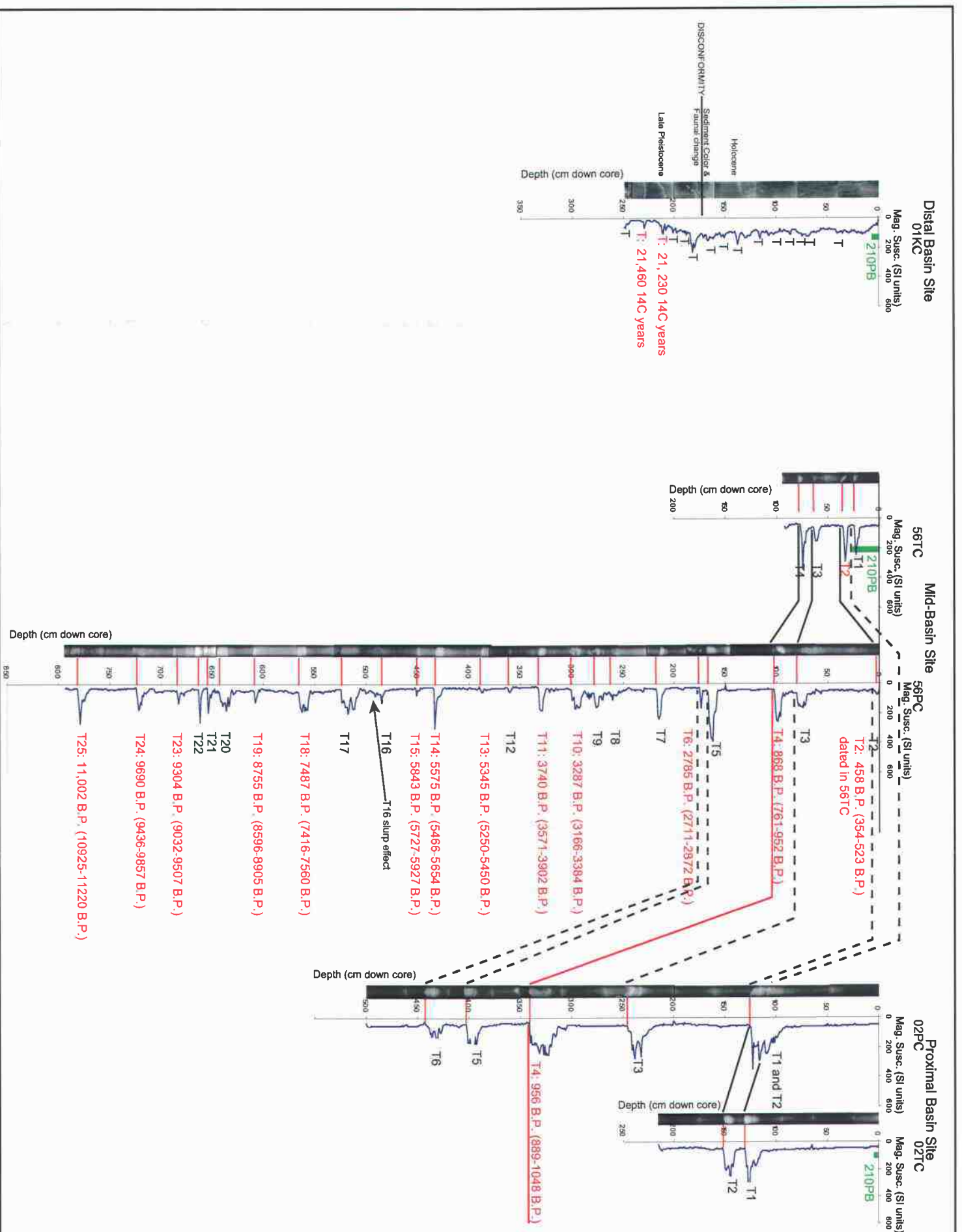


Figure 4-2. Stratigraphic records from the three core sites located across the western slope basin. Core x-rays are shown next to the high resolution point magnetic susceptibility logs for each core. Turbidite events are numbered from the top down at the proximal and mid-basin sites and are labeled (e.g. T3). Radiocarbon ages and 2 sigma error ranges (red) are also shown for all dated turbidites within the stratigraphy. Correlation of sites is based on the overlap between the calibrated radiocarbon age of T4 at the proximal and mid-basin sites. 210Pb measurements (shown in green) at the core tops assisted in correlation of the youngest event (T1), and confirmed it is missing from the top of 56PC. The distal kasten core, although dated at the base, cannot be correlated with the remaining stratigraphy, due to a lack of preserved hemipelagic intervals within the upper stratigraphy above the disconformity discussed in the text. Ages shown in the distal kasten core, are uncalibrated radiocarbon years B.P. 1950. The radiocarbon data are shown in Table 4-3.

Core: RR0207-01KC

	Depth down core (cm)	Planktonic foraminifera	Radiolaria	
Olive Green Sediments	10.0	1	3	Radiolaria dominance (Holocene)
	20.0	8	65	
	30.0	0	17	
	40.0	1	7	
Grey Sediments	171.5	0	10	Foraminifera dominance (Pleistocene)
	175.5	346	36	
	190.0	65	5	
	200.0	63	15	
	213.0	75	12	
	235.0	152	20	

DISCONFORMITY

Table 4-2. Down core faunal change documented from smear slide analyses taken in the RR0207-01 kasten core. The grey to olive green color change (discussed in the text) was also identified in this core at the same position as the faunal shift. Old radiocarbon ages obtained from the base of the the 01 kasten core (discussed in the text) in close proximity to this faunal and color change suggest a disconformity exists at this boundary.

or not it is a complete Holocene section cannot be determined because it is possible that not only some of the late Pleistocene section is missing near the disconformity, but also part of the early Holocene.

Correlation of Turbidites Across the Basin

Examination of the cores at the proximal and mid-basin sites reveals a general decrease in thickness of turbidites from the proximal to mid-basin sites and to the distal core site, which is suggestive of an eastern source region, likely linked to the canyon on the west side of Hydrate Ridge (Fig. 4-1). We are able to correlate the turbidites across the basin between the proximal and mid-basin sites using a correlative radiocarbon age for turbidite T4 (Fig. 4-2) and the correlation of events above and below that datum. Based on this correlation and measured excess ^{210}Pb activity in cores 56TC and 02TC, confirming near complete recovery of the seafloor sediment surface (this work also suggests the top of the core is missing in 56PC, i.e. turbidite 1 is absent there). Although a correlatable time datum was not found in the distal kasten core (01KC), comparison of the total number of Holocene turbidites (approximately 9 above the disconformity) preserved at the distal kasten core site (01KC) to the mid-basin site (56PC/TC), where there are more in the Holocene (25 total), suggests either not all of the turbidites sourced to the east were deposited at the kasten core site or the record at the kasten core site only represents part of the Holocene, as suggested above. However, because the turbidites across the basin, as observed at the three sites, are thinner to the west, and a complete Holocene record could be preserved at the distal kasten site, the discrepancy in total number of turbidites between the mid-basin and kasten sites could simply indicate that not all of the events recorded at the mid-basin site had sufficient run out distance to be deposited at the distal kasten site. Although it is tempting to speculate on the correlation of events at the distal kasten site and the mid-basin site, without Holocene radiocarbon results from the kasten core, an event for event correlation between the distal and mid-basin sites cannot be established with certainty and thus, is not attempted here.

Dating the Turbidites

High abundances (800-1000 or more individuals, >2.0 mg) of foraminifera from well preserved hemipelagic intervals between turbidites are required for obtaining reliable radiocarbon ages within the stratigraphic sequence. When sampling for foraminifera in the cores, discrimination between turbidite clay tails (deposited during the waning stages of a turbidity current and likely containing reworked foraminifera) and hemipelagic clay (the sediment that slowly rains out through the water column) was made based on the relative grain size contrast between the sediments. Turbidite tail clay is slightly coarser grained, containing a larger proportion of silt- or even very fine sand-sized material, compared to hemipelagic sediment, which is dominated by the clay-size fraction. The abundance of foraminifera, and other biogenic material (e.g. radiolarians), within sediments in the tail of a turbidity current is also diluted compared to the biogenic fraction in hemipelagic samples.

Obtaining sufficient foraminifera from hemipelagic intervals beneath turbidites can be difficult if the amount of foraminifera falling to the seafloor varies with time, or if hemipelagic intervals containing the foraminifera have been eroded during the emplacement of the overlying turbidite. Consistent abundances of foraminifera (~900-1100 individuals/3 cm hemipelagic sample; Table 4-3) throughout the Holocene at the mid-basin site suggests that the flux to the seafloor has not varied significantly over this time period. Thus, the low foraminifera counts observed at the proximal site for 4 of the 6 events preserved here (T2, T3, T5, and T6) may be a result of erosive emplacement of these events (thus the sample included turbidite tail material), which is consistent with the proximal location of the site to the source region for the slope failures, and the thicker deposits observed there, which thin to the west, presumably due to deposition during waning turbidity currents. Because foraminifera counts were low beneath some turbidites, perhaps due to erosion, and hemipelagic intervals were lacking between others (either from erosion or short recurrence time between events) and thus not sampled, we were only able to obtain sufficient foraminifera abundances to radiocarbon date 1 out of

Turbidite #	Sample #	Cruise #	Core #	Depth (cm)	Foram Estimate	Foram Count	Foram Weight (mg)	LLNL CAMS #	AMS Age RCYBP	AMS Age	Calibrated AMS Age**	1 sigma Range	2 sigma Range	Calib DR (yr)***	+
T2	HRW-18	RR02-07	02PC	123.5-126.5	420	-	-	-	-	-	-	-	-	-	-
T2	HRW-25	RR02-07	02TC	151-154	650	689	1.00	-	-	-	-	-	-	-	-
T2	HRW-24	RR02-07	56TC	32-35	1000	1166	3.40	103549	1220	40	458	428-497	354-523	398	25
T3	HRW-22	RR02-07	02PC	243-246	350	358	0.30	-	-	-	-	-	-	-	-
Samples HRW-21 and 21B were combined for dating															
T3*	HRW-21	RR02-07	56PC	81-84	1000	1005	1.70	-	-	-	-	-	-	-	-
T3*	HRW-21B	RR02-07	56PC	84-85	85-100	749	5.88 combined w	105104	1885	40	1030	966-1074	935-1140	398	25
T4	HRW-03	RR02-07	56PC	98-101	1000+	1076	3.90	98748	1725	40	868	921-822	952-761	398	25
T4	HRW-19	RR02-07	02PC	341.5-344.5	900+	1030	2.37	100251	1810	35	956	991-913	1048-889	398	25
T5	HRW-23	RR02-07	02PC	403-406	200	244	0.10	-	-	-	-	-	-	-	-
T6	HRW-04	RR02-07	56PC	175-178	1000+	1129	3.80	98749	3415	40	2785	2821-2739	2872-2711	398	25
T6	HRW-20	RR02-07	02PC	444-447	380	-	-	-	-	-	-	-	-	-	-
T7	HRW-05	RR02-07	56PC	217-220	820	1019	4.70	-	-	-	-	-	-	-	-
Samples HRW-06, 06b, and 06c were combined for dating															
T10	HRW-06	RR02-07	56PC	299-302	330	839	1.45	103550	3815	40	3287	3238-3343	3168-3384	398	25
T10	HRW-06b	RR02-07	56PC	298-302.5	480	both	both 6 and 6b	-	-	-	-	-	-	-	-
T10	HRW-06c	RR02-07	56PC	302.5-303.5	250+	568	2.4 (6c only)	-	-	-	-	-	-	-	-
Samples HRW-07, 07b, and 07c were combined for dating															
T11	HRW-07	RR02-07	56PC	332.5-335.5	430	669	1.59	103551	4200	60	3740	3659-3823	3571-3902	398	25
T11	HRW-07b	RR02-07	56PC	332.5-335.5	160	both	both	-	-	-	-	-	-	-	-
T11	HRW-07c	RR02-07	56PC	335.5-337	200+	431	0.3 c only	-	-	-	-	-	-	-	-
T12	HRW-08	RR02-07	56PC	361.5-364.5	790	783	-	-	-	-	-	-	-	-	-
T13	HRW-09	RR02-07	56PC	388-391	1000+	1000	3.50	98750	5385	40	5345	5395-5285	5450-5250	398	25
T14	HRW-10	RR02-07	56PC	431-434	800+	985	3.50	98751	5610	40	5575	5622-5525	5654-5466	398	25
T15	HRW-13	RR02-07	56PC	451-454	900+	985	3.28	100247	5870	40	5843	5900-5788	5927-5721	398	25
T16	HRW-14	RR02-07	56PC	484-487	280	-	-	-	-	-	-	-	-	-	-
T17	HRW-02	RR02-07	56PC	523.5-525.5	-	351	0.45	-	-	-	-	-	-	-	-
T18	HRW-11	RR02-07	56PC	564.5-567.5	900+	927	5.00	98752	7390	40	7487	7518-7434	7560-7416	398	25
T19	HRW-12	RR02-07	56PC	608.5-611.5	900+	1173	3.90	98753	8650	45	8755	8827-8654	8906-8598	398	25
T22*	HRW-15	RR02-07	56PC	664.5-667.5	1000+	915	5.13	100248	9785	35	10048	10714-9931	10296-9811	398	25
T23	HRW-16	RR02-07	56PC	684.5-687.5	1000+	1006	4.89	100249	9195	35	9304	9250-9074	9507-9032	398	25
T24	HRW-17	RR02-07	56PC	723-726	900+	1093	5.31	100250	9480	35	9690	9834-9590	9657-9436	398	25
T25	HRW-01	RR02-07	56PC	780.5-783	-	1179	4.00	97786	10520	60	11002	11178-10940	1220-1092	398	25
base	HRW-26	RR02-07	01KC	217-219.5	>1000	1124	1/2 = 9.08	105105	21230	70	-	too old for calibration	-	-	-
base	HRW-27	RR02-07	01KC	231-233.5	>1000	994	1/2 = 8.28 archived	105106	21460	70	-	too old for calibration	-	-	-
							1/2 = 8.89 archived								

Table 4-3. Radiocarbon results and correlative *Reversed age
 foraminifera data obtained from hemipelagic samples
 taken beneath each turbidite. Grey shaded rows are
 samples and ages discussed in the text. Additional
 samples for which forams were obtained and weighed are
 also shown, however, because of their low abundances or
 weights radiocarbon ages were not possible.

**B.P. (1950), Calib 4.4.2, Median Probability
 *** Total marine reservoir correction used was 798 years
 (standard ocean correction of 400 years + local correction of 398 years (Calib. DR)

at total of 6 turbidites at the proximal site, 13 out of total of 25 turbidites at the mid-basin site, and only 2 out of at least 15 turbidites that were deposited at the distal kasten core site (Table 4-3) We obtained reversed ages for T3 and T22 at the mid-basin site, both older than the enclosing hemipelagic sediments. The source of this contamination, could be the inclusion of some older foraminifera, possibly derived from the underlying turbidite tail of the previous event, although sample handling, or lab errors cannot be excluded. We intentionally did not sample intervals bearing silty clay, between closely spaced turbidites lacking significant hemipelagic material. The closely spaced turbidites not sampled for radiocarbon dating at the mid-basin site included T1, T5, T8, T9, T20, and T21. Turbidite T1 in core 02TC at the proximal site was also not sampled due to its proximity to turbidite T2. In addition to these events without radiocarbon dates, a lab error at LLNL resulted in the loss of the forams for the dating of turbidite T6 and a micropaleo sample error contaminated the forams that were to be used to date turbidite T11. Both of these samples were from the mid-basin site. Nevertheless, we do have good time constraints for enough of the turbidites at the mid-basin site to capture the entire Holocene slope basin record (Fig. 4-2).

Discussion

The radiocarbon results from the mid-basin site suggest that the entire Holocene (~11,000 year) turbidite record was recovered at this site. 25 total turbidites are preserved if we interpret all turbidites, including closely spaced ones, as separate slope failure events. The average recurrence of slope failure during the last 11,000 years is 440 years. To understand what processes may control the frequency of slope failure events at Hydrate Ridge, and in the likelihood that those same processes control the frequency of slope failures across the entire continental margin, we discuss the possible triggers for slope failures in the marine environment and their potential applicability as triggers for the slope failure events recorded at Hydrate Ridge.

Triggers for Slope Failure

Slope failures in the marine environment can be triggered by (1) oversteepening of slopes due to rapid sedimentation, (2) or tectonic growth of structures, (3) storm waves, (4)

distal tsunamis, (5) excess pore water pressure caused by bubble phase gas, (6) destabilized gas hydrate, (7) crustal or slab earthquakes, and (8) subduction zone earthquakes. At Hydrate Ridge, several of these triggers can be eliminated as likely causes for the Holocene slope failure record in the western slope basin because of its location within the accretionary wedge. A lack of submarine canyon and channel systems on the central Oregon margin suggests that oversteepening of slopes due to rapid sediment flux is not occurring in the Hydrate Ridge region. In fact, the uplifted and isolated nature of the source region (Hydrate Ridge) for the slope failures in the western slope basin suggests sedimentation on the ridge has been dominated by slow hemipelagic clay accumulation since the uplift and isolation of the ridge during accretion from the abyssal plain (~1.7-0.3 Ma; Johnson et al., in prep). Because the tectonic growth of structures within the accretionary wedge at Hydrate Ridge occurs at timescales (10^5 years) longer than the Holocene timescale discussed here, it is also not a likely mechanism for triggering the Holocene slope failures at Hydrate Ridge. Hydrate Ridge is also located in water depths (>700 m) too deep to be affected by storm wave disturbances and distant tsunamis. The 1964 Alaskan earthquake tsunami wave did not even trigger a slope failure in the shallow water upper canyon systems on the Washington and southern Oregon continental shelf (Adams, 1990; Goldfinger, 2003). Because Hydrate Ridge lies within the gas hydrate stability zone, that leaves excess pore water pressure caused by bubble phase gas or destabilized gas hydrate, crustal or slab earthquakes, and subduction zone earthquakes as possible triggers for the slope failure record preserved in the western slope basin.

Slope Failure Triggers at Hydrate Ridge

Of the remaining triggers potentially responsible for the Holocene slope failure record at Hydrate Ridge, long term records recording the frequency of degassing events or the destabilization of gas hydrates unfortunately do not exist. In the last few years, however, hydrate coated gas bubble plumes have been observed emanating from the seafloor at southern Hydrate Ridge (Heeschen et al., 2003), and geochemical studies of the authigenic carbonates preserved at the crest of Hydrate Ridge suggests carbon from destabilized gas hydrate has contributed to their precipitation in the past (Bohrmann et al.,

1998), suggesting that both of these processes occur in the Hydrate Ridge region. Thus, some slope failures preserved in the western slope basin at Hydrate Ridge may have been triggered by bubble phase gas escape and/or destabilized gas hydrate events at some time during the Holocene.

Although instrumental records of crustal and slab earthquakes along the Cascadia margin region have only become available in the last ~40 years, these records indicate very little offshore seismicity within the central Cascadia margin (e.g. Miller et al., 2001). In the Hydrate Ridge region the outer portion of the accretionary wedge likely deforms aseismically, limiting earthquakes in this region to slab events in the Juan de Fuca plate (Goldfinger et al., 1992; Clarke and Carver 1992). In the Hydrate Ridge region, although active (Holocene slip) strike slip faults rooted in Juan de Fuca basement exist (Goldfinger et al., 1997), they have not produced an offshore earthquake over the short time period of instrumentally recorded seismicity. The only instrumentally recorded earthquake in the Hydrate Ridge region occurred in 1973 and was a m_b 5.8 event in the slab (Spence, 1989). Because we did not record a recent (<100 year old) turbidite at the top of our cores (confirmed by a lack of excess ^{210}Pb activity above and beneath the youngest turbidite, T1), this event apparently did not trigger a slope failure recorded at any of our three core sites. Although evidence for slope failure triggered by slab or crustal earthquakes is lacking in the modern record, that does not preclude that one or more of these types of events could have triggered a slope failure at some time during the past 11,000 years. Thus, slab and crustal earthquakes remain possible triggers for Holocene slope failures at Hydrate Ridge.

Along the northern and central portion of the Cascadia margin, the longest paleoseismic records are those from past subduction zone earthquakes. In the marine environment, this record consists of synchronously triggered submarine canyon and channel turbidites (Adams, 1990 and Goldfinger et al., 2003). If subduction zone earthquakes can trigger slope failures recorded in the submarine canyon and channel cores along the margin, it seems likely that they might also trigger slope failures in the slope basin environment at Hydrate Ridge as well. Because the earthquake triggered turbidite record spans the entire Holocene, we can determine if any of the events at Hydrate Ridge

occurred at the same time as slope failures accompanying subduction zone earthquakes by direct comparison of the Hydrate Ridge record with the record of past subduction zone earthquakes from Goldfinger et al. (2003). To make this comparison, we use the radiocarbon results and physical property data described below.

Correlation to the Earthquake Triggered Turbidite Record

The average recurrence interval for earthquake triggered turbidites deposited over the last ~9800 years is 540 years, during which 18 turbidites were deposited (Goldfinger et al., 2003). Over the same time interval at Hydrate Ridge, there are 24 turbidites deposited in ~9700 years, yielding a more frequent average recurrence interval of about 400 years. To determine if any of the events at Hydrate Ridge are the same age as subduction zone earthquake triggered turbidites, we compare the radiocarbon results from the Juan de Fuca Canyon site offshore Washington (Goldfinger et al., 2003) to the Hydrate Ridge record (Fig. 4-3).

Because the Holocene Hydrate Ridge record is thicker relative to the Holocene Juan de Fuca Canyon record, likely due to the proximal location of the Hydrate Ridge cores to the source region, we have expanded the Juan de Fuca Canyon record and broken it into segments (Fig. 4-3a) that correspond in time and in some cases physical property character, to the stratigraphy at Hydrate Ridge (Fig. 4-3b). We define correlative events by overlapping radiocarbon ages (2 sigma error ranges; Fig. 4-3b; Table 4-3), which imply a subduction zone earthquake trigger at Hydrate Ridge, and hang our correlation based on those events. Based on the available radiocarbon ages, this results in the correlation of 7 of the events at Hydrate Ridge (T2, T4, T6, T10, T18, T23, and T24) to subduction zone earthquake triggered events at the Juan de Fuca Canyon site (solid green lines in Fig. 4-3). The remaining radiocarbon ages at Hydrate Ridge show that events (T11, T13, T14, and T15) do not correlate with any of the events at the Juan de Fuca site, and are thus probably not subduction zone earthquake triggered. Because at least 4 events were not triggered by subduction zone earthquakes, the potential other triggers exists. Because we have ages for events attributed to subduction zone earthquakes events throughout the Holocene and several of the events at Hydrate Ridge, although undated,

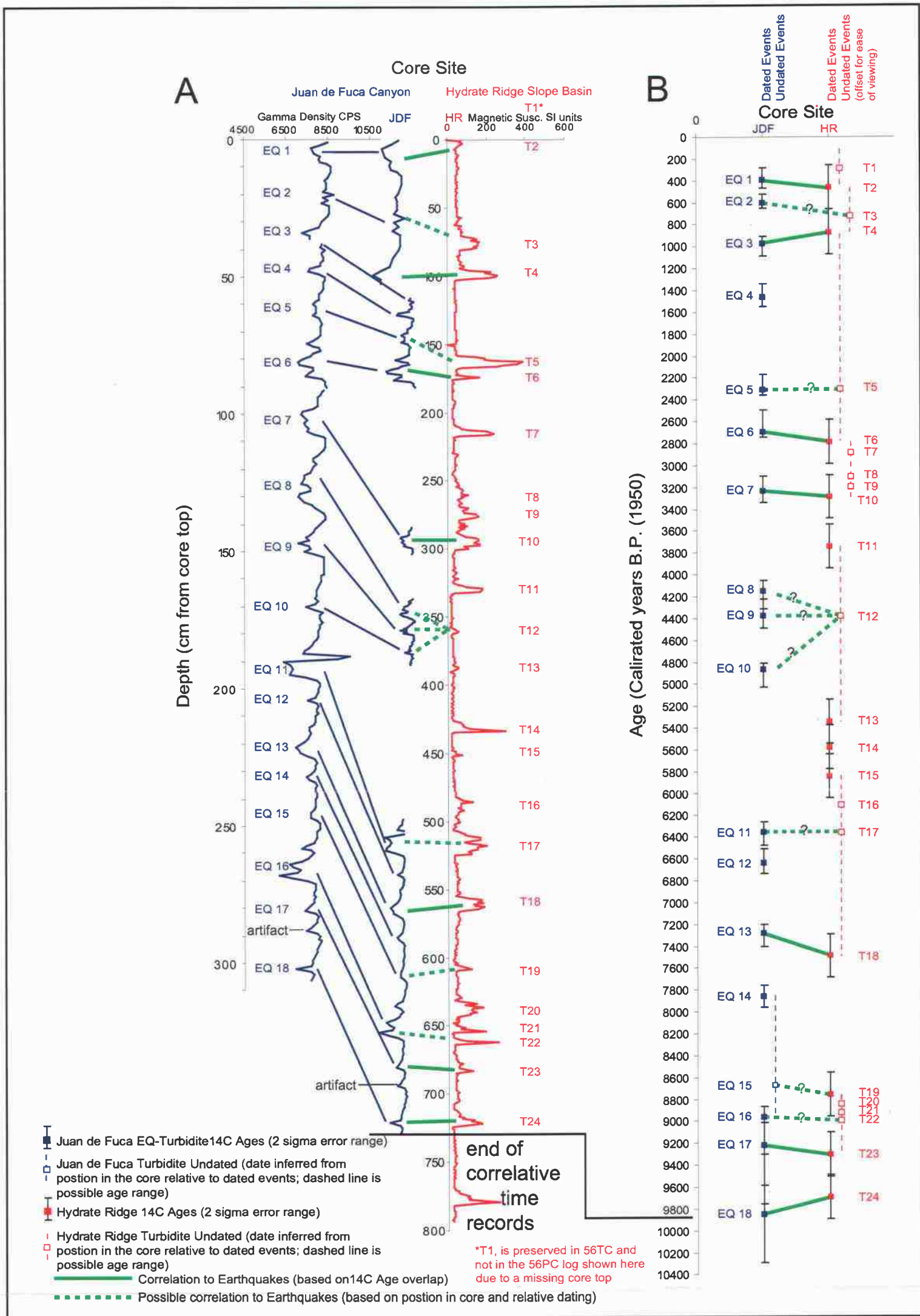


Figure 4-3. (A) Comparison of the Holocene Hydrate Ridge record (RR0207-56PC; in red) to the Holocene subduction zone earthquake triggered turbidite record at the Juan de Fuca Canyon site (M9907-12PC; in blue) of Goldfinger et al. (2003). The Juan de Fuca Canyon density log is expanded and broken into segments that correspond in time and in some cases physical property character to the record at Hydrate Ridge. High resolution point magnetic susceptibility logs best capture the signatures of the turbidites, however, comparison of the JDF density log to the high resolution magnetic susceptibility log of core 56PC (Hydrate Ridge) is necessary because high resolution magnetic data is not available for the Juan de Fuca Canyon site. Examination of gamma density and high resolution magnetic susceptibility records from the same stratigraphy, however, reveals that they record virtually the same turbidite patterns in the stratigraphy and thus, the stratigraphic comparison made here, based on these two seemingly different physical property measurements, is warranted. (B) Calibrated radiocarbon ages for the Juan de Fuca Canyon and Hydrate Ridge turbidite events (closed symbols, with 2 sigma error ranges also shown). Other events without radiocarbon ages (open symbols) are shown and placed on the graph based on their proximity to other dated events (dashed line indicated maximum range in age based on surrounding dated events). The numerical radiocarbon data is shown in Table 4-3.

are bracketed by ages, we can evaluate if some of the additional undated events are subduction zone earthquake triggered by using the relative positions of other turbidites between dated events coupled with the physical property signatures of the turbidites (character of individual events, relative size of events, and relative spacing of events). The results of this comparison, suggests a likely earthquake trigger for 6 other turbidites at Hydrate Ridge (dashed green lines in Fig. 4-3). This comparison also reveals that 5 of the margin wide earthquakes did not result in a slope failure deposit at Hydrate Ridge (at least one that was recovered at the 56PC core site) and up to 7 additional events were not triggered by subduction zone earthquakes (Fig. 4-3). Below we discuss the evidence for our interpretation of other likely earthquake triggered events, other non subduction zone earthquake triggered events, and the missing earthquake triggered events at the Hydrate Ridge site.

Comparison of the physical property character of individual correlative earthquake triggered turbidites from canyon and channel records along the entire margin, suggests the earthquake shaking characteristics during individual events, may be recorded in the turbidites (Goldfinger et al., 2004). Some of those signals may also be recorded in some of the events at Hydrate Ridge as well. We notice a remarkable similarity, particularly in the older portion of the record, between the physical property signature and relative sizes of some turbidites compared to others at both sites (e.g. JDF T11 and HR T17 have a similar box shape; JDF T11, T13, and T16 are also large deposits at the Juan de Fuca site and margin wide and have large correlative deposits at Hydrate Ridge, T17, T18, and T22-T20, respectively; discussed below). Coupled with the radiocarbon dates, these physical characteristics serve as an additional tool for event correlation. For example, we infer an earthquake origin for T17, T19, and T22 at Hydrate Ridge based on the following lines of evidence. We can lock in the lower portion of the stratigraphy at Hydrate Ridge, events (T17 to T24), using the 3 radiocarbon ages for events T18, T23, and T24, which have overlapping ages with earthquake events EQ13, EQ17, and EQ 18, respectively (Fig. 4-3) as a starting point. Next we dated events T15 and T18 at Hydrate Ridge. We can infer that undated events T16, and T17 were deposited in the time

between them (dashed red age range for T17; Fig. 4-3b) and that T16 is younger than T17 and older than T15 (Fig. 4-3b). Because of the similarity in the physical properties between T17 and EQ 11 and the age for EQ 11 is consistent with the age range possible for T17 at Hydrate Ridge (Fig. 4-3b), we suspect that these events are correlatable, suggesting turbidite T17 was earthquake triggered. If this relationship is correct, it means that turbidite T16 at Hydrate Ridge was not triggered by a subduction zone earthquake (its relative dating places it younger than the T17-EQ11 age and older than the EQ10 age). It also implies that EQ12 was not recorded as a turbidite deposit at Hydrate Ridge (because there is no turbidite between T17 and T18, both of which correlate with EQ11 and EQ13 earthquakes. With T17 likely correlated to EQ 11, and the other T18/ EQ13, T23/EQ17 and T24/EQ18 overlapping radiocarbon constrained correlations, we can determine additional relationships between the two records between T18 and T23 at Hydrate Ridge. Because we lack an age for EQ15, we can only infer that it occurred between EQ14, and EQ16 (dashed blue age range line; Fig. 4-3b). We have an age for T19 at Hydrate Ridge that overlaps with this time range and therefore we suggest T19 is correlatable with EQ15. The relative spacing of events above and below in both cores also supports this correlation. With this correlation, that implies that EQ14 did not trigger a slope failure at Hydrate Ridge. If T19 is correlative with EQ15, and we know T23 is correlative with EQ17 (from radiocarbon age overlap), then EQ16 could be coincident with T22, T21, or T20, which although not dated, all lie between the dated T19 and T23 events. The overlapping bracketed ages suggests EQ16 is recorded as either T22, T21, or T20 at Hydrate Ridge. In terms of physical properties, we notice a remarkable similarity between the EQ16 event at Juan de Fuca canyon (a triple coarse pulse turbidite) and the closely spaced T22, T21, and T20 events. Although it is possible that the characteristics of the EQ 16 shaking resulted in a triplet event across the margin, and this same shaking signal is recorded at Hydrate Ridge as the triplet T22, T21, and T20, we cannot rule out erosive emplacement of separately-triggered T20 into T21, and T21 into T22 during subsequent deposition, as the cause of this apparent sequence of events. Another possible interpretation for the close spacing of events in this proximal

slope basin environment is that the slope failures were triggered by one mechanism that initiated slope failure at slightly different distances from the core site, thus arriving at the core site slightly separated in time and resulting in an amalgamated deposit. This same scenario may have resulted in the close spacing of events T10, T9, and T8 and even T2 and T1 as well, discussed below. Nevertheless, we suspect that EQ16 is correlative with at least 1 of the three (if separate) events T22, T21, or T20, and because of the relative spacing of events surrounding them, we have correlated EQ16 with the base of this sequence, at T22. This leaves open the possibility that T21 and T22 are separate events triggered by other non subduction zone earthquakes after the EQ16/T22 event or part of a triplet event, with a base at T22, and two subsequent coarse grained pulses, all three of which may have been triggered by EQ16.

In the middle portion of the Holocene section at Hydrate Ridge, turbidite T12, although not dated, is bracketed by two dated events T11 and T13, neither of which correlate in time with EQ8, EQ9, or EQ10 that occurred between them (Fig. 4-3). This means the deposition of T12 overlaps with the occurrence in time of three earthquakes (EQ8, EQ9, and EQ10). Because of this coincidence, we suspect that T12 at Hydrate Ridge correlates with one of these events. Also implied is that two subduction zone earthquakes in this time interval did not deposit a turbidite at the Hydrate Ridge core site. Exactly which 2 of the 3 events, however, cannot be determined. The close spacing of turbidites T5 and T6 (T6 is correlated in time to EQ6) and the potential for a time overlap between the occurrence of T5 with EQ5 suggests that T5 was triggered by an earthquake (Fig. 4-3). We correlate T5 with EQ5 rather than EQ4, because of the closer proximity of T5 to T6 rather than T4 and the closer proximity in time between EQ5 and EQ6 rather than EQ5 to EQ4. This correlation implies that EQ4 did not deposit a turbidite at the Hydrate Ridge site. Because turbidite T3 is bracketed by correlative earthquake triggered turbidites above and below it and EQ2 is coincident in time with the time range for the deposition of T3 (after T2 and before T4) we correlate T3 with EQ2. Thus, T3 is likely earthquake triggered. At the top of the section at Hydrate Ridge, we consider T1 to be an event not related to a subduction zone earthquake.

A Mix of Earthquakes and Other Triggers

Of the 24 Holocene turbidites at Hydrate Ridge, radiocarbon age matches suggest that 7 of the margin wide earthquakes resulted in the deposition of 7 of the turbidites at Hydrate Ridge. An additional 6 turbidites are also inferred to match the subduction zone earthquake record based on relative age dating and physical property signatures of events. If 13 of the 24 events at Hydrate Ridge were triggered by subduction zone earthquakes, that leaves 11 other events that must have other triggers. The number of other triggered events (11) may be less by up to 5 events if we interpret the closely spaced T1-T2, T8-T9-T10, and T22-T21-T20 portions of the record as couplet and triplet events triggered by event. In this case, the bases of the couplet and two triplets are correlated with subduction zone earthquakes. As multiple pulsed turbidite deposits can occur when triggered by earthquakes, due to coalescing slope failures, this interpretation may be consistent with the inferred earthquake trigger for these events (Shiki et al., 2000). These results and interpretations suggest at least 13 of 24 or slightly more than 50% and potentially up to 70% (13 of 19 total events) of the slope failures at Hydrate Ridge were likely triggered by subduction zone earthquakes. The remaining events (11 of 24 or slightly less than 50% or as low as 6 of 24 or 25%) were triggered by other mechanisms. As mentioned earlier, other possible triggers for the slope failure record at Hydrate Ridge include (1) crustal or slab earthquakes, (2) bubble phase gas escape and (3) destabilization of gas hydrate. Perhaps future work will yield insight into which of these remaining triggers are more likely than others.

We also note that based on the record preserved at the mid-basin site at Hydrate Ridge, 5 of the margin wide earthquakes did not trigger a slope failure at Hydrate Ridge. There are two possible explanations for this observation. First, perhaps only the largest subduction zone earthquakes are capable of triggering slope failures on the lower slope of the accretionary wedge. Although it is tempting to speculate on the size of an earthquake and the effect it may have on a slope failure, along the Cascadia margin subtle variations in earthquake magnitude from paleoseismic records is difficult at best to determine. The lack of intermediate seismicity along the margin and correlative paleoseismic records

across the margin suggests consistently large magnitude events (M 8-9) are likely common. Secondly, and perhaps a more likely explanation, is perhaps all of the subduction zone earthquakes did trigger slope failure at Hydrate Ridge, but only 13 of the total 18 earthquake triggered slope failures were deposited at the mid-basin core site. Other events, may have had shorter run out distances, or been sourced in regions away from the large canyon upslope from the mid-basin site, resulting in a bypassing of the core site. Additional coring in this slope basin or other lower slope basins could test this hypothesis. Nevertheless, a majority (13) of the total (18) Holocene margin wide earthquakes triggered many of the Holocene slope failures at Hydrate Ridge and this has important implications for the stability of margin wide gas hydrates

Implications for the Mobilization of Seafloor Gas Hydrates

If slope failures are an important mechanism for destabilizing seafloor and shallow seafloor gas hydrates, determining their frequency of occurrence and understanding their potential triggering mechanism(s) can yield insight into the processes that affect the frequency and spatial extent of gas hydrate destabilization events on the seafloor. In order to have the greatest potential for mobilizing the largest volume of seafloor gas hydrates during slope failure, either the slope failures have to be massive in scale, instantaneously mobilizing a large region of the seafloor, or the trigger for the slope failure has to be massive in scale, effectively causing numerous smaller synchronous slope failures across a broad region. Along the Cascadia margin, evidence for young large scale individual slope failures triggered during the Holocene is lacking, instead, examination of the margin wide bathymetry shows it is riddled with fresh, smaller slope failure scars suggestive of small and frequent slope failures with a margin wide distribution of occurrence.

In this paper we present a complete and well dated Holocene record of slope failures derived from gas hydrate bearing sediments in an active margin setting down slope from one of these small slope failure scars. The slope basin turbidite record west of Hydrate Ridge indicates slope failures occur with an average recurrence ranging from 400 years (9700 B.P./24 events) to 500 years (9700 B.P./19 events, if couplet and triplets are

single events). Comparison of the Hydrate Ridge record to the marine record of subduction zone earthquakes suggests slightly more than 50% and perhaps as much as 70% of the slope failures at Hydrate Ridge are related to subduction zone earthquakes. Because subduction zone earthquakes along the Cascadia margin are interpreted to have long rupture lengths (as much as 700 km), based on correlative paleoseismic records, and subduction zone earthquake triggered slope failures occur at Hydrate Ridge, they are likely to occur along much of the lower slope of the accretionary wedge within the gas hydrate stability zone (water depths >500 m). This suggests that margin wide subduction zone earthquakes could be a trigger for 50-70% of the slope failures in many if not all of the gas hydrate portions of the margin, perhaps serving to a large extent to regulate the short term frequency of gas hydrate destabilization events (via slope failure mobilization) along the Cascadia margin at least during the Holocene.

In addition to subduction zone earthquake triggered slope failures however, there are other slope failure triggers that could operate in the gas hydrate bearing regions of the Cascadia margin. From the Hydrate Ridge slope basin record discussed here, the most likely other triggers include (1) slab or crustal earthquakes, (2) bubble phase gas escape and (3) destabilization of gas hydrate. Of these remaining triggers only bubble phase gas escape and the destabilization of gas hydrate are likely to be triggers for margin wide slope failures and only if they are controlled by a margin wide or large scale process. Recent work on the Norwegian continental margin has suggested bottom water temperature changes during the Holocene were responsible for destabilizing the seafloor gas hydrate there, resulting in massive slope failure (Jung and Vogt, 2004). Perhaps some of the events not triggered by subduction zone earthquakes, could be a result of this same type of process operating at Hydrate Ridge and even throughout the gas hydrate stability zone across the margin. With no supporting evidence, however, for thermally destabilized gas hydrate events, much less their timing during the Holocene, testing this hypothesis will remain the subject of future research.

Conclusions

In this paper, we document the Holocene frequency of occurrence of slope failure at an active margin gas hydrate province. The average recurrence of events during the last 9700 years is ~400-500 years. The possible triggers for these slope failures include slab earthquakes, bubble phase gas escape, the destabilization of gas hydrate, and/or subduction zone earthquakes. Comparison of the timing of slope failures between the Hydrate Ridge slope basin site, and the subduction zone earthquake turbidite Juan de Fuca site of Goldfinger et al. (2003) suggests subduction zone earthquakes are responsible for triggering 50-70% of the slope failures at Hydrate Ridge during the Holocene. Because subduction zone earthquakes are a margin wide process and they triggered many of the slope failures at Hydrate Ridge, it is likely that they triggered other slope failures within the gas hydrate stability zone, across the margin, thus potentially regulating to a large extent the frequency of margin wide mobilization of seafloor gas hydrates during the Holocene. Identification of subduction zone earthquake triggered slope failures as an important mechanism for margin wide mobilization of seafloor gas hydrates suggests this type of process may be common on other active continental margins as well.

Acknowledgements

Acknowledgement is also made to the Donors of The Petroleum Research Fund, administered by the American Chemical Society, for support of this research and the COAS Chipman-Downs Fellowship at Oregon State University. We also thank Richard Boettcher for picking the foraminifera for radiocarbon dating, Michelle Arsenault (OSU) for sieving radiocarbon samples, and Rob Wheatcroft (OSU) and Roger Lewis (OSU) for radioisotope measurements (OSU). Additional thanks to Bob Yeats (OSU), Anne Tréhu (OSU), and Marta Torres (OSU) for valuable discussions.

References

- Adams, J., 1990, Paleoseismicity of the Cascadia subduction zone: Evidence from turbidites off the Oregon-Washington margin: *Tectonics*, 9, 569-583.
- Atwater, B.F., and Hemphill-Haley, E., 1997, Recurrence Intervals for Great Earthquakes of the Past 3,500 Years at Northeastern Willapa Bay, Washington: U. S. Geological Survey Professional Paper 1576, 108 p.
- Bohrmann, G., Greinert, J., Suess, E., and Torres, M., 1998, Authigenic carbonates from the Cascadia subduction zone and their relation to gas hydrate stability: *Geology*, 26, 647-650.
- Brewer, P.G., Paull, C., Peltzer, E.T., Ussler, W., Rehder, G., and Friederich, G., 2002, Measurements of the fate of gas hydrates during transit through the ocean water column: *Geophys. Res. Lett.*, 29, doi:10.1029/2002GL014727.
- Carlson, P.R., and Nelson, C.H., 1987, Marine geology and resource potential of Cascadia Basin, *in* Scholl, G., and Vedder, ed., *Geology and Resource Potential of the Continental Margin of Western North America and Adjacent Ocean Basins*, Volume 6: Houston TX, Circum-Pacific Council for Energy and Mineral Resources, Earth Sciences Series, 523-535.
- Clarke Jr., S.H., and Carver, G.A., 1992, Late Holocene tectonics and paleoseismicity, southern Cascadia subduction zone: *Science*, 255, 188-191.
- Duncan, J.R., Fowler, G.A., and Kulm, L.D., 1970, Planktonic Foraminiferan-Radiolarian Ratios and Holocene-Late Pleistocene Deep Sea Stratigraphy off Oregon: *Geol. Soc. Am. Bull.*, 81, 561-566.
- Field, M.E., Gardner, J.V., Jennings, A.E., and Edwards, B.D., 1982, Earthquake-induced sediment failures on a 0.25° slope, Klamath River delta, California: *Geology*, 10, 542-546.
- Goldfinger, C., Kulm, L.D., Yeats, R.S., Appelgate, B., MacKay, M.E., and Moore, G.F., 1992, Transverse structural trends along the Oregon convergent margin: Implications for Cascadia earthquake potential and crustal rotations: *Geology*, 20, 141-144.
- Goldfinger, C., Kulm, L.D., Yeats, R.S., McNeill, L., and Hummon, C., 1997, Oblique strike-slip faulting of the central Cascadia submarine forearc: *J. of Geophys. Res.*, 102, 8217-8243.
- Goldfinger, C., Nelson, C.H., and Johnson, J.E., 2003, Holocene Earthquake Records From the Cascadia Subduction Zone and Northern San Andreas Fault Based on Precise Dating of Offshore Turbidites: *Annual Rev.-Earth and Planetary Sci.*, 31, 555-577.
- Goldfinger, C., Nelson, C.H., Johnson, J.E., Chaytor, J.D., Eriksson, D., Karabanov, E., Morey-Ross, A., and R/V Revelle and R/V Melville Shipboard Scientific Parties, 2004, Long-term paleoseismic records along the Cascadia subduction zone and northern San Andreas Fault based on turbidite stratigraphy, Japan Earth and Planetary Science Joint Meeting: Tokyo, Japan, JEPS.
- Greinert, J., Bohrmann, G., and Suess, E., 2001, Gas Hydrate-Associated Carbonates and Methane-Venting at Hydrate Ridge: Classification, Distribution, and Origin of

- Authigenic Lithologies, *in* Paull, C.K., and Dillon, W.P., eds., *Natural Gas Hydrates: Occurrence, Distribution, and Detection*, Volume Geophysical Monograph 124: Washington D.C., American Geophysical Union, 99-113.
- Heeschen, K.U., Tréhu, A.M., Collier, R.W., Suess, E., and Rehder, G., 2003, Distribution and height of methane bubble plumes on the Cascadia margin characterized by acoustic imaging: *Geophysical Research Letters*, v. 30, p. 1643-1646.
- Heezen, B.C., and Ewing, M., 1952, Turbidity currents and submarine slumps, and the 1929 Grand Banks earthquake: *American Journal of Science*, 250, 849-878.
- Inouchi, Y., Kinugasa, Y., Kumon, F., Nakano, S., Yasumatsu, S., and Shiki, T., 1996, Turbidites as records of intense palaeoearthquakes in Lake Biwa, Japan: *Sedimentary Geology*, 104, 117-125.
- Johnson, J.E., Goldfinger, C., Bangs, N., Tréhu, A.M., and Chevallier, J., in prep 2004, Structural vergence variation and clockwise block rotation in the Hydrate Ridge region, Cascadia accretionary wedge: *Tectonics*.
- Johnson, J.E., Goldfinger, C., and Suess, E., 2003, Geophysical constraints on the surface distribution of authigenic carbonates across the Hydrate Ridge region, Cascadia margin: *Marine Geology*, 202, 79-110.
- Jung, W., and Vogt, P.R., 2004, Effects of bottom water warming and sea level rise on Holocene hydrate dissociation and mass wasting along the Norwegian-Barents Continental Margin: *J. of Geophys. Res.*, 109, doi:10.1029/2003JB002738.
- Kelsey, H.M., Witter, R.C., and Hemphill-Haley, E., 2002, Plate-boundary earthquakes and tsunamis of the past 5500 yr, Sixes River estuary, southern Oregon: *Geol. Soc. Am. Bull.*, 114, 298-314.
- Kennett, J.P., Cannariato, K.G., Hendy, I.L., and Behl, R.J., 2003, *Methane Hydrates in Quaternary Climate Change The Clathrate Gun Hypothesis*: Washington D.C., American Geophysical Union, 216 p.
- Klein, G.d., 1984, Relative rates of tectonic uplift as determined from episodic turbidite deposition in marine basins: *Geology*, 12, 48-50.
- Miller, M.M., Johnson, D.J., Rubin, C.M., Dragert, H., Wang, K., Qamar, A., and Goldfinger, C., 2001, GPS-determination of along-strike variation in Cascadia margin kinematics: Implications for relative plate motion, subduction zone coupling, and permanent deformation: *Tectonics*, 20, 161-176.
- Nelson, H., 1976, Late Pleistocene and Holocene depositional trends, processes, and history of Astoria deep-sea fan, northeast Pacific: *Marine Geology*, 20, 129-173.
- Paull, C.K., Brewer, P.G., Ussler III, W., Peltzer, E.T., Rehder, G., and Clague, D., 2003, An experiment demonstrating that marine slumping is a mechanism to transfer methane from seafloor gas-hydrate deposits into the upper ocean and atmosphere: *Geo-Marine Lett.*, 22, 198-203.
- Paull, C.K., Buelow, W.J., Ussler III, W., and Borowski, W.S., 1996, Increased continental-margin slumping frequency during sea-level lowstands above gas hydrate-bearing sediments: *Geology*, 24, 143-146.

- Rothwell, R.G., Thomson, J., and Kähler, G., 1998, Low-sea-level emplacement of a very large Late Pleistocene 'megaturbidite' in the western Mediterranean Sea: *Nature*, 392, 377-380.
- Shiki, T., Cita, M.B., and Gorsline, D.S., 2000, Sedimentary features of seismites, seismoturbidites and tsunamites—an introduction: *Sedimentary Geology*, 135, vii-ix.
- Spence, W., 1989, Stress Origins and Earthquake Potentials in Cascadia: *J. of Geophys. Res.*, 94, 3076-3088.
- Stuiver, M., and Reimer, P.J., 1993, Extended 14C database and revised CALIB radiocarbon calibration program: *Radiocarbon*, 35, 215-230.
- Stuiver, M., Reimer, P.J., and Braziunas, T.F., 1998, High-precision radiocarbon age calibration for terrestrial and marine samples.: *Radiocarbon*, 40, 1127-1151.
- Suess, E., Torres, M.E., Bohrmann, G., Collier, R.W., Rickert, D., Goldfinger, C., Linke, P., Heuser, A., Sahling, H., Heeschen, K., Jung, C., Nakamura, K., Greinert, J., Pfannkuche, P., Tréhu, A., Klinkhammer, G., Whiticar, M.J., Eisenhauer, A., Teichert, B., and Elvert, M., 2001, Sea floor methane hydrates at Hydrate Ridge, Cascadia Margin, *in* Paull, C.K., and Dillon, W.P., eds., *Natural Gas Hydrates Occurrence, Distribution, and Detection*, Volume 124: American Geophysical Union Monograph: Washington D.C., American Geophysical Union, 87-98.
- Teichert, B.M.A., Eisenhauer, A., Bohrmann, G., Haase-Schramm, A., Bock, B., and Linke, P., 2003, U/Th systematics and ages of authigenic carbonates from Hydrate Ridge, Cascadia convergent margin: recorders of fluid composition and sealevel changes: *Geochimica et Cosmochimica Acta*, 67, 3845-3857.
- Tréhu, A.M., Bohrmann, G., Rack, F., Collett, T., Goldberg, D., Long, P.E., Milkov, A.V., Riedel, M., Schultheiss, P., Torres, M.E., Bangs, N.L., Barr, S.R., Borowski, W.S., Claypool, G.E., Delwiche, M.E., Dickens, G.R., Gracia, E., Guerin, G., Holland, M., Johnson, J.E., Lee, Y.-J., Liu, C.-S., Su, X., Teichert, B., Tomaru, H., Vanneste, M., Watanabe, M., and Weinberger, J.L., 2004, Three-dimensional distribution of gas hydrate beneath southern Hydrate Ridge: constraints from ODP Leg 204: *Earth and Planetary Sci. Lett.*, 222, 845-862.
- Tréhu, A.M., Bohrmann, G., Rack, F.R., Torres, M.E., and *al., e.*, 2003, Proc. ODP, Init. Repts. [CD-ROM], Volume 204: College Station, TX, Ocean Drilling Program.
- Tréhu, A.M., and Flueh, E.R., 2001, Estimating the thickness of the free gas zone beneath Hydrate Ridge, Oregon continental margin, from seismic velocities and attenuation: *J. of Geophys. Res.*, 106, 2035-2045.
- Tréhu, A.M., Torres, M.E., Moore, G.F., Suess, E., and Bohrmann, G., 1999, Temporal and spatial evolution of a gas hydrate-bearing accretionary ridge on the Oregon continental margin: *Geology*, 27, 939-942.
- Westbrook, G.K., Carson, B., Musgrave, R.J., et al., 1994, Proc. ODP, Init. Repts.: College Station, TX, Ocean Drilling Program.
- Witter, R.C., Kelsey, H.M., and Hemphill-Haley, E., 2003, Great Cascadia earthquakes and tsunamis of the past 6700 years, Coquille River estuary, southern coastal Oregon: *Geol. Soc. Am. Bull.*, 115, 1289-1306.

Chapter V

Conclusions

The research presented in this dissertation describes some of the geologic processes that can influence the gas hydrate system at Hydrate Ridge. It is likely that these same processes occur within other portions of the Cascadia margin within the gas hydrate stability zone as well, and they may also be applicable at other active margin gas hydrate systems.

The results presented here, suggest the regional distribution of pore fluid venting sites and likely gas hydrate occurrences within the Hydrate Ridge region is largely controlled by the deformation intensity and dewatering history across the margin (Chapter II). Within large accretionary ridges like Hydrate Ridge, the surface expression of fluid venting appears to be highly focused. Migrating up dip through stratigraphic and/or structural conduits, pore fluids serve to feed a well developed shallow gas hydrate system observed at the summit. These fluids can escape directly to the ocean water, where they precipitate authigenic carbonates or they can simply supply the gas hydrate stability zone with methane, which occasionally escapes during the destabilization of gas hydrate, also resulting in the precipitation of authigenic carbonates. Identification of regional fluid venting patterns on high resolution sidescan sonar data coupled with seismic reflection data and gridded bathymetry offers good insight into the processes that may be operating within a given margin transect, and can greatly aid in guiding more specific seafloor investigations. Understanding the structural evolution of the region hosting a gas hydrate system is also valuable in evaluating the distribution and concentration of marine gas hydrates across a continental margin transect. The results presented here documented the structural vergence variability across the Hydrate Ridge region, its relative timing to external geologic processes (deposition of the Astoria fan on the abyssal plain and strike slip fault propagation into the wedge) and the interaction between these processes, which results in the present configuration of this portion of the accretionary wedge (Chapter III). Understanding this evolution is important as it may

help explain the absence or presence of gas hydrate and provide insight to the evolution of other gas hydrate systems across the margin. On short timescales the slope failure frequency induced by subduction zone earthquakes, with minimal contributions from other triggers, may influence the margin wide slope failure history within the gas hydrate stability zone. This could mean that a significant portion of seafloor and shallow subseafloor gas hydrates could be synchronously mobilized during a subduction zone earthquake, resulting in a potentially large methane release from the seafloor into the ocean and even the atmosphere.

Although the above research has significantly contributed to our understanding of the gas hydrate system at Hydrate Ridge and has the potential for extrapolation to other portions of the Cascadia margin, there is always more insight that can be gained through continued research efforts, not only here at Hydrate Ridge, but in other active margin gas hydrate bearing environments.

Bibliography

- Adams, J., 1990, Paleoseismicity of the Cascadia subduction zone: Evidence from turbidites off the Oregon-Washington margin: *Tectonics*, 9, 569-583.
- Atwater, B.F., and Hemphill-Haley, E., 1997, Recurrence Intervals for Great Earthquakes of the Past 3,500 Years at Northeastern Willapa Bay, Washington: U. S. Geological Survey Professional Paper 1576, 108 p.
- Blondel, P. and Murton, B.J., 1997. *Handbook of Seafloor Sonar Imagery*. Wiley-Praxis Series in Remote Sensing. John Wiley & Sons Ltd. in association with Praxis Publishing Ltd., West Sussex, England, 314 p.
- Bohrmann, G., Greinert, J., Suess, E., and Torres, M., 1998, Authigenic carbonates from the Cascadia subduction zone and their relation to gas hydrate stability: *Geology*, 26, 647-650.
- Bohrmann, G., Linke, P., Suess, E. and Pfannkuche, O., 2000. RV SONNE Cruise Report SO143 TECFLUX-I-1999. GEOMAR Report 93.
- Brewer, P.G., Paull, C., Peltzer, E.T., Ussler, W., Rehder, G., and Friederich, G., 2002, Measurements of the fate of gas hydrates during transit through the ocean water column: *Geophys. Res. Lett.*, 29, doi:10.1029/2002GL014727.
- Brown, K.M., 1990. The nature and hydrogeologic significance of mud diapirs and diatremes for accretionary systems: *J. Geophys. Res.*, 95 (B6), 8969-8982.
- Burbidge, D.R., and Braun, J., 1998, Analogue models of obliquely convergent continental plate boundaries: *J. of Geophys. Res.*, 103, 15,221-15,237.
- Byrne, D.E., Wang, W., and Davis, D.M., 1993, Mechanical role of backstops in the growth of forearcs: *Tectonics*, 12, 123-144.
- Carlson, P.R., and Nelson, C.H., 1987, Marine geology and resource potential of Cascadia Basin, *in* Scholl, G., and Vedder, ed., *Geology and Resource Potential of the Continental Margin of Western North America and Adjacent Ocean Basins*, 6: Houston TX, Circum-Pacific Council for Energy and Mineral Resources, Earth Sciences Series, 523-535.
- Carson, B., Seke, E., Paskevich, V. and Holmes, M.L., 1994. Fluid expulsion sites on the Cascadia accretionary prism: Mapping diagenetic deposits with processed GLORIA imagery: *J. Geophys. Res.*, 99 (B6), 11,959-11,969.
- Caulet, J.-P., 1995, Radiolarians from the Cascadia Margin, leg 146, *in* Carson, B., Westbrook, G.K., Musgrave, R.J., and Suess, E., eds., *Proc. ODP, Sci. Results, Volume 146 (Pt. 1)*: College Station, TX, Ocean Drilling Program, 47-61.
- Chevallier, J., 2004, Seismic sequence stratigraphy and tectonic evolution of Southern Hydrate Ridge [M.S. thesis]: Corvallis, OR, Oregon State University, 117 p.
- Clague, D.A., Maher, N., and Paull, C.K., 2001. High-resolution multibeam survey of Hydrate Ridge, offshore Oregon. *In*: Paull, C.K. and Dillon, W.P. (Eds.), *Natural Gas Hydrates: Occurrence, Distribution, and Detection*. Geophysical Monograph 124. American Geophysical Union, Washington, D.C., 297-303.

- Clarke Jr., S.H., and Carver, G.A., 1992, Late Holocene tectonics and paleoseismicity, southern Cascadia subduction zone: *Science*, 255, 188-191.
- Davis, D., Suppe, J., and Dahlen, F.A., 1983, Mechanics of Fold-and-Thrust Belts and Accretionary Wedges: *J. of Geophys. Res.*, B2, 1153-1172.
- Davis, E.E., and Hyndman, R.D., 1989, Accretion and recent deformation of sediments along the northern Cascadia subduction zone: *Geol. Soc. Am. Bull.*, 101, 1465-1480.
- Duncan, J.R., Fowler, G.A., and Kulm, L.D., 1970, Planktonic Foraminiferan-Radiolarian Ratios and Holocene-Late Pleistocene Deep Sea Stratigraphy off Oregon: *Geol. Soc. Am. Bull.*, 81, 561-566.
- Echavarría, L., Hernández, R., Allmendinger, R., and Reynolds, J., 2003, Subandean thrust and fold belt of northwestern Argentina: Geometry and timing of the Andean evolution: *AAGP Bull.*, 87, 965-985.
- Field, M.E., Gardner, J.V., Jennings, A.E., and Edwards, B.D., 1982, Earthquake-induced sediment failures on a 0.25° slope, Klamath River delta, California: *Geology*, 10, 542-546.
- Fleming, S.W. and Tréhu, A., 1999. Crustal structure beneath the central Oregon convergent margin from potential-field modeling: Evidence for a buried basement ridge in local contact with a seaward dipping backstop: *J. Geophys. Res.*, 104 (B9), 20,431-20,447.
- Flueh, E.R., Fisher, M.A., Bialas, J., Childs, J.R., Klaeschen, D., Kukowski, N., Parsons, T., Scholl, D.W., ten Brink, U., Tréhu, A.M., and Vidal, N., 1998, New seismic images of the Cascadia subduction zone from cruise SO108-ORWELL: *Tectonophysics*: 293, 69-84.
- Fourtanier, E., 1995, Neogene diatom biostratigraphy of site 892, Cascadia Margin, *in* Carson, B., Westbrook, G.K., Musgrave, R.J., and Suess, E., eds., *Proc. ODP, Sci. Results, Volume 146 (Pt. 1): College Station, TX, Ocean Drilling Program*, 63-77.
- Fourtanier, E., and Caulet, J.-P., 1995, Siliceous microfossil stratigraphic synthesis of site 892, Cascadia Margin, *in* Carson, B., Westbrook, G.K., Musgrave, R.J., and Suess, E., eds., *Proc. ODP, Sci. Results, Volume 146 (Pt. 1): College Station, TX, Ocean Drilling Program*, 369-374.
- Goldfinger, C., Kulm, L.D., Yeats, R.S., Appelgate, B., MacKay, M.E., Moore, G.F., 1992. Transverse structural trends along the Oregon convergent margin: Implications for Cascadia earthquake potential and crustal rotations: *Geology*, 20, 141-144.
- Goldfinger, C., Kulm, L.D., Yeats, R.S., Hummon, C., Huftile, G.J., Niem, A.R., McNeill, L.C., 1996. Oblique strike-slip faulting of the Cascadia submarine forearc: The Daisy Bank fault zone off central Oregon. In: Bebout, G.E., Scholl, D.W., Kirby, S.H., Platt, J.P. (Eds.), *Subduction: Top to Bottom. Geophysical Monograph 96. American Geophysical Union, Washington, D.C.*, 65-74.
- Goldfinger, C., Kulm, L.D., Yeats, R.S., McNeill, L., and Hummon, C., 1997, Oblique strike-slip faulting of the central Cascadia submarine forearc: *J. of Geophys. Res.*, 102, 8217-8243.

- Goldfinger, C., Kulm, L.D., Yeats, R.S., Appelgate, B., MacKay, M.E., and Cochrane, G.R., 1996, Active strike-slip faulting and folding of the Cascadia subduction-zone plate boundary and forearc in central and northern Oregon, *in* Rogers, A.M., Walsh, T.J., Kockleman, W.J., and Priest, G.R., eds., *Assessing earthquake hazards and reducing risk in the Pacific Northwest, Volume 1: Washington*, United States Government Printing Office.
- Goldfinger, C., Kulm, L.D., Yeats, R.S., McNeill, L., and Hummon, C., 1997, Oblique strike-slip faulting of the central Cascadia submarine forearc: *J. of Geophys. Res.*, 102, 8217-8243.
- Goldfinger, C., Kulm, L.D., McNeill, L.C., and Watts, P., 2000, Super-scale failure of the southern Oregon Cascadia margin: *Pure and Applied Geophysics*, 157, 1189-1226.
- Goldfinger, C., Nelson, C.H., and Johnson, J.E., 2003, Holocene Earthquake Records From the Cascadia Subduction Zone and Northern San Andreas Fault Based on Precise Dating of Offshore Turbidites: *Annual Rev.-Earth and Planetary Sci.*, 31, 555-577.
- Goldfinger, C., Nelson, C.H., Johnson, J.E., Chaytor, J.D., Eriksson, D., Karabanov, E., Morey-Ross, A., and R/V Revelle and R/V Melville Shipboard Scientific Parties, 2004, Long-term paleoseismic records along the Cascadia subduction zone and northern San Andreas Fault based on turbidite stratigraphy, Japan Earth and Planetary Science Joint Meeting: Tokyo, Japan, JEPS.
- Greiner, J., Bohrmann, G. and Suess, E., 2001. Gas hydrate-associated carbonates and methane-venting at Hydrate Ridge: Classification, distribution, and origin of authigenic lithologies. In: Paull, C.K., Dillon, W.P. (Eds.), *Natural Gas Hydrates: Occurrence, Distribution, and Detection*. Geophysical Monograph 124. American Geophysical Union, Washington D.C., 99-113.
- Gulick, S.P.S., Bangs, N.L.B., Shipley, T.H., Nakamura, Y., Moore, G., and Kuramoto, S., 2004, Three dimensional architecture of the Nankai accretionary prism's imbricate thrust zone off Cape Muroto, Japan: Prism reconstruction via an echelon thrust propagation: *J. of Geophys. Res.*, 109, doi: 10.1029/2003JB002654.
- Gulick, S.P.S., Meltzer, A.M., and Clarke Jr., S.H., 1998, Seismic structure of the southern Cascadia subduction zone and accretionary prism north of the Mendocino triple junction: *J. of Geophys. Res.*, 103, 27207-27222.
- Gutscher, M.-A., Kukowski, N., Malavielle, J., and Lallemand, S., 1996, Cyclical behavior of thrust wedges: Insights from high basal friction sandbox experiments: *Geology*, 24, 135-138.
- Gutscher, M.-A., Klaeschen, D., Flueh, E., and Malavielle, J., 2001, Non-Coulomb wedges, wrong-way thrusting, and natural hazards in Cascadia: *Geology*, 29, 379-382.
- Haugerud, R.A., 1999. Digital elevation model (DEM) of Cascadia, latitude 39N-53N, longitude 116W-133W. U.S. Geological Survey Open-file Report 99-369.

- Heeschen, K.U., Tréhu, A.M., Collier, R.W., Suess, E., and Rehder, G., 2003. Distribution and height of methane bubble plumes on the Cascadia margin characterized by acoustic imaging: *Geophys. Res. Letts.* v. 30, 1643-1646.
- Heezen, B.C., and Ewing, M., 1952, Turbidity currents and submarine slumps, and the 1929 Grand Banks earthquake: *American Journal of Science*, 250, 849-878.
- Henry, P., Lallemand, S.J., Le Pichon, X. and Lallemand, S.E., 1989. Fluid venting along Japanese trenches: Tectonic context and thermal modeling: *Tectonophysics*, 160, 277-291.
- Hovland, M., Lysne, D. and Whiticar, M., 1995. Gas hydrate and sediment gas composition, Hole 892A. In: Carson, B., Westbrook, G.K., Musgrave, R.J., Suess, E. (Eds.), *Proceedings of the Ocean Drilling Program, Scientific Results. Ocean Drilling Program, College Station, Texas*, 151-161.
- Humphreys, E. and Hemphill-Haley, M.A., 1996, Causes and characteristics of western U.S. deformation: *Geol. Soc. Am. Abstracts*, 28.
- Hyndman, R.D. and Spence, G.D., 1992. A seismic study of methane hydrate marine bottom simulating reflectors: *J. Geophys. Res.*, 97 (B5), 6683-6698.
- Hyndman, R.D., Spence, G.D., Yuan, T., and Davis, E.E., 1994, Regional geophysics and structural framework of the Vancouver Island Margin Accretionary Prism, In Westbrook, G.K., Carson, B., Musgrave, R.J., et al., eds., *Proc. ODP, Init. Repts.*, Volume 146 (Pt. 1): College Station, TX, Ocean Drilling Program, 399-419.
- Ingle, J.C., 1973, Neogene foraminifera from the Northeastern Pacific Ocean, Leg 18, Deep Sea Drilling Project, in Kulm, L.D., von Huene, R., et al., *Initial reports of the Deep Sea Drilling Project, Volume 18*: Washington, U.S. Government Printing Office, 517-567.
- Inouchi, Y., Kinugasa, Y., Kumon, F., Nakano, S., Yasumatsu, S., and Shiki, T., 1996, Turbidites as records of intense palaeoearthquakes in Lake Biwa, Japan: *Sedimentary Geology*, 104, 117-125.
- Johnson, J.E., Goldfinger, C., Bangs, N., Tréhu, A.M., and Chevallier, J., in prep 2004, Structural vergence variation and clockwise block rotation in the Hydrate Ridge region, Cascadia accretionary wedge: *Tectonics*.
- Johnson, J.E., Goldfinger, C., and Suess, E., 2003, Geophysical constraints on the surface distribution of authigenic carbonates across the Hydrate Ridge region, Cascadia margin: *Marine Geology*, 202, 79-110.
- Johnson, J.E., Goldfinger, C., and Tréhu, A.M., 2000, Structural development and deformation styles of the Hydrate Ridge region, Cascadia accretionary prism. *Geol. Soc. Am. Abstracts with Programs*, 32 (7), A36.
- Johnson, H.P. and Helferty, M., 1990. The geological interpretation of side-scan sonar: *Rev. Geophys.*, 28 (4), 357-380.
- Jung, W., and Vogt, P.R., 2004, Effects of bottom water warming and sea level rise on Holocene hydrate dissociation and mass wasting along the Norwegian-Barents Continental Margin: *J. of Geophys. Res.*, 109, doi:10.1029/2003JB002738.

- Kelsey, H.M., Witter, R.C., and Hemphill-Haley, E., 2002, Plate-boundary earthquakes and tsunamis of the past 5500 yr, Sixes River estuary, southern Oregon: *Geol. Soc. Am. Bull.*, 114, 298-314.
- Kennett, J.P., Cannariato, K.G., Hendy, I.L., and Behl, R.J., 2003, Methane Hydrates in Quaternary Climate Change The Clathrate Gun Hypothesis: Washington D.C., American Geophysical Union, 216 p.
- Klein, G.d., 1984, Relative rates of tectonic uplift as determined from episodic turbidite deposition in marine basins: *Geology*, 12, 48-50.
- Kopf, A.J., 2002, Significance of Mud Volcanism. *Rev. Geophys.*, 40, B1-B49.
- Kulm, L.D. and Fowler, G.A., 1974. Cenozoic sedimentary framework of the Gorda-Juan de Fuca Plate and adjacent continental margin- A Review. In: Dott, R.H. Jr., Shaver, R.H. (Eds.), *Modern and Ancient Geosynclinal Sedimentation: Society of Economic Paleontologists and Mineralogists, Special Publication 19*, 212-229.
- Kulm, L.D. and Suess, E., 1990. Relationship between carbonate deposits and fluid venting: Oregon accretionary prism: *J. of Geophys. Res.*, 95 (B6), 8899-8915.
- Kulm, L.D., Suess, E., Moore, J.C., Carson, B., Lewis, B.T., Ritger, S.D., Kadko, D.C., Thornburg, T.M., Embley, R.W., Rugh, W.D., Massoth, G.J., Langseth, M.G., Cochrane, G.R., Scamman, R.L., 1986. Oregon subduction zone: Venting, fauna, and carbonates: *Science*, 231, 561-566.
- Kulm, L.D. and von Huene, R., et al., 1973, Initial reports of the Deep Sea Drilling Project, Volume 18: Washington, U.S. Government Printing Office.
- Kvenvolden, K.A., 1993. Gas hydrates - Geological perspective and global change: *Rev. Geophys.*, 31 (2), 173-187.
- Linke, P. and Suess, E., 2001. RV SONNE Cruise Report SO148 TECFLUX-II-2000. GEOMAR Report 98.
- Le Pichon, X., Kobayashi, K. and Crew, K.-N.S., 1992. Fluid venting activity within the eastern Nankai Trough accretionary wedge: A summary of the 1989 Kaiko-Nankai results: *Earth Planet. Sc. Lett.*, 109, 303-318.
- Lewis, B.T.R. and Cochrane, G.C., 1990. Relationship between the location of chemosynthetic benthic communities and geologic structure on the Cascadia subduction zone: *J. Geophys. Res.*, 95 (B6), 8783-8793.
- Marshak, S., 1986, Structure and tectonics of the Hudson Valley fold-thrust belt, eastern New York State: *Geol. Soc. Am. Bull.*, 97, 354-368.
- MacKay, M.E., Moore, G.F., Klaeschen, D., and von Huene, R., 1995, The case against porosity change: Seismic velocity decrease at the toe of the Oregon accretionary prism: *Geology*, 23, 827-830.
- MacKay, M.E., 1995. Structural variation and landward vergence at the toe of the Oregon accretionary prism: *Tectonics*, 14 (5), 1309-1320.
- MacKay, M.E., Jarrard, R.D., Westbrook, G.K., Hyndman, R.D., Shipboard Scientific

- Party of Ocean Drilling Program Leg 146, 1994. Origin of bottom-simulating reflectors: Geophysical evidence from the Cascadia accretionary prism: *Geology*, 22, 459-462.
- MacKay, M.E., Moore, G.F., Cochrane, G.R., Moore, G.F., and Kulm, L.D., 1992, Landward vergence and oblique structural trends in the Oregon margin accretionary prism: Implications and effect on fluid flow: *Earth and Planetary Science Letters*: 109, 477-491.
- McCaffrey, R., Long, M.D., Goldfinger, C., Zwick, P.C., Nabelek, J.L., Johnson, C.K., and Smith, C., 2000, Rotation and plate locking at the southern Cascadia subduction zone: *Geophys. Res. Lett.*, 27, 3117-3120.
- McNeill, L.C., Goldfinger, C., Kulm, L.D., and Yeats, R.S., 2000, Tectonics of the Neogene Cascadia forearc basin: Investigations of a deformed late Miocene unconformity: *Geol. Soc. Am. Bull.*, 112 (8), 1209-1224.
- Miller, M.M., Johnson, D.J., Rubin, C.M., Dragert, H., Wang, K., Qamar, A., and Goldfinger, C., 2001, GPS-determination of along-strike variation in Cascadia margin kinematics: Implications for relative plate motion, subduction zone coupling, and permanent deformation: *Tectonics*, 20, 161-176.
- Moore, J.C., and Silver, E.A., 1987, Continental Margin Tectonics: Submarine Accretionary Prisms: *Rev. of Geophys.*, 25, 1305-1312.
- Moore, C. J., Mascle, A., Taylor, E., Andreieff, P., Alvarez, F., Barnes, R., Beck, C., Bhermann, J., Blanc, G., Brown, K., Clark, M., Dolan, J., Fisher, A., Gieskes, J., Hounslow, M., McLellan, P., Moran, K., Ogawa, Y., Sakai, T., Schoonmaker, J., Vrolijk, P., Wilkens, R., and Williams, C., 1988, Tectonics and hydrogeology of the northern Barbados Ridge: Results from Ocean Drilling Program Leg 110: *Geol. Soc. Am. Bull.*, 100, 1578-1593.
- Moore, J.C. and Vrolijk, P., 1992. Fluids in accretionary prisms: *Rev. of Geophys.*, 30, 113-135.
- Nelson, H., 1976, Late Pleistocene and Holocene depositional trends, processes, and history of Astoria deep-sea fan, northeast Pacific: *Marine Geology*, 20, 129-173.
- Ohta, S. and Laubier, L., 1987. Deep biological communities in the subduction zone of Japan from bottom photographs taken during "Nautile" dives in the Kaiko project: *Earth Planet Sc. Lett.*, 83, 329-342.
- Paull, C.K., Brewer, P.G., Ussler III, W., Peltzer, E.T., Rehder, G., and Clague, D., 2003, An experiment demonstrating that marine slumping is a mechanism to transfer methane from seafloor gas-hydrate deposits into the upper ocean and atmosphere: *Geo-Marine Lett.*, 22, 198-203.
- Paull, C.K., Buelow, W.J., Ussler III, W., and Borowski, W.S., 1996, Increased continental-margin slumping frequency during sea-level lowstands above gas hydrate-bearing sediments: *Geology*, 24, 143-146.
- Price, R.A., 1981, The Cordilleran foreland thrust and fold belt in the southern Canadian Rocky Mountains: In McClay, K.R., and Price, N.J., eds., *Thrust and Nappe Tectonics*, Volume 9, Geological Society of London Special Paper, 427-448.

- Ritger, S.D., Carson, B. and Suess, E., 1987. Methane-derived authigenic carbonates formed by subduction-induced-pore-water expulsion along the Oregon/Washington margin: *Geol. Soc. Am. Bull.*, 98, 147-156.
- Rothwell, R.G., Thomson, J., and Kähler, G., 1998, Low-sea-level emplacement of a very large Late Pleistocene 'megaturbidite' in the western Mediterranean Sea: *Nature*, 392, 377-380.
- Sample, J.C., 1996. Isotopic evidence from authigenic carbonates for rapid upward fluid flow in accretionary wedges: *Geology*, 24 (10), 897-900.
- Sample, J.C. and Reid, M.R., 1998. Contrasting hydrogeologic regimes along strike-slip and thrust faults in the Oregon convergent margin: Evidence from the chemistry of syntectonic carbonate cements and veins: *Geol. Soc. Am. Bull.*, 110 (1), 48-59.
- Sample, J.C., Reid, M.R., Tobin, H.J. and Moore, J.C., 1993. Carbonate cements indicate channeled fluid flow along a zone of vertical faults at the deformation front of the Cascadia accretionary wedge (northwest U.S. coast): *Geology*, 21, 507-510.
- Scheidegger, K.F., Kulm, L.D., and Piper, D.J.W., 1973, Heavy mineralogy of unconsolidated sands in Northeastern Pacific sediments: Leg 18, Deep Sea Drilling Project, *in* Kulm, L.D., von Huene, R., and *al., e.*, eds., Initial Reports of the Deep Sea Drilling Project, Volume 18: Washington, U.S. Government Printing Office, 877-887.
- Seely, D.R., 1977. The significance of landward vergence and oblique structural trends on trench inner slopes. In: Talwani, M., Pitman, W.C. (Eds.), *Islands Arcs, Deep Sea Trenches, and Back-Arc Basins*, Maurice Ewing Series. American Geophysical Union, Washington, D.C., 187-198.
- Shiki, T., Cita, M.B., and Gorsline, D.S., 2000, Sedimentary features of seismites, seismo-turbidites and tsunamiites—an introduction: *Sedimentary Geology*, 135, vii-ix.
- Shipboard Scientific Party, 1994, Explanatory Notes, *in* Westbrook, G.K., Carson, B., Musgrave, R.J., and *al., e.*, eds., *Proc. ODP, Init. Repts.*, Volume 146 (Pt. 1): College Station, TX, Ocean Drilling Program, 15-48.
- , 1994, Site 891, *in* Westbrook, G.K., Carson, B., Musgrave, R.J., et al., *Proc. ODP, Init. Repts.*, Volume 146 (Pt. 1): College Station, TX, Ocean Drilling Program, 241-300.
- , 1994, Site 892, *in* Westbrook, G.K., Carson, B., Musgrave, R.J., et al., *Proc. ODP, Init. Repts.*, Volume 146 (Pt. 1): College Station, TX, Ocean Drilling Program, 301-378.
- , 2003, Site 1244, *in* Tréhu, A.M., Bohrmann, G., Rack, F., Torres, M.E., et al., *Init. Repts. [CD-ROM]*, Volume 204: College Station, TX, Ocean Drilling Program, 1-132.
- , 2003, Site 1245, *in* Tréhu, A.M., Bohrmann, G., Rack, F., Torres, M.E., et al., *Init. Repts. [CD-ROM]*, Volume 204: College Station, TX, Ocean Drilling Program, 1-131.

- Smit, J.H.W., Brun, J.P., and Sokoutis, D., 2003, Deformation of brittle-ductile thrust wedges in experiments and nature: *J. of Geophys. Res.*, 108, doi:10.1029/2002JB002190.
- Snively, P.D. Jr., 1987. Tertiary Geologic Framework, Neotectonics, and Petroleum Potential of the Oregon-Washington Continental Margin. In Scholl, D.W., Grantz, A., and Vedder, J.G. (Eds.), *Geology and resource potential of the continental margin of western North America and adjacent Ocean - Beaufort Sea to Baja California*. Circum-Pacific Council for Energy and Mineral Resources, Earth Science Series 6, 305-335.
- Snively, P.D., Jr., Wagner, H.C., and Lander, D.L., 1980, Geologic cross section of the central Oregon continental margin: Boulder, CO, Plate Tecton. Group, U.S. Geodyn. Comm., Geol. Soc. of Am.
- Spence, W., 1989, Stress Origins and Earthquake Potentials in Cascadia: *J. of Geophys. Res.*, 94, 3076-3088.
- Stuiver, M., Reimer, P.J., and Braziunas, T.F., 1998, High-precision radiocarbon age calibration for terrestrial and marine samples: *Radiocarbon*, 40, 1127-1151.
- Stuiver, M., and Reimer, P.J., 1993, Extended 14C database and revised CALIB radiocarbon calibration program: *Radiocarbon*, 35, 215-230.
- Suess, E., Carson, B., Ritger, S., Moore, J.C., Jones, M.L., Kulm, L.D., Cochrane, G.R., 1985. Biological communities at vent sites along the subduction zone off Oregon. The hydrothermal vents of the eastern Pacific: An overview. *Biological Society of Washington Bulletin*, 6, 474-484.
- Suess, E., Torres, M.E., Bohrmann, G., Collier, R.W., Greinert, J., Linke, P., Rehder, G., Tréhu, A., Wallmann, K., Winckler, G., Zuleger, 1999. Gas hydrate destabilization: Enhanced dewatering, benthic material turnover and large methane plumes at the Cascadia convergent margin. *Earth Planet Sc. Lett.*, 170, 1-15.
- Suess, E., Torres, M.E., Bohrmann, G., Collier, R.W., Rickert, D., Goldfinger, C., Linke, P., Heuser, A., Sahling, H., Heeschen, K., Jung, C., Nakamura, K., Greinert, J., Pfannkuche, P., Tréhu, A., Klinkhammer, G., Whiticar, M.J., Eisenhauer, A., Teichert, B., Elvert, M., 2001. Sea floor methane hydrates at Hydrate Ridge, Cascadia Margin. In. Paull, C.K. and Dillon, W.P. (Eds.), *Natural Gas Hydrates Occurrence, Distribution, and Detection*. American Geophysical Union. *Geophysical Monograph* 124, 87-98.
- Suppe, J., 1983. Geometry and kinematics of fault-bend folding: *American Journal of Science* 283, 684-721.
- Teichert, B.M.A., Eisenhauer, A., Bohrmann, G., Haase-Schramm, A., Bock, B., and Linke, P., 2003, U/Th systematics and ages of authigenic carbonates from Hydrate Ridge, Cascadia convergent margin: recorders of fluid composition and sealevel changes: *Geochimica et Cosmochimica Acta*, 67, 3845-3857.
- Tobin, H.J., Moore, J.C., MacKay, M.E., Orange, D.L., and Kulm, L.D., 1993, Fluid flow along a strike-slip fault at the toe of the Oregon accretionary prism: Implications for the geometry of frontal accretion: *Geol. Soc. Am. Bull.*, 105, 569-582.

- Torres, M.E., Bohrmann, G., Brown, K., deAngelis, M., Hammond, D., Klinkhammer, G., McManus, J., Suess, E., Tréhu, A., 1999. Geochemical observations on Hydrate Ridge, Cascadia margin, July 99. Reference 99-3, Oregon State University Data Report 174.
- Tréhu, A., Asudah, I., Brocher, T.M., Luetgert, J.H., Mooney, W.D., Nabelek, J.L., and Nakamura, Y., 1994, Crustal architecture of the Cascadia forearc: *Science*, 266, 237-243.
- Tréhu, A.M., Bangs, N.L., Arsenault, M.A., Bohrmann, G., Goldfinger, C., Johnson, J.E., Nakamura, Y., Torres, 2002. Complex Subsurface Plumbing Beneath Southern Hydrate Ridge, Oregon Continental Margin, from High-resolution 3D Seismic Reflection and OBS Data. Proceedings of the Fourth International Conference on Gas Hydrates, Yokohama, Japan, 90-96.
- Tréhu, A.M., Bohrmann, G., Rack, F., Collett, T., Goldberg, D., Long, P.E., Milkov, A.V., Riedel, M., Schultheiss, P., Torres, M.E., Bangs, N.L., Barr, S.R., Borowski, W.S., Claypool, G.E., Delwiche, M.E., Dickens, G.R., Gracia, E., Guerin, G., Holland, M., Johnson, J.E., Lee, Y.-J., Liu, C.-S., Su, X., Teichert, B., Tomaru, H., Vanneste, M., Watanabe, M., and Weinberger, J.L., 2004, Three-dimensional distribution of gas hydrate beneath southern Hydrate Ridge: constraints from ODP Leg 204: *Earth and Planetary Sci. Lett.*, 222, 845-862.
- Tréhu, A.M., Bohrmann, G., Rack, F.R., Torres, M.E., et al., 2003, Proc. ODP, Init. Repts. [CD-ROM], Volume 204: College Station, TX, Ocean Drilling Program.
- Tréhu, A.M., Flemings, P.B., Bangs, N., Chevallier, J., Gracia, E., Johnson, J.E., Liu, C.-S., Liu, X., Riedel, M., and Torres, M.E., 2004, Feeding methane vents and gas hydrate deposits at south Hydrate Ridge: *Science*, submitted.
- Tréhu, A.M. and Flueh, E.R., 2001. Estimating the thickness of the free gas zone beneath Hydrate Ridge, Oregon continental margin, from seismic velocities and attenuation. *J. Geophys. Res.*, 106 (B2), 2035-2045.
- Tréhu, A.M., Torres, M.E., Moore, G.F., Suess, E. and Bohrmann, G., 1999. Temporal and spatial evolution of a gas hydrate-bearing accretionary ridge on the Oregon continental margin. *Geology*, 27 (10), 939-942.
- Underwood, M.B., Moore, G.F., Taira, A., Klaus, A., Wilson, M.E.J., Fergusson, C.L., Hirano, S., Steurer, J., and Party, L.S.S., 2003, Sedimentary and Tectonic Evolution of a Trench-Slope Basin in the Nankai Subduction Zone of Southwest Japan: *Sedimentary Geology*, 73, 589-602.
- von Huene, R., Pecher, I.A., and Gutscher, M.-A., 1996, Development of the accretionary prism along Peru and material flux after subduction of Nazca Ridge: *Tectonics*, 15, 19-33.
- von Huene, R., and Suess, E., 1988, Ocean Drilling Program Leg 112, Peru continental margin: Part 1, Tectonic history: *Geology*, 16, 934-938.
- Wells, R.E., and Simpson, R.W., 2001, Northward migration of the Cascadia forearc in the northwestern U.S. and implications for subduction deformation: *Earth, Planets and Space*, 53, 275-283.

- Westbrook, G.K., 1994, Growth of Accretionary Wedges off Vancouver Island and Oregon, *in* Westbrook, G.K., Carson, B., and Musgrave, R.J., eds., Proceedings of the Ocean Drilling Program, Initial Reports, Volume 146 (part 1): College Station, TX, Ocean Drilling Program, 381-388.
- Westbrook, G., Carson, B., Musgrave, R., and Shipboard Scientific Party, 1994. Initial reports of the Ocean Drilling Program, 146. Ocean Drilling Program, College Station, Texas, 630 p.
- Witter, R.C., Kelsey, H.M., and Hemphill-Haley, E., 2003, Great Cascadia earthquakes and tsunamis of the past 6700 years, Coquille River estuary, southern coastal Oregon: *Geol. Soc. Am. Bull.*, 115, 1289-1306.
- Zellers, S.D., 1995, Foraminiferal Biofacies, paleoenvironments, and biostratigraphy of Neogene-Quaternary sediments, Cascadia Margin, *in* Carson, B., Westbrook, G.K., Musgrave, R.J., and Suess, E., eds., Proc. ODP, Sci. Results, Volume 146 (Pt. 1): College Station, TX, Ocean Drilling Program, 79-113.